

Chapter 7

GLACIERS AND GLACIAL GEOLOGY

Fire and Ice

*Some say the world will end in fire
Some say in ice.
From what I've tasted of desire
I hold with those who favor fire.
But if I had to perish twice,
I think I know enough of hate
To say that for destruction ice
Is also great
And would suffice.*

Robert Frost

In this chapter we address the processes behind the modification of the landscape by glaciers. These large mobile chunks of ice are very effective modifiers of the landscape, sculpting very distinctive landforms, and generating prodigious amounts of sediment. Our task is broken into understanding the physics of how glaciers work, the discipline of glaciology, which is prerequisite for understanding how glaciers erode the landscape, the discipline of glacial geology.

Although glaciers are interesting in their own right, and lend to alpine environments an element of beauty of their own, they are also important actors geomorphically. Occupation of alpine valleys by glaciers leads to the generation of such classic glacial signatures as U-shaped valleys, steps and overdeepenings of the long valley profiles that are now occupied by lakes, hanging valleys that now spout waterfalls. Even the coastlines have been greatly affected by glacial processes. Major fjords, some of them extending to water depths of several hundreds of meters, punctuate the coastlines of western North America, New Zealand and Norway.

It is the variation in glacial extent, largely of continental scale ice sheets in the northern hemisphere, that has driven the 120-150 m fluctuations in sea level over the last 3-5 million years. On tectonically rising coastlines, this results in the generation of marine terraces, each carved at a sea level highstand, corresponding to an interglacial period.

Ice sheets and glaciers also contain high-resolution records of climate change. Extraction and analysis of cores of ice reveal detailed layering, chemistry and air bubble contents that are our best terrestrial paleoclimate archive, against which to contrast the deep sea records obtained through ocean drilling programs.

The interest is not limited to Earth, either. As we learn more about other planets in the solar system, attention has begun to focus on the potential that Martian ice caps could also contain paleoclimate information. And further out into the solar system are bodies whose surfaces are at mostly water ice. Just how these surfaces deform upon impacts of bolides, and the potential for unfrozen water at depth, are topics of considerable interest in the planetary sciences community.

Finally, glaciers themselves are worth understanding as they present obstacles encountered by climbers en route to the summits of alpine peaks. The surfaces of glaciers are littered with cracks and holes, some of which are dangerous. But these hazards can either be avoided or lessened if we approach them with some knowledge of their origin. How deep are crevasses? How are crevasses typically oriented, and why? What is a moulin? What is a medial moraine, what is a lateral moraine? Are they mostly ice or mostly rock? How does the water discharge from a glacial outlet stream vary through a day, and through a year?

Glaciers: what are they and how they work

A glacier is a natural accumulation of ice that is in motion due to its own weight. The ice is derived from snow, which slowly loses porosity to approach a density of pure ice (Figure 1). Consider a small alpine valley. In general, it snows more at high altitudes than it does at low altitudes. And it melts more at low altitudes than it does at high. If there is some place in the valley where it snows more in the winter than it melts in the summer, there will be a net accumulation of snow there. The down-valley limit of this accumulation is the snowline, the first place where you would encounter snow on a climb of the valley in the late fall. If this happened year after year, a wedge of snow would accumulate each year, compressing the previous years' accumulations. The snow slowly compacts to more and more dense phase, called firn, in a process akin to the metamorphic reactions in a mono-mineralic rock near its pressure melting point. Once thick enough, this growing wedge of snow-ice can begin to deform under its own weight, and to move downhill. At this point, we would call the object a glacier. It is only by the motion of the ice that we would ever have a chunk of ice poking further down the valley than the annual snowline.

The anatomy of a glacier

A glacier can be broken into two parts (Figure 2): the accumulation area, where there is net accumulation of ice over the course of a year, and the ablation area, where there is net loss of ice. The two are separated by the equilibrium line, at which point there is a balance (or equilibrium) between accumulation and ablation. This corresponds to a long-term average of the snowline position. The equilibrium line altitude, or the ELA, is a very important attribute of a glacier. In a given climate, it is remarkably consistent from one valley to another.

Types of glaciers: a bestiary of ice

First of all, note that sea ice is fundamentally different from a glacier. Sea ice is frozen sea water; it is not born of snow. It is usually a few meters thick at the best, with pressure ridges and their associated much deeper keels being a few tens of meters thick. Ice breakers can plow through sea ice. They cannot plow through icebergs, which are calved from the fronts of tidewater glaciers, and can be more than a hundred meters thick. It is icebergs that pose a threat to shipping.

Glaciers can be classified in several ways, using size, the thermal regime, the location in the landscape, and even the regularity of a glacier's speed. Some of these classifications overlap, as we will see. We will start with the thermal distinctions, as they play perhaps the most important role in determining the degree to which a glacier can modify the landscape.

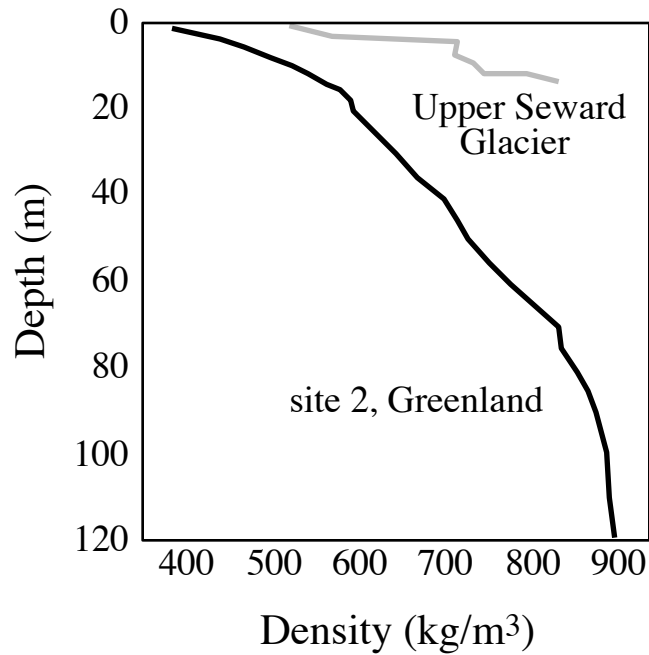


Figure 7.1 Density profiles in two very different glaciers, the upper Seward Glacier in coastal Alaska being very wet, the Greenland site being very dry. The metamorphism of snow is much more rapid in the wetter case; firn achieves full ice densities by 20 m on the upper Seward and takes 100 m in Greenland. Ice with no pore space has a density of 917 kg/m^3 . (after Paterson, 1992)

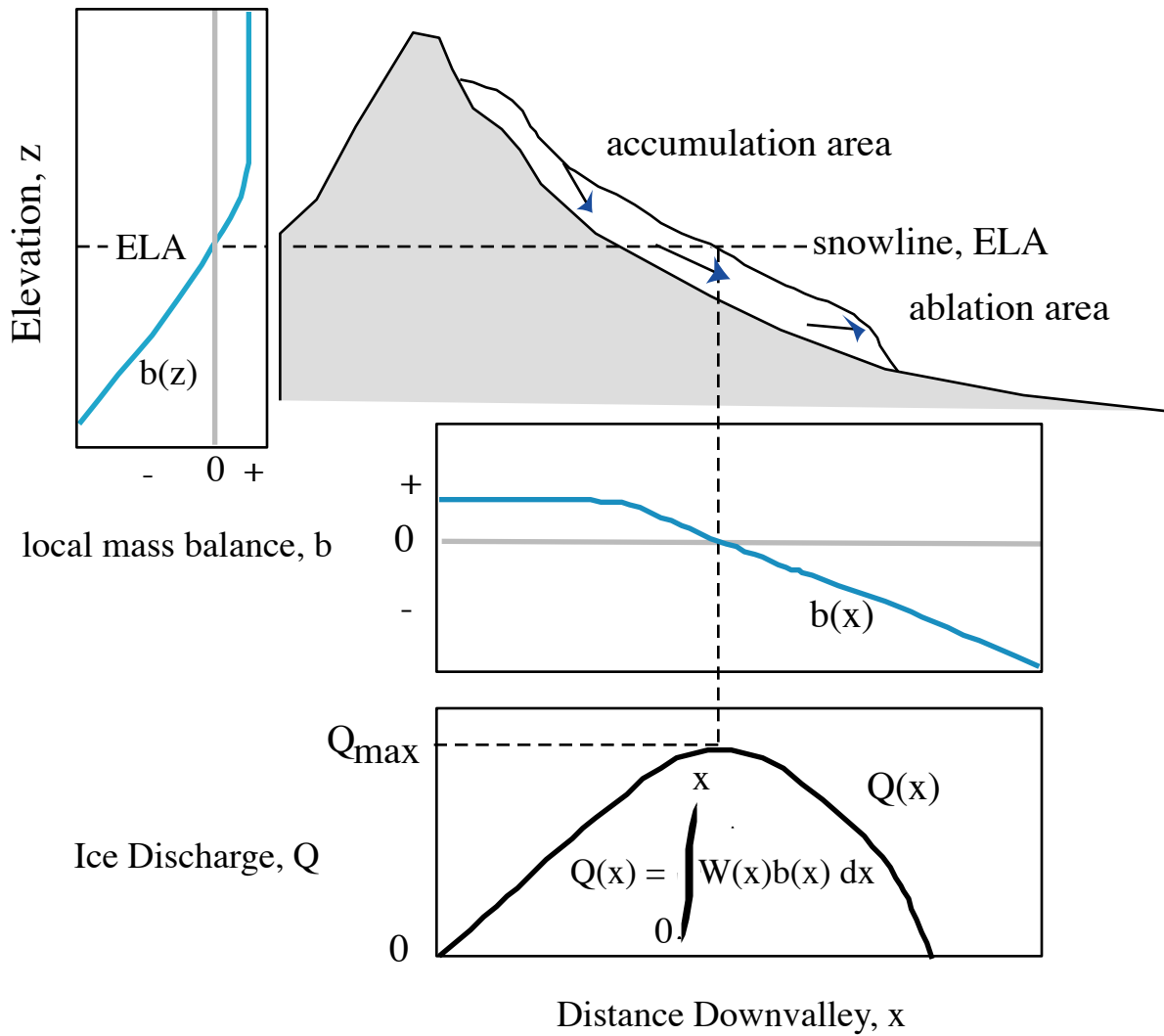


Figure 7.2 Schematic diagrams of a glacier (white) in a mountainous topography (gray) showing accumulation and ablation areas on either side of the equilibrium line altitude (ELA). Mapped into the vertical, z (left diagram), the net mass balance profile, $b(z)$, is negative at elevations below the ELA and positive above it. We also show the net balance mapped onto the valley-parallel axis, x (follow dashed line downward), generating the net balance profile $b(x)$. At steady state the ice discharge of the glacier must reflect the integral of this net balance profile (bottom diagram). The maximum discharge should occur at roughly the down-valley position of the ELA. Where the discharge goes again to zero determines the terminus position.

The temperatures of *polar glaciers* are well below the freezing point of water throughout. They are found at both very high latitudes and very high altitudes, reflecting the very cold mean annual temperatures there. To first order, a thermal profile in these glaciers would look like one in rock, increasing with depth in a geothermal profile that differs from one in rock only in that the conductivity and density of ice is different from that of rock (Figure 3).

In contrast to these glaciers, *temperate glaciers* are those in which the mean annual temperature is very close to the pressure-melting point of ice, all the way to the bed. They derive their name from their location in temperate climates whose mean annual temperatures are closer to 0°C than at much higher elevations or latitudes. The importance of the thermal regime lies in the fact that being close to the melting point at the base allows the ice to slide along the bed in a process called regelation (see below). It is this process of sliding that allows temperate glaciers to erode their beds through both abrasion and quarrying. Polar glaciers are gentle on the landscape, perhaps even protecting it from subaerial mechanical weathering processes that would otherwise attack it. How does a temperate glacier remain close to the melting point throughout, being almost isothermal? Recall that associated with the phase change of water is a huge amount of energy. In a temperate glacier, significant water melts at the surface, and is translated to depth within the firn, and even deeper in the glacier along grain boundaries. Glacier ice is after all a porous substance. If this water encounters any site that is below the freezing point, it will freeze, yielding its energy, which in turn warms up the surrounding ice. So heat is efficiently moved from the surface to depth by moving water – it is advected. This is a much more efficient process than conduction, and can maintain the entire body of a glacier at very near the freezing point.

A straight-forward distinction can be made in terms of size. Valley glaciers occupy single valleys. Ice caps cover the tops of peaks and drain down several valleys on the sides of the peak. Ice sheets can exist in the absence of any pre-existing topography, and can be much larger by orders of magnitude than ice caps. The greatest living examples are the ice sheets of east and west Antarctica, and of Greenland, whose diameters are thousands of kilometers, and thicknesses are kilometers. Their even larger relatives in the last glacial maximum, the combined Laurentide and Cordillera, and the Fennoscandian icesheets, covered half of North America and half of Europe, respectively.

Tidal glaciers are those that dip their toes in the sea, and lose some fraction of their mass through the calving of icebergs (as opposed to melt). These are the glaciers of concern to shipping, be it the shipping plying the waters of the Alaskan coastline, or the ocean liners plying the waters off Greenland.

Most glaciers obey what we mean when we use the adjective ‘glacial’. Glacial speeds might be a few meters per year to a few kilometers per year, and they will be the same the next year and the next. We speak of glacial speeds as being slow and steady. The exceptions to this are the surging glaciers and their cousins embedded in icesheet margins, the ice streams, which appear to be in semi-perpetual surge. These ill-behaved glaciers (meaning they don’t fit our expectations) are the subject of intense modern study. They may hold the key to understanding the rapid fluctuations of climate in the late Pleistocene, which in turn are important to understand as they lay the context for the modern climate system that Humans are modifying significantly.

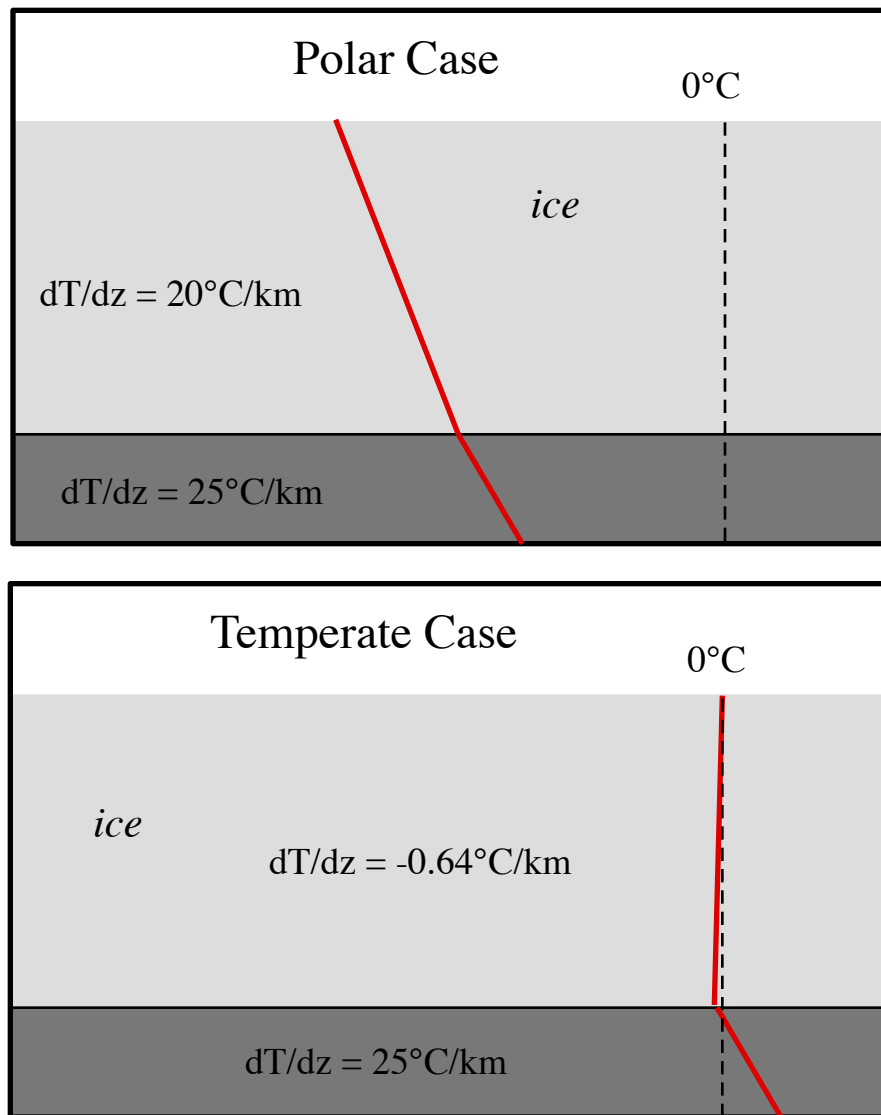


Figure 7.3 Temperature profiles in polar (top) and temperate (bottom) glacier cases. Kink in profile in the polar case reflects the different thermal conductivities of rock and ice. Roughly isothermal profile in the temperate case is allowed by the downward advection of heat by meltwaters. Temperature is kept very near the pressure-melting point throughout, meaning it declines slightly (see phase diagram of water).

All of these we will visit in turn, but first let us lay out the basics of how glaciers work, in general.

Mass Balance

The glaciological community, traditionally an intimate mix of mountain climbers and geophysicists, has a long and proud tradition of being quite formal in its approach to the health of glaciers and their mechanics. Once again, the problem comes down to a balance, this time of mass of ice. One may find in the bible of the glaciologists, Paterson's *The Physics of Glaciers*, now in its 3rd edition, at least one chapter on mass balance alone (see Further Reading for more suggestions of summary texts). One may formalize the illustration of the mass balance shown in [Figure 2](#) with the following equation:

$$\frac{\partial H}{\partial t} = b(z) - \frac{1}{W(z)} \frac{\partial Q}{\partial x} \quad (7.1)$$

where H is ice thickness, W is the glacier width, and Q the ice discharge per unit width [=] L^2/T . Mass can be lost or gained through all edges of the block we have depicted (the top, the base, and the up- and down-ice sides). Here b represents the "local mass balance" on the glacier surface, the mass lost or gained over an annual cycle. It is usually expressed as a change in height of the ice surface, i.e., meters of ice equivalent. This quantity is positive where there is a net gain of ice mass over an annual cycle, and negative where there is a net loss. The elevation at which the mass balance crosses zero defines the "equilibrium line altitude", or the ELA, of the glacier (see [Figure 2](#)). The mass balance reflects all of the meteorological forcing of the glacier, both the snow added over the course of the year, and the losses dealt by the combined blows of ablation (melt) and sublimation. Where the annual mass balance is positive, it has snowed more than it melts in a year, and vice versa. To first order, because it snows more at higher altitudes, and melts more at lower altitudes, the mass balance always has a positive gradient with elevation. Examples of mass balance profiles from a variety of glaciers in differing climates are shown in [Figure 4](#). Note the positive mass balance gradient in each case, which is especially well marked in the ablation or wastage zones. One can easily pick out the ELA for each glacier. The ELA varies greatly, being lowest in high latitudes (where it is cold and the ablation is low) and nearest coastlines (where the winter accumulation is high due to proximity of oceanic water sources). A classic illustration of the latitudinal dependence is drawn from work of Porter ([Figure 5](#)). The modern ELAs, as deduced from snowlines and mass balance surveys, are everywhere much lower than the ELAs reconstructed (more on how to do this later; see [Figure 19](#)) from the last glacial maximum (LGM) at roughly 18 ka. In places the decline in ELA is up to 1 kilometer!

One may measure the health of a glacier by the total mass balance, reflecting whether in a given year there has been a net loss or gain of ice from the entire glacier. This is simply the spatial integral of the product of the local mass balance with the hypsometry (area vs elevation) of the valley:

$$B = \int_0^{z_{\max}} b(z)W(z)dz \quad (7.2)$$

This exercise is carried out on at least a dozen Norwegian glaciers on an annual basis (see [Figure 6](#) for an example from the Nigardsbreen). The Norwegians are interested in the health of their glaciers in large part because a significant portion of their electrical power comes from subglacially tapped hydropower sources.

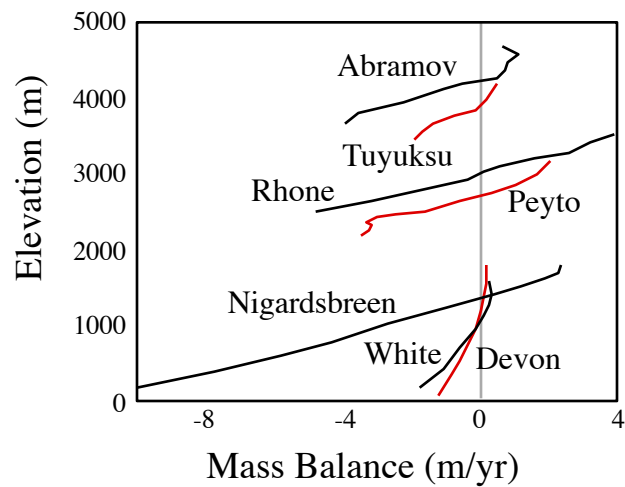


Figure 7.4 Specific mass balance profiles from several glaciers around the world, showing the variability of the shape of the profiles. Mass balance gradients (slopes on this plot) are quite similar, especially in ablation zones (where the balance <0), except for those in the Canadian Arctic (Devon and White ice caps). (adapted from Oerlemans, Nature October 7, 1992)

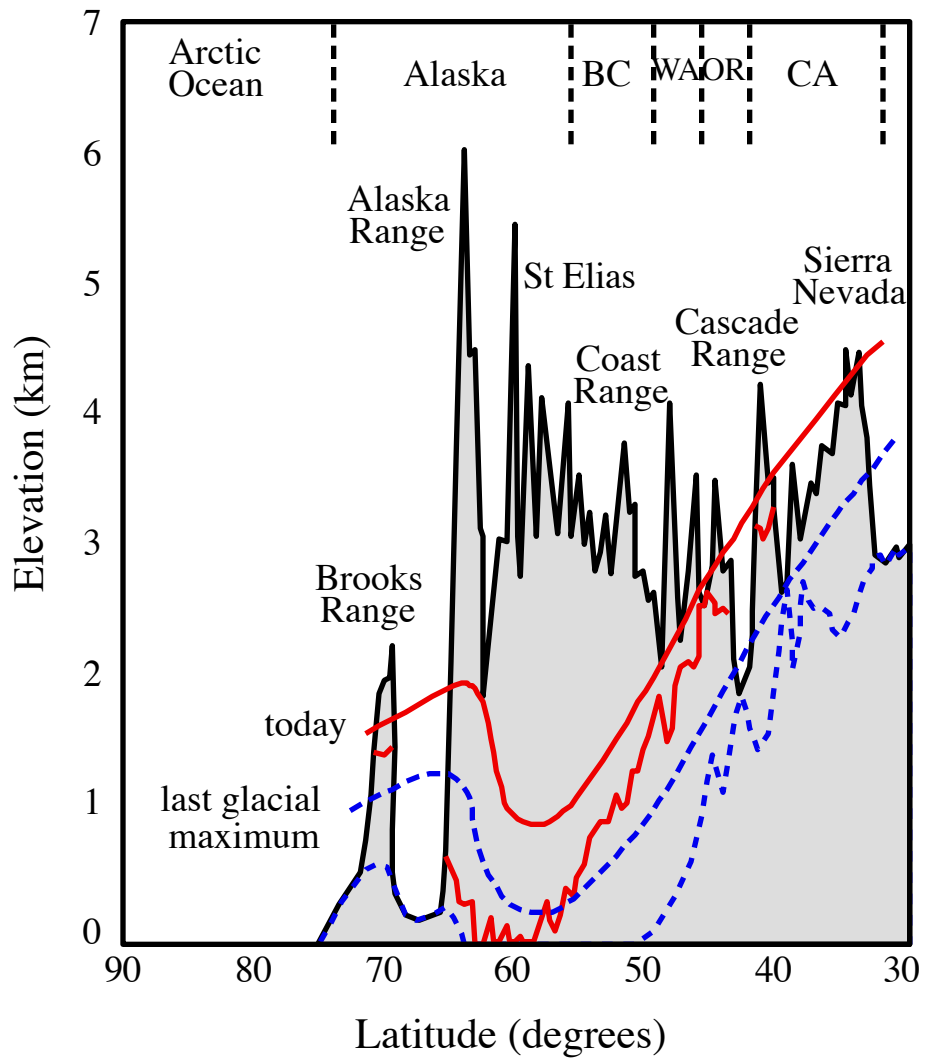


Figure 7.5 Profiles of topography (solid line), equilibrium line elevation (ELA) and glacial extent (solid, present day; dashed, last glacial maximum (LGM)) along the spine of Western North America from California to the Arctic Ocean. Note many-hundred meter lowering of the ELA in the LGM, and corresponding greater extent of the glacial coverage of the topography. (after Skinner and Porter, 19xx)

Nigardsbreen, Norway
1998

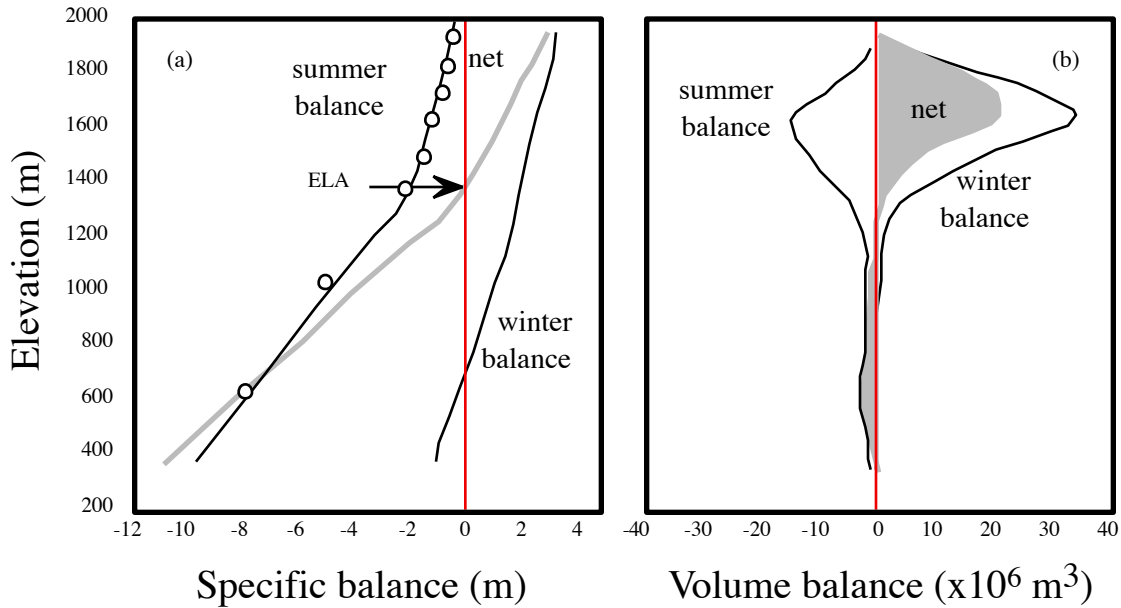


Figure 7.6 Mass balance profiles for the year 1998 on the Nigardsbreen, a coastal Norwegian glacier. a) Specific balance in meters of water equivalent. Winter balance from snow probe surveys, summer balance from stake network (circles). Net balance is shown in gray; net balance is zero at 1350 m, the ELA. b) The volume balance derived by the product of the specific balance with the altitudinal distribution or hypsometry of the glacier. That the glacier has so much more area at high elevations is reflected in the highly contribution of accumulation to the net balance of the glacier (gray fill). In 1998, the net balance is highly positive; there is more gray area to the right of the 0 balance line than to the left), so that the integral of the gray fill is > 0 . In this year the positive total balance represents a net increase of roughly 1 m water equivalent over the entire glacier. (after NVE, 1999)

It is a common misconception that a considerable amount of melting takes place at the base of a glacier, because after all the Earth is hot. Note the scales on the mass balance profiles. In places, many meters can be lost by melting associated with solar radiation. Recall that the heat flux through the Earth's crust is about 41 mW/m^2 (defined as one heat flow unit, HFU). This is sufficient to melt about 5 cm of ice per year, a trivial amount when contrasted with the high heat fluxes powered in one or another way by the sun. As far as the mass balance of a glacier is concerned, then, there is little melt at the base of a glacier.

If nothing else were happening but the local mass gain or loss from the ice surface, a new wedge of snow would accumulate, which would be tapered off by melt to a tip at the ELA (or snowline) each year. Each successive wedge would thicken the entire wedge of snow above the snowline, and would increase the slope everywhere. But something else *must* happen, because we find glaciers poking their snouts well below the ELA, below the snowline. How does this happen? Ice is in motion. This is an essential ingredient in the definition of a glacier. Otherwise we are dealing with a snowfield. The Q terms in the mass balance expression reflect the fact that ice can move downhill, powered by its own weight. Ice has two technologies for moving, one by basal sliding, in which the entire glacier moves at a rate dictated by the slip at the bed, the other by internal deformation, like any other fluid (see [Figure 7](#)). We will return to a more detailed treatment of these processes in a bit. Know for now that the ice discharge per unit width of glacier, Q , may be defined by the mean velocity of the ice column, \bar{U} with the thickness of the glacier, H .

Given only this knowledge, we can construct a model of a glacier in steady state, one in which none of the variables of concern in the mass balance expression are changing with time. Setting the left hand side (lhs) to zero, then, we see that there must be a balance between the local mass balance of ice dictated by the meteorological forcing (the climate) and the local gradient in the ice discharge.

$$Q(x) = \int_0^x b(x)W(x)dx \quad (7.3)$$

Here we have taken x to be 0 at the up-valley end of the glacier. Ignoring for the moment the width function $W(x)$, reflecting the geometry (or really the hypsometry) of the valley, we see that for small x , high up in the valley, since the local mass balance is positive there the ice discharge must increase with distance downvalley; conversely, it must decrease for distances below that associated with the ELA. The ice discharge must therefore go through a maximum at the ELA. In addition, since the discharge Q must increase at least as fast as the ice thickness (Q has H in the expression already, and if \bar{U} increases with H it will be even more sensitive to H), we might expect that the ice thickness is also a maximum at the ELA. To illustrate this, we show in [Figure 8](#) a simulation of the evolution of a small alpine glacier in its valley, starting with no ice and evolving to steady state. We impose a mass balance profile shown in the figure, and hold it steady from the start of the model run. The simulations shown represent 600 years, and the glacier comes into roughly steady state within 400 years. Similar modeling exercises have been used recently to explore the sensitivity of alpine glaciers to climate changes in the past and in the future ([refs to Greuell, Oerlemans, also latest Oerlemans 2007](#)).

This exercise also yields another interesting result. In steady state, we find that within the accumulation area, the ice discharge must be increasing down-valley in order to accommodate

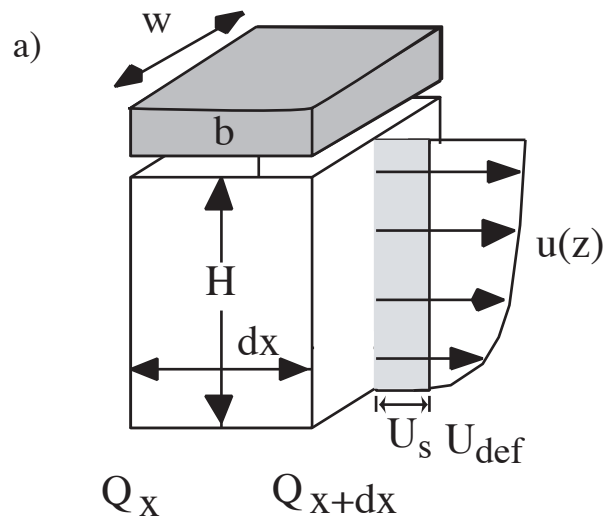


Figure 7.7 a) Mass balance for a section of glacier of width W , down-glacier length dx , and height H . Inputs or outputs through the top of the box are captured as the local mass balance, b . Downglacier discharge of ice into left side of box, Q_x , and out the right side of box, Q_{x+dx} , include contributions from basal sliding (shading) and internal ice deformation. (after MacGregor et al., 2002)

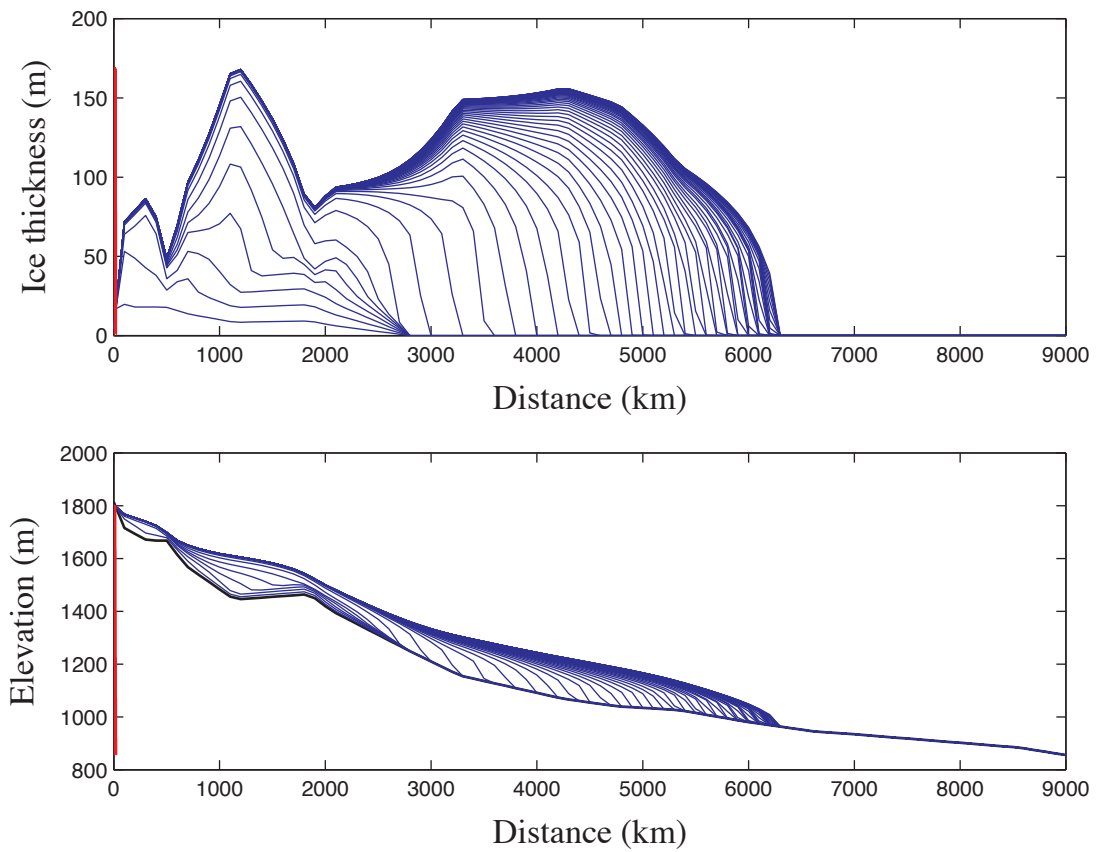


Figure 7.8 Model of glacier evolution on bedrock profile from Bench Glacier valley, Alaska, shown in evenly spaced time steps out to 600 years. Climate is assumed to be steady, with a prescribed mass balance profile. top: profiles of ice thickness through time. bottom: glacier draped on bedrock profile. The glacier reaches approximately steady state at ~500 years. Measured maximum ice thickness of 180 m is well reproduced by the final glacier.

the new snow (ultimately ice) arriving on its top. Conversely, the ice discharge must be decreasing with downvalley distance in the ablation region. This has several important glaciological and glacial geological consequences. First, the vertical component of the trajectories of the ice parcels must be downward in the accumulation zone and upward in the ablation zone, as shown in all elementary figures of glaciers, including [Figure 2](#). As a corollary, debris embedded in the ice is taken toward the bed in the accumulation zone and away from it in the ablation zone. Glaciers tend to have concave up-valley contours above the ELA, and convex contours below (hence you can locate the ELA on a map of a glacier simply by finding the contour that most directly crosses the glacier without bending either up- or down-valley). Debris therefore moves away from the valley walls in the accumulation zone and toward them in the ablation zone. This is reflected in the fact that lateral moraines begin at roughly the ELA. This observation is useful if one is trying to reconstruct past positions of glaciers in a valley, or more particularly to locate the past position of the ELA. As the ELA is often taken as a proxy for the 0° isotherm, it is a strong measure of climate, and hence a strong target for paleoclimate studies.

This straight-forward exercise should serve as a motivation for understanding the mechanics of ice motion. This mechanics is at the core of all such simulations. It is what separates one type of glacier from another. And whether a glacier can slide on its bed or not dictates whether it can erode the bed or not -- and hence whether the glacier can be an effective means of modifying the landscape.

Ice deformation

Like any other fluid on a slope, ice deforms under its own weight. It does so at very slow rates, which are dictated by the high viscosity of the ice. As the viscosity is temperature dependent, growing greatly as the temperature declines, the colder the glacier is the slower it deforms. Although the real picture is considerably more complicated than that we will describe here (see Hooke and Patterson for recent detailed treatments), the essence of the physics is as follows. Consider a slab of ice resting on a plane inclined at an angle to the horizontal ([Figure 9](#)). We wish to write a force balance for this chunk of ice. It is acted upon by body forces (fields like gravitational fields and magnetic fields). As ice is not magnetic, the relevant body force is simply that due to gravity. The weight of any element of ice is mg where m is the mass of the slab, or its density times its volume, $(dx dy dz)$. One may decompose the weight vector into one acting parallel to the bed and one acting normal to the bed. As shown in the figure, the normal stress, σ , (recall that a stress is a force divided by the area of the surface, $dx dy$) acting on the slab on its top side is $\rho g(H-z)\cos(\alpha)$, and at its base $\rho g(H-z-dz)\cos(\alpha)$.

Now that we have an expression for the stresses within the slab, we introduce its material behavior, or rheology, the relationship describing the reaction of the material to the stresses acting upon it. To anticipate, our goal is to derive an expression for the velocity of the ice as a function of height above the bedrock-ice interface, or the bed of the glacier. The rheology will relate the stresses to the spatial *gradient* of the velocity. We will then have to integrate this expression to obtain the velocity.

In a simple fluid, Newton demonstrated that there is a linear relation between the shear stress acting on a parcel of the fluid and the shear strain rate of that fluid. These are therefore called 'linear' or Newtonian fluids. Although ice is more complicated, we will walk through the

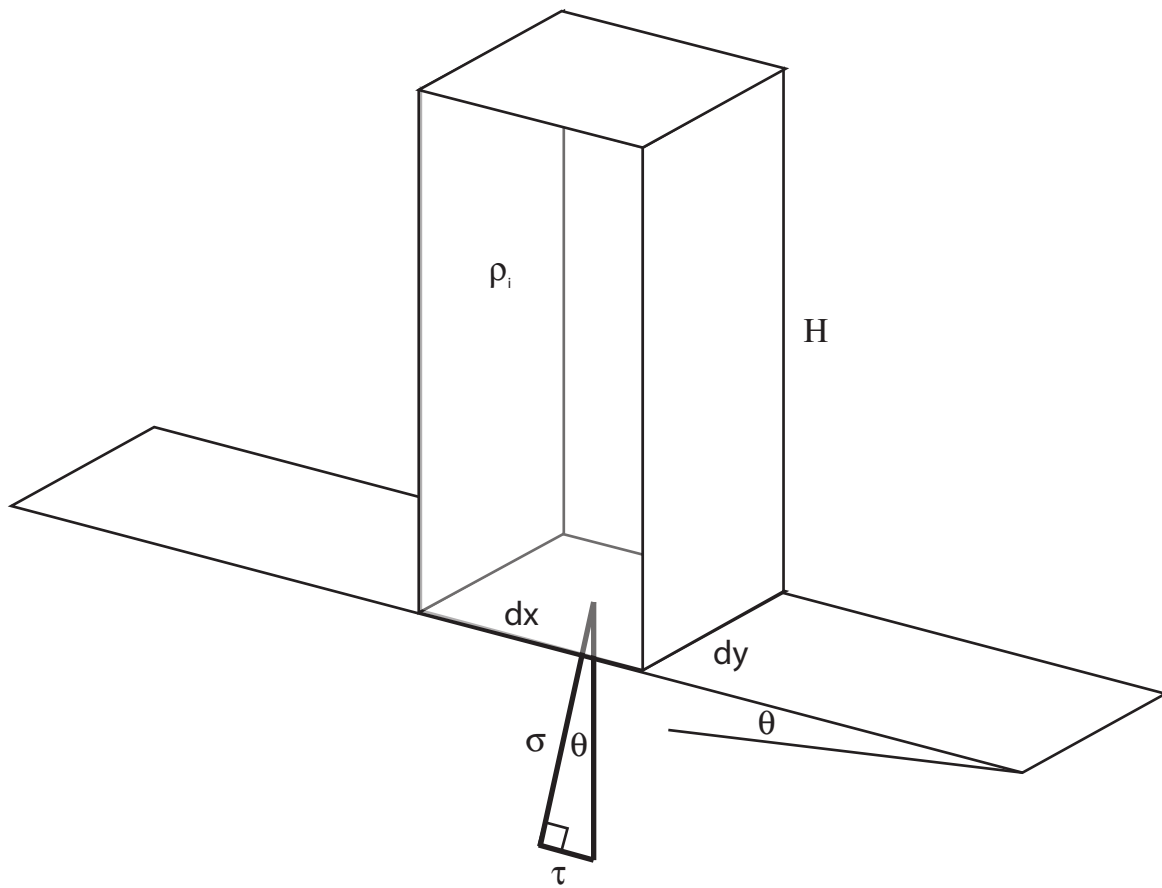


Figure 7.9 Definition of normal and shear stresses imposed by a column of material (here ice) resting on a sloping plane.

derivation using a linear fluid first, and then take the parallel path through the expressions relevant to ice. The problem requires several steps: development of

1. an expression for the pattern of shear stress within the material
2. an expression describing the rheology of the material
3. combination of these to obtain an expression relating the rate of strain to the position within the material
4. integration of the strain rate to obtain the velocity profile.

The pattern of stress. At any level within a column of material resting on a slope, the shear stress is the component of the weight of the overlying material that acts parallel to the bed, divided by the cross-sectional area of the column (Figure 9), while the normal stress is that acting normal to the surface. The weight is of course the mass times the acceleration, here that due to gravity, and the mass is the density times the volume. If we take the density to be uniform with depth in the column, this yields the expression for the shear stress as a function of height above the bed, z :

$$\tau = \rho_i g (H - z) \sin(\theta) \quad (7.4)$$

Here the quantity $H-z$ represents the height of the overlying column of material, which is exerting the stress on the underlying material. Note that we have not yet identified the nature of the material -- i.e., we have not yet specified how the material responds to this stress. This is a general expression for the vertical profile of shear stress within a brick, a column of rock on a slope, or in a fluid like water or lava or ice on a slope. The stress linearly increases with depth into the material (Figure 10), reaching a maximum at the bed. Importantly, the shear stress is said to "vanish" at the surface; nothing magic here, it is simply zero where $z=H$. The shear stress exerted by the overlying column of air is negligible (until we begin worrying about entrainment of small sand and dust particles in the chapter on sediment transport).

The rheology

Now we must address the response of the material to this applied shear stress. This is called the rheology of the material. In the case of a solid or elastic rheology, there is a finite and specific strain of the material that results from an applied stress. Consider a rubber band. You apply a stress to it, a force per unit area of the rubber. The band stretches a certain amount. The strain of the rubber, ϵ , is defined to be the change in length divided by the original length:

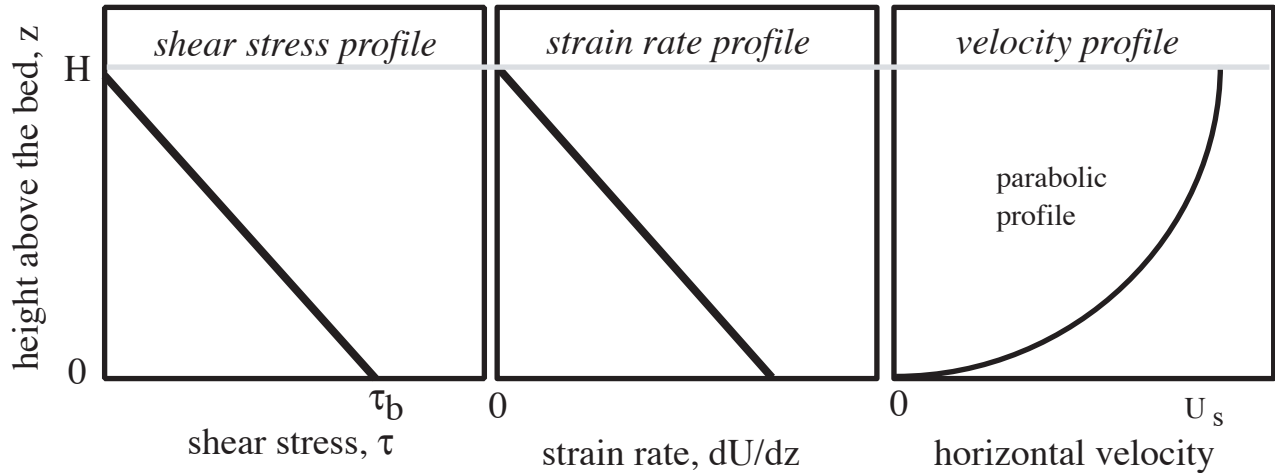
$$\epsilon = \frac{\Delta L}{L_o} \quad (7.5)$$

where L_o is the original length. This is called the linear strain, the strain of the material along a line, the changes of length in the direction of the applied force, here a normal force. Note that strain is dimensionless. In the case of elastic solids, this strain is both finite and reversible: when the force is taken away, the material returns to its original shape. The relationship between the stress and the resulting strain is captured by this simplified rheological statement for an elastic solid:

$$\epsilon = \frac{1}{E} \sigma \quad (7.6)$$

where σ is the applied stress, and E is called Young's modulus. The higher the Young's modulus, the more stress it takes to accomplish a given strain. For completeness, we must recognize that in an elastic material the strain in one dimension is connected to the strain in another direction; the rubber band thins as you stretch it. The material constant that relates strain in one dimension to strain in orthogonal directions is Poisson's ratio, ν .

Linear or Newtonian Fluid



Nonlinear Fluid

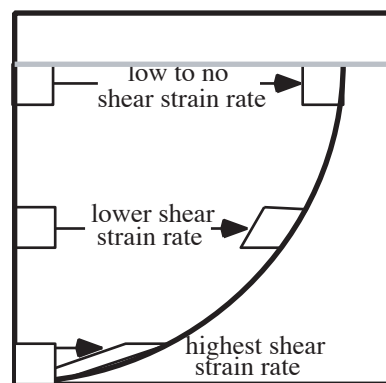
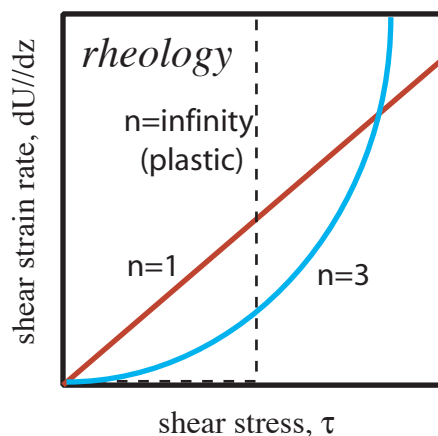
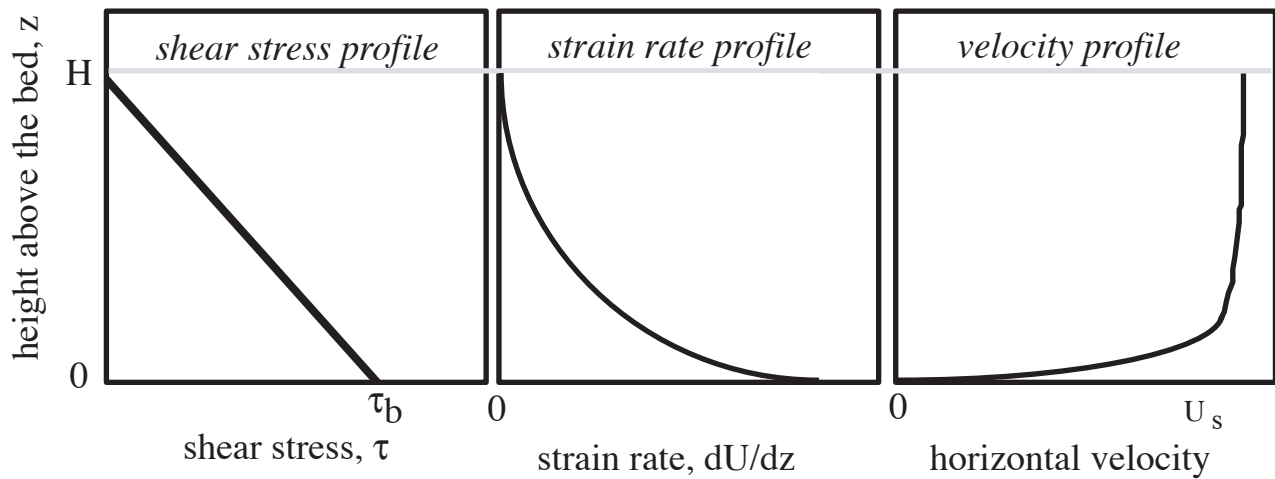


Figure 7.10 Diagrams to aid in the derivation of the velocity profiles in linear fluids (top row) and in nonlinear fluids (second row). In each row the shear stress profile is the same, linearly increasing from 0 at the top of the fluid to the basal shear stress τ_b at the base. The middle box shows the shear deformation rate profile, $dU/dz(z)$, and the third box shows its integral, the velocity profile, $U(z)$. Bottom box shows graphically the shear strain associated with three different levels in the fluid. Recall that shear strain can be measured by the change in angles in a box with originally orthogonal sides.

There is another type of strain, called a shear strain, which results from a shear stress. Rather than changes in length, this is captured as changes in angles. Consider a material on which we have magically scribed a right angle. Shear strain of the material results in changes in this angle. Again, it is dimensionless (radians). Again, a given stress results in a given strain, here a shear stress and a shear strain:

$$\epsilon_{xz} = \frac{1 + \nu}{E} \tau_{xz} \quad (7.7)$$

For further discussion of strains and stresses in elastic materials, see for example Turcotte and Schubert.

Now let us consider a fluid rather than a solid. They differ fundamentally because an applied stress can result in an infinite strain of the material. Imagine a plate on which you pour a bit of molasses. Tip the plate; in so doing you exert a shear stress on the molasses. The molasses keeps moving as long as you keep the plate tilted. There is no specific strain associated with an applied stress, and we cannot therefore use an elastic rheology to describe the behavior. It was noted, however, that one could instead relate a specific *rate* of strain to the applied stress. In the case of a shear stress, the resulting shear strain rate is equivalent to the velocity gradient in the direction of shear (see [Figure 10](#)). In other words, for the case at hand of a fluid on a tipped plate (or bedrock valley floor), the shear stress results in a strain rate that is captured in the gradient of the horizontal velocity with respect to the vertical, dU/dz :

$$\dot{\epsilon}_{xz} = \frac{dU}{dz} = \frac{1}{\mu} \tau_{xz} \quad (7.8)$$

The parameter μ that dictates the scale of the response is called the viscosity of the fluid. This is called variously a Newtonian viscous rheology, or a linear viscous rheology. The shear strain rate is related linearly to the shear stress.

Combining this mathematical representation of a linear viscous fluid with that for the shear stress as a function of depth (the stress profile), we obtain an expression for the shear strain rate at all levels within the fluid ([Figure 10](#)).

$$\frac{dU}{dz} = \frac{\rho_i g \sin(\theta)}{\mu} (H - z) \quad (7.9)$$

Note that the profile of shear strain rate mimics the shear stress profile in that it is zero at the surface of the fluid, and linearly increases to a maximum at the bed. What does this mean for the velocity profile? At the surface, there can be no shear strain rate. Equivalently, the velocity profile must have no slope to it at the surface. The gradient (slope) of the velocity profile then increases linearly toward the bed.

We obtain the velocity itself by integrating the strain rate with respect to z . This is a definite integral, from 0 to some level z in the fluid.

$$U(z) = \frac{\rho_i g \sin(\theta)}{\mu} \left(Hz - \frac{z^2}{2} \right) \quad (7.10)$$

While the contribution due to internal deformation (flow) is indeed zero at the bed, to this must be added any slip along the bed. In most fluids, the “no slip condition” is applied, as molecules within the fluid interact with stationary ones in the bed to bring the velocity smoothly to zero at the bed. Ice, we will see below, is different. First, it can change phase at the bed, and

second, it can slide as a block against the bed. Ignoring this for the moment, the resulting profile of velocity is shown in [Figure 10](#), where you can see that the features we expected are displayed: there is no gradient at the top of the flow, and the highest gradient in the velocity is found at the bed.

Three other quantities are easily extracted from this analysis: the surface velocity, which we would like to have because we can measure it, the average velocity, and the integral of the velocity, which is equivalent to the ice discharge per unit width of the glacier, something we discussed above in our mass balance analysis. The surface velocity is simply $u(H)$, which is

$$U_s = \frac{\rho g H^2 \sin \theta}{2\mu} \quad (7.11)$$

The average velocity can be obtained formally by application of the mean value theorem to the problem:

$$\bar{y} = \frac{1}{b-a} \int_a^b y(x) dx \quad (7.12)$$

In the case at hand, the variable is the velocity, and the limits are 0 and H:

$$\bar{U} = \frac{1}{H-0} \int_0^H U(z) dz. \quad (7.13)$$

We find that the average velocity is

$$\bar{U} = \frac{\rho g H^2 \sin \theta}{3\mu} = \frac{2}{3} U_s, \quad (7.14)$$

or 2/3 of the surface velocity. Note on the graph of velocity vs. depth ([Figure 10](#)) where this mean velocity would be encountered in the profile. It is closer to the bed than to the surface, and is in fact at about 6/10 of the way to the bed from the surface.

The integral of the velocity, or the discharge per unit width of flow, is the product of the mean velocity and the flow depth, and is therefore

$$Q = \bar{U} H = \frac{\rho g H^3 \sin \theta}{3\mu}. \quad (7.15)$$

Note the strong (cubic) dependence on the depth of the flow.

Ice wrinkles: 1. Glenn's flow law

While the equations derived above illustrate the approach one takes to flow problems in general, they are not appropriate for ice. Ice differs from many fluids in that the relationship between the shear stress and the strain rate (the rheology) is not linear. Instead, the rheology is roughly cubic ([Figure 10](#)). Ice is therefore said to have a non-linear rheology. [[Historical note here on Glenn's flow experiments](#)] Below we trace back through the steps in the derivation of the flow profile, and redo the analysis appropriate for the ice deformation rate profile. This generates the second row of diagrams in [Figure 10](#). A more general rheological relation can be written

$$\frac{dU}{dz} = A \tau^n = [A \tau^{n-1}] \tau \quad (7.16)$$

where n is an exponent that one needs to determine experimentally, and the constant A is called the “flow law parameter”. We have already dealt with the linear ($n=1$) case. Glenn’s experiments revealed that n is approximately 3. The term in brackets represents the inverse of an

effective viscosity: $\frac{1}{[A\tau^{n-1}]}$. This expression implies that as the shear stress increases, the

effective viscosity declines, and radically so for all $n > 1$. The consequence is that ice near the bed (under high shear stress) behaves as if it is much less stiff than ice near the surface. We can now again combine this formula for the relationship between the shear strain rate and the shear stress (the rheology) with that for shear stress profile to obtain the profile of shear strain rate:

$$\frac{dU}{dz} = A[\rho_i g \sin(\theta)]^3 (H - z)^3 \quad (7.17)$$

This may then be integrated to yield the velocity profile:

$$U(z) = A[\rho_i g \sin(\theta)]^3 \left[H^3 z - \frac{3z^2 H}{2} + z^3 H - \frac{z^4}{4} \right] \quad (7.18)$$

The resulting velocity profile is significantly different from that for the linear rheology case (Figure 10 and 11). In particular, much more of the change in speed of the ice with distance from the bed is accomplished very near the bed. The flow looks much more 'plug-like'.

Again, we can obtain the surface speed by evaluation of the velocity at $z=H$

$$U(H) = U_s = A[\rho_i g \sin(\theta)]^3 \left[\frac{H^4}{4} \right] \quad (7.19)$$

The specific discharge of ice is obtained by integrating the profile from 0 to H :

$$Q = A[\rho_i g \sin(\theta)]^3 \left[\frac{H^5}{5} \right] \quad (7.20)$$

and the average speed is obtained by using the mean value theorem, or by recognizing that the average speed is simply Q/H :

$$\bar{U} = A[\rho_i g \sin(\theta)]^3 \left[\frac{H^4}{5} \right] \quad (7.21)$$

(Figure 11). Note that this average speed is related to the mean speed through

$$\bar{U} = \frac{4}{5} U_s = \frac{n+1}{n+2} U_s \quad (7.22)$$

As the nonlinearity of the flow law, expressed by n , increases, the mean speed approaches the surface speed. The flow profiles for $n=1$ and $n=3$ cases are compared in Figure 11, in which we also show the mean speeds. That the velocities are normalized to the maximum speed (that at the surface, U_s), makes it straightforward to see the how the mean speed relates to the maximum in both cases. As n increases, the maximum speed becomes a better proxy for the mean speed, and the maximum speed could be measured more and more close to the bed.

Note that in the formulations above, we have assumed that the flow law parameter, A , is uniform with depth. While this is a good approximation in temperate glaciers, in which the temperatures are close to the pressure melting point throughout, the assumption breaks down badly in polar glaciers. Both experiments and theory show that the flow law parameter is very sensitive to temperate:

$$A = f(T) = A_o e^{-\frac{E_a}{RT}} \quad (7.23)$$

where A_o is a reference flow law parameter, E_a is the activation energy, R is the universal gas constant, and T_k is the absolute temperature. As the temperature decreases, the argument of the exponential factor becomes more negative and A declines. Since the effective viscosity goes as $1/A$, the viscosity therefore increases. (For discussion see Turcotte and Schubert, chapter 7.) Using the values of activation energy for ice (61×10^3 J/mole) and the universal gas constant (8.31

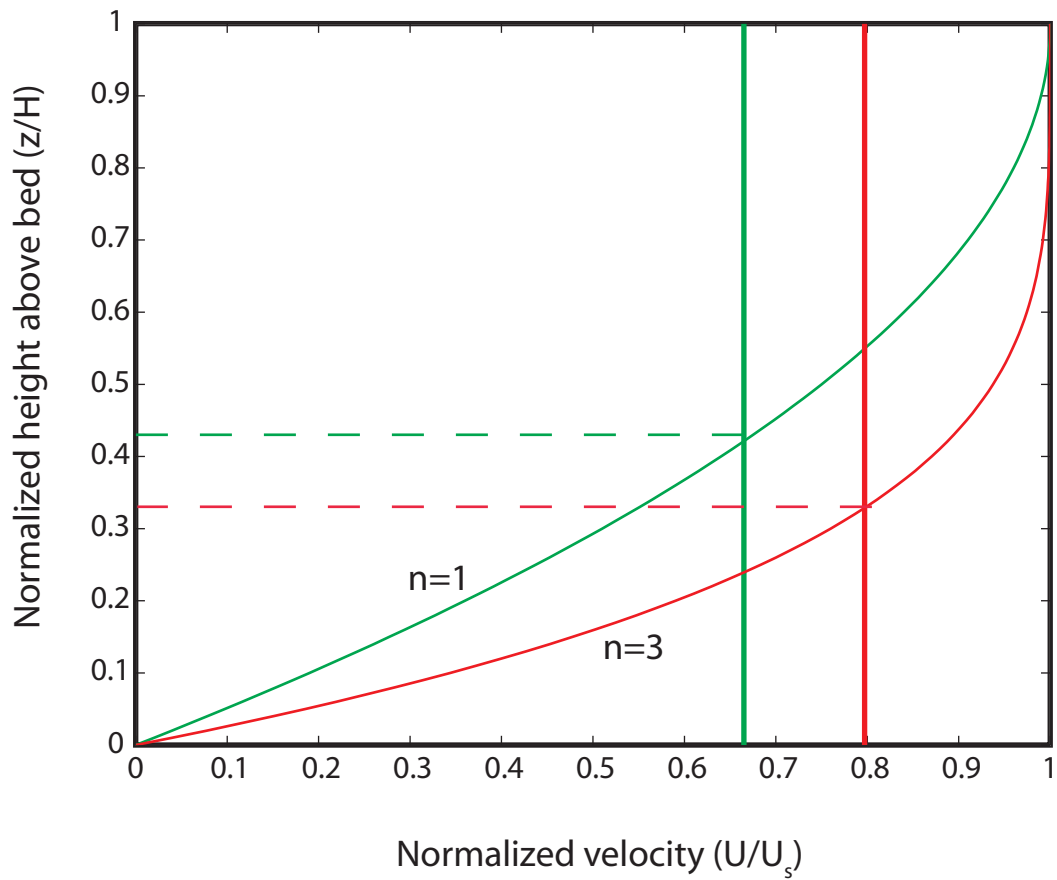


Figure 7.11 Flow profiles for $n=1$ (green) and $n=3$ (red) fluids, normalized against maximum height above bed and maximum flow speed. The mean speed is shown as the vertical lines, and the position above the bed at which this mean speed would be measured is signified by the dashed horizontal lines. As the nonlinearity of the rheology increases, the mean speed approaches the surface speed, and the depth at which it would be measured is found nearer the bed.

J/mole-°K), the flow law parameter and hence the effective viscosity are expected to vary over 4 orders of magnitude in the temperature range relevant for Earth's glaciers and ice sheets (Figure 12). Let's think about the implications for the shape of the velocity profile. As temperature decreases with height above the bed, z , the flow law parameter will decrease rapidly. The ice effectively stiffens with height above the bed. This reduces the rate of strain, or the velocity gradient, and the flow profile should look even more plug-like than in the uniform temperature case. This extreme sensitivity of the rheology to temperature requires that the modeling of ice sheets must incorporate the evolution of the temperature field. Such models are said to require thermo-mechanical coupling.

Ice wrinkles 2. Sliding/Regelation

While the physics of internal deformation is interesting and can accomplish the translation of large masses of ice down valleys, some large segment of the glacier population has yet another trick to allow transport of ice down valleys. If the ice near the bed of the glacier is near the melting point, the ice can actually slide across the bed. As it is only by this mechanism that the bed of the glacier can be modified by the motion of ice above it, it is sliding that is the focus of glacial geologic studies.

The mechanism of sliding of the ice is allowed by this special property of water: high pressure promotes melting. A corollary to this is that the high pressure phase of water is ice, its solid phase. This makes ice very different from, say quartz or olivene, whose melted liquid state is lighter than its solid, and for which higher pressure therefore promotes the change of phase from the solid to the liquid. This can be seen in the phase diagram for the water system (Figure 13). The negative slope (of $-0.0074^\circ\text{C}/\text{bar}$) on the P-T plot, separating the water and ice phases, is what differentiates water from most other substances. Now how does this help a glacier slide on its bed?

Consider the conditions at the bed of a temperate glacier, which by definition is at its freezing point throughout (meaning at all points the temperature lies along the phase boundary, declining at $0.0074^\circ\text{C}/11\text{m}$ of depth) (Figure 13). The glacier rests on a sloping valley floor that is not perfectly smooth, but has bumps and swales in it. I think we would all agree that the ice is not accelerating (changing its velocity) very much. If it is doing so, it is doing so very slowly, meaning that the accelerations are very slight. This means, through Newton's law $F = ma$, that the forces on the ice are essentially balanced. There is also heat arriving at the base of the glacier from cooling of the earth, at a rate sufficient to melt about 5 cm of ice per year. Not much melt, but given that the ice is already at the pressure melting point, there ought to be a thin layer of water present at the bed. You might think this would make it pretty slippery. For a slab of ice dx long in the downvalley direction, the force promoting down-valley motion is the down-valley component of the weight of the ice, or $dx\rho g H\sin(\theta)$. What is resisting this ... especially if there is a thin layer of water there, which is very weak in shear? Given that the shear resistance is therefore nearly zero, the forces resisting the down-valley motion of the ice are those associated with pressures fluctuations associated with the bumps in the bed. In order to prevent acceleration of the ice, there must be a net component of the normal stress that is directly up-glacier. There must therefore be higher pressures on the up-valley sides of bumps than on the down-valley sides of bumps. Of course in the direction normal to the mean bed, the pressure must be that exerted by the normal component of the ice weight, or $dx\rho g H\cos(\theta)$.

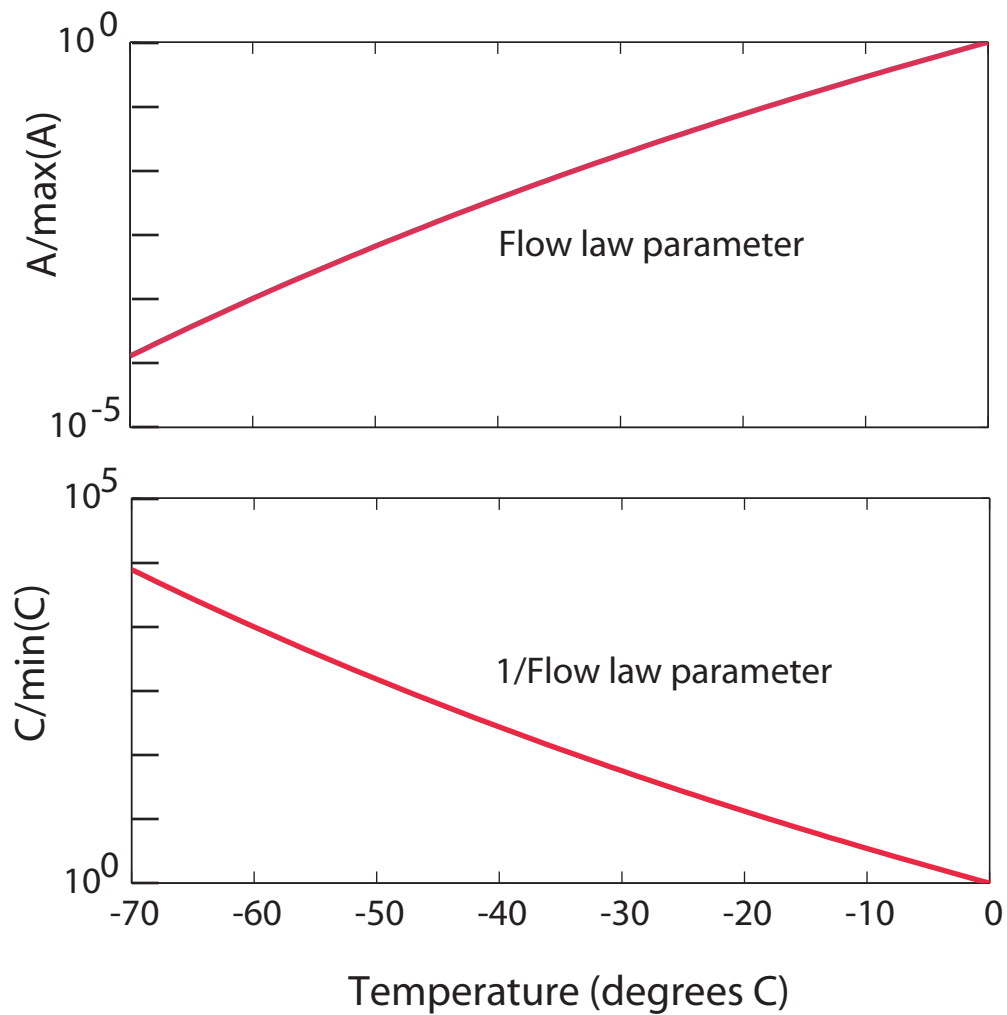


Figure 7.12. Dependence of flow law parameter on temperature. A) flow law parameter, A , and B) inverse of flow law parameter, which scales the effective viscosity. Vertical axes are normalized to their values at the pressure melting point. Noting the log vertical axis, the effective viscosity will rise by 4 orders of magnitude over the 70 degree range depicted.

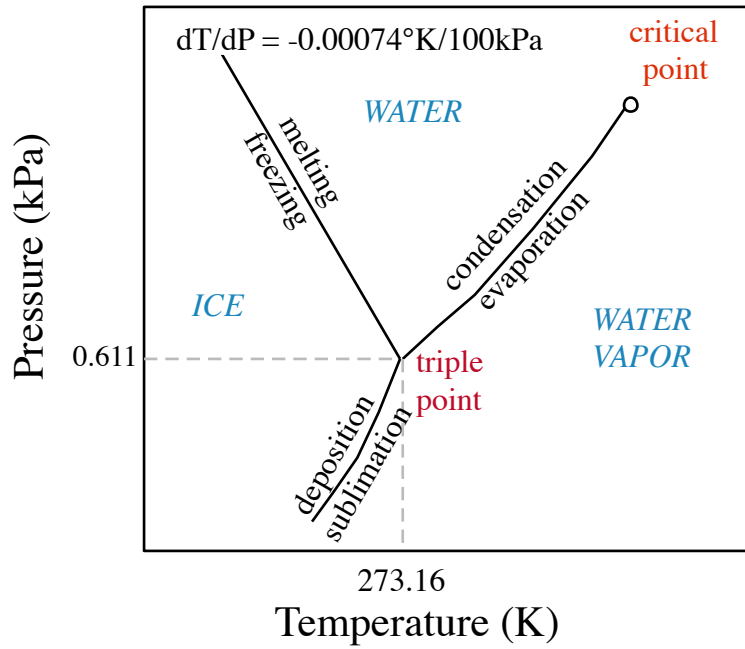


Figure 7.13 Phase diagram $P(T^{\circ})$ for the molecule H_2O . Note the negative slope of the melting curve separating water and ice. This allows melting, favoring the higher density phase, when pressure is increased, and is at the root of the regelation process. (after Locke, 19xx)

But if the pressure fluctuates about some mean, say that of the pressure melting point of ice, then increasing the pressure a smidge on the up-valley side of a bump will promote melting of the ice, and decreasing it a smidge on the back of the bump will promote freezing of water. This must happen given the phase diagram of the H₂O system. In fact, the water film so generated on the up-valley side of the bumps is forced into motion for the very same reason: liquid water responds to pressure gradients by flowing from high pressures toward low pressures. Putting the two stories together, we find that that a parcel of basal ice performs something of a magic act to get past bumps in the bed. The ice melts on the up-valley sides of bumps, flows around the bump as a thin water film, and refreezes on the low pressure downvalley sides of the bump. This process is called regelation, for “refreezing” in French.

This regelation process is most effective in moving ice past small-scale bumps in the bed. Why might that be? At issue is the energy part of the story, the heat pump involved in the process. Recall the energetic nature of a phase change. Melting of water consumes energy, and refreezing of water releases energy, the same amount per unit volume of ice. That’s nice, as no net energy must be added to the system. The problem is that the site where energy is needed to melt ice is different from where it is released upon refreezing. They are separated by the length of the bump. This heat energy must be transported through the bump by conduction (Figure 14). Recall that heat conduction is dictated by the temperature gradient, which in turn is the temperature difference between the two sites, divided by the distance between them. Therefore the closer the sites, or the smaller wavelength the bump, the more efficient the process.

It turns out that very large bumps can be circumvented by another process that makes them easy to get around as well. For long wavelength bumps, only a small-scale perturbation of the flow field in the ice itself is required to get past the bump (Figure 15), meaning that the ice does not have to perform the magic act of regelation to get by the bump. This leaves intermediate sized bumps, with wavelengths of around 0.5-1 meter, as the hardest bumps for the basal ice to move past. These are called the “controlling wavelengths” for the basal sliding process. We will see that these details of the sliding process are strongly reflected in the patterns of erosion at the bed of a temperate glacier.

Direct evidence for the existence of this thin film of subglacial water, and the operation of the regelation mechanism, comes from several sources. One of the more striking is to be found on limestone bedrock, where the susceptibility of the calcite to solution allows the subglacial water system to be read in great detail. One sees on the upslope sides of small bumps little dissolution pits, and on the down-glacier sides precipitates. In fact, the precipitates take the form of small stalactites that grow almost horizontally, anchored to the downslope sides of the bumps (see photo in Figure 16). This pattern of solution and re-precipitation is argued to represent the solution of calcite by the very pure water film, and its expulsion from solution as the water refreezes on the downslope side of the bump. How thick is the water film? It is thought to be only microns thick. The ice produced by the regelation process is distinct in at least two senses from that produced originally from snow. It has a strong isotopic signature associated with fractionation that occurs upon both melting and refreezing. And it is largely bubble-free. Recall that typical glacial ice is bubbly; air originally trapped in the ice as it metamorphoses from firn to more and more dense ice. The bubbles give rise to the white color of the ice. In the regelation process, the air in the bubbles is allowed to escape upon melting on the stoss sides of bumps, and is not incorporated into the regelation ice in the lee of the bumps. Thus basal ice can take on a

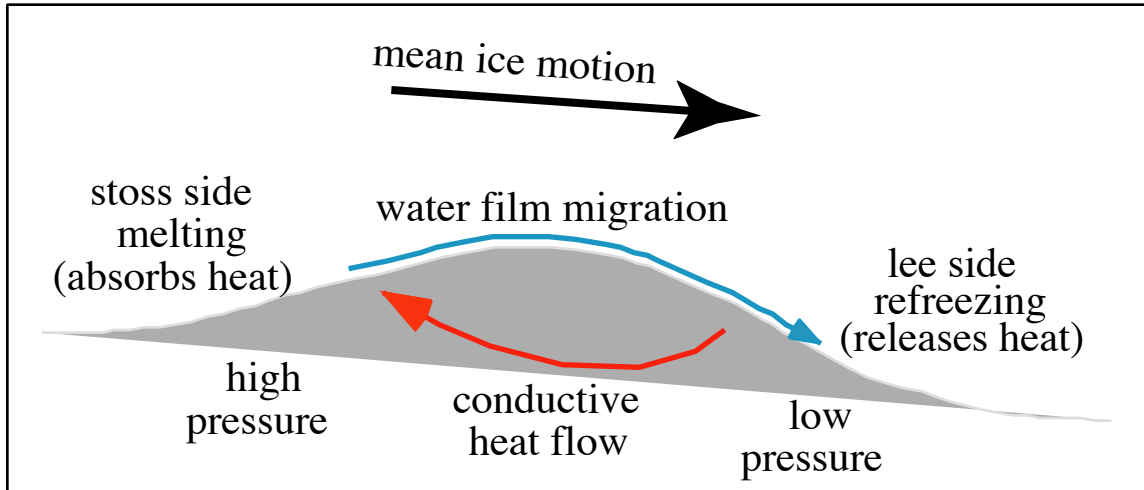


Figure 7.14 Schematic diagram of the regelation process by which temperate glaciers move around small bumps on the glacier bed. ice melts on the high pressure (stoss) side of the bump, moves around it as a thin water film, and refreezes in the low pressure shadow on the lee side. The heat released by the refreezing is conducted back through the bump to be used in the melting process. It is therefore an excellent case of coupling between thermal and fluid mechanics problems.

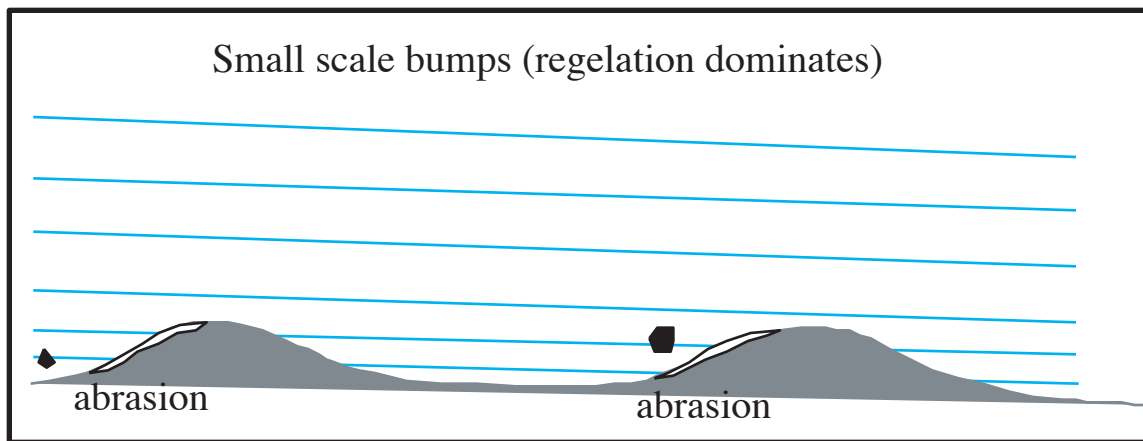
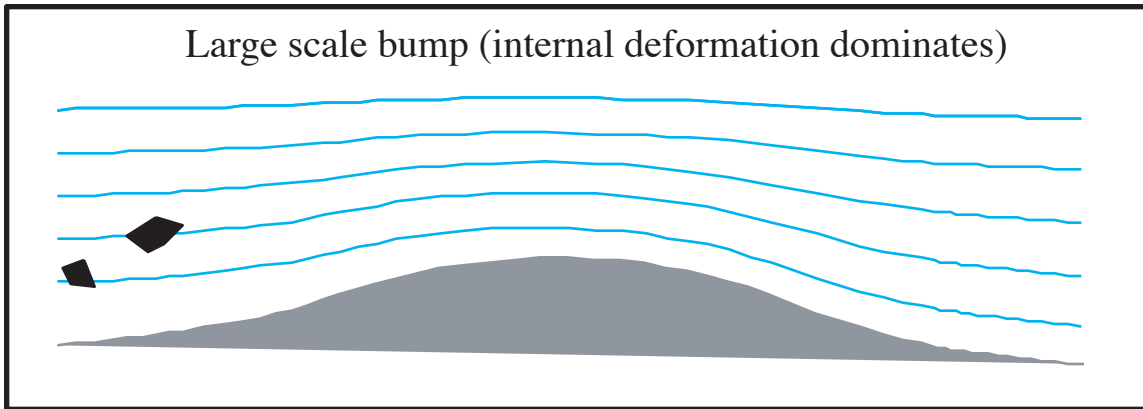


Figure 7.15 b) Trajectories of clasts embeded in basal ice as it encounters big (top) and little (bottom) bumps in the bed. Ice can deform sufficiently to accommodate the larger bumps, allowing clasts in the ice to ride over the bumps. In the small-bump case, the ice trajectories intersect the bed, reflecting the regelation mechanism. Clasts in the ice will be brought forcefully into contact with the bed, and cause abrasion of the front sides (stoss) of these bumps, leading to their elimination.



Figure 7.16 Details of the recently deglaciated bed of Blackfoot Glacier, Montana. Top: view downglacier. Bumps in the bed localized by argillitic partings in the limestone bedrock show dissolutional roughening on the stoss (upvalley) sides, and reprecipitation of calcite (white) in the lee. Bottom: detail of the subglacially precipitated calcite, glacier flow top to bottom.

beautifully complex blue and white streaked look, clear blue in the regelation ice and white due to bubbles in the original ice.

Concurrent measurement of glacier sliding and of local water pressure in the glacier has led to the hypothesis that sliding is promoted by high water pressures. This is captured in the expression

$$U_{slide} = c \frac{\tau_b^p}{\{P_i - P_w\}^q}. \quad (7.24)$$

where c is a constant that serves to scale the sliding speed, and p and q determine the sensitivity of the sliding to basal stress and to effective stress, respectively. The expression in the denominator, the difference between the normal stress exerted by the ice overburden ($\rho_i g H$) and the local water pressure, P_w , is called the effective stress. As the water pressure approaches that of the ice overburden, the effective stress goes to zero and sliding ought to become very rapid (infinite, if we take it to the limit of zero effective pressure). This state we also call the flotation condition: the full pressure of the column of ice overhead is being supported by the water pressure. Given the density difference between water and ice, this would correspond to a water table in the glacier at a height of ρ_i/ρ_w or roughly 9/10 of the ice thickness.

While the details of the relationship between water pressure and sliding rate are the target of modern glacial research, it is clear enough that there is some sort of relationship that we must address what sets the water pressures at the bed. These are very difficult to measure in the field, as they require drilling holes in the glacier that connect to the water system at the bed. When this is done, the pressures vary considerably both in time and in space. The bottom line, however, is that the glacial hydrologic system evolves anew every year (see review in Walder and Fountain, 19xx). This system is complex, and consists of several interacting elements (Figure 17). Water is generated at the glacier surface by melt. This percolates into the snow and/or runs off on the ice surface to find a conduit that takes it into the subsurface. This often consists of a moulin (a vertical hollow shaft) or the base of a crevasse. At the bed, the hydrologic system consists of 3 elements: a thin film of water at the ice-bedrock interface we have already talked about, a set of cavities in the lee of bumps in the bed, and conduits or tunnels. These large-scale elements close down significantly in the winter when the melt water input is turned off, as the water drains out of the system leaving cavities and tunnels as voids that collapse by viscous closure of the ice. They must therefore be born anew each melt season. This is what makes the glacial hydrologic system so interesting, and it is intimately related to the seasonal cycle of sliding that is now well-documented. As the melt season begins, water that makes its way toward the bed does not have an efficient set of conduits through which to drain. It therefore backs up in the glacier, raising the water table and therefore pressurizing the subglacial system as the column of water piles up. This allows sliding to begin, which in turn opens up cavities in the lee of bumps. Nearest the terminus, a tunnel system begins to grow, forced open by the high water pressures driving a high water pressure gradient toward the terminus. As water flows through this nascent system, it widens due to frictional dissipation of heat, winning against the tendency of the ice to move toward the conduit. The lower pressure conduit is therefore inserted into the glacier from the terminus upglacier. As it reaches a particular location, it serves as a low pressure boundary condition for the adjacent cavities, and can serve to bleed the water out of cavities, which in turn lowers the water pressure in the local glacier. As the conduit system elongates, it therefore bleeds off the pressures that were sustaining the sliding of the glacier, and terminates the sliding event. In the meanwhile, the water delivery to the exit stream grows until it can accommodate the rate of water input from the glacier surface. This basic explanation of the “spring sliding

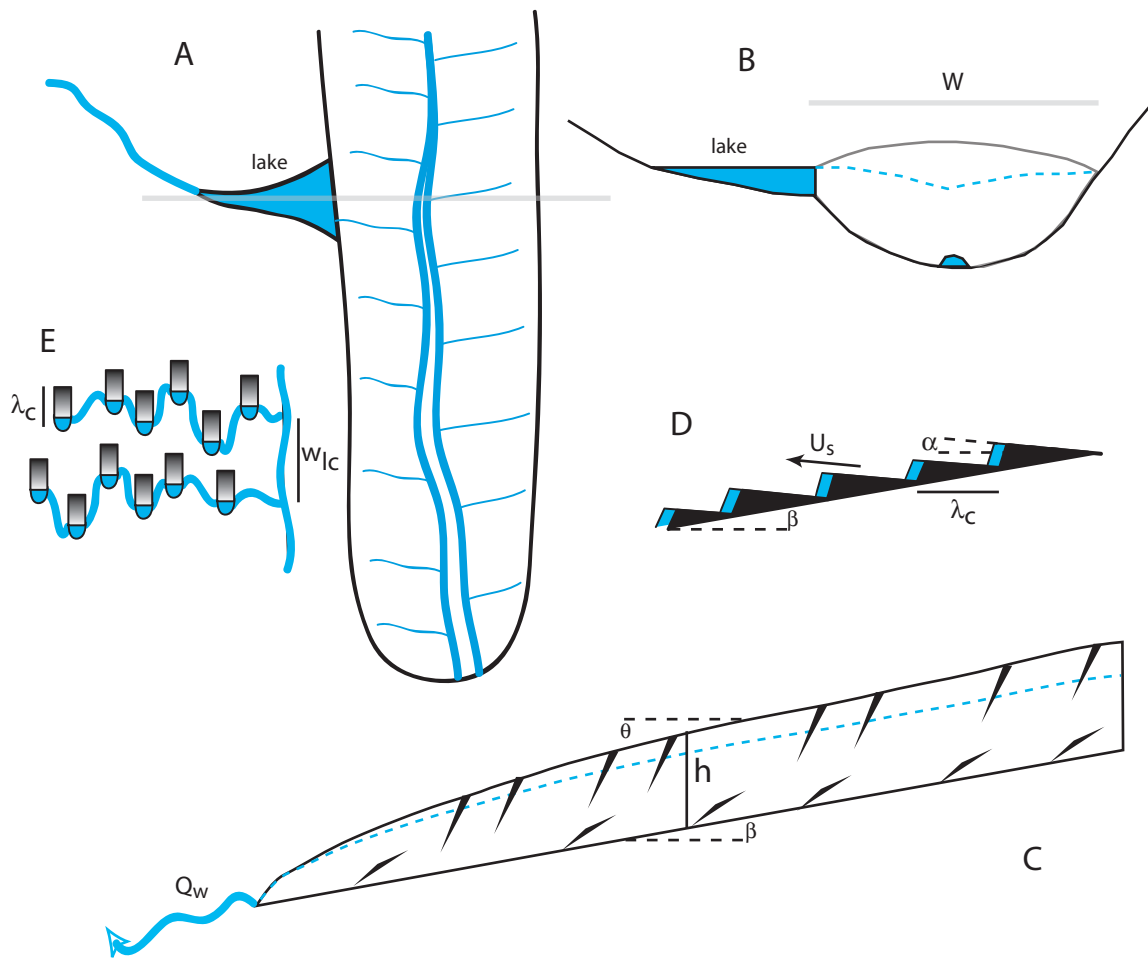


Figure 7.17. Sketch of the hydrological system in a glacier. A) Map view showing subglacial tunnel system and tributaries to it that are in turn connect sets of cavities in the lee of bumps (shown in plan view in E and in cross-section in D). B) Cross-valley profile through the glacier at the location of a side-glacier lake ponded by the ice, showing subglacial tunnel and a hypothetical water table (dashed). C) Long-valley cross-section of the glacier showing crevasses and the water table, with water discharging in the exit stream. (after Kessler and Anderson, 2005, Fig. 1)

events” has been modeled as well, and shows the up-glacier evolution of the system (see Kessler and Anderson 2005).

Recent work on small to medium alpine glaciers has begun to utilize GPS measurements to document surface motion history of a glacier through a melt season (Figure 18). While the uplift of glaciers during these speedup events has led to models of enhanced sliding over upglacier tilted blocks in the bed for some time, these new measurements in concert with records of stream discharge coalesce into a coherent model of alpine glacier sliding mechanics. [also discussion and Figure xx from work on Kennicott glacier]

Simulations of alpine glaciers are now being performed in 2 planview dimensions (e.g., Kessler et al. on Kings canyon 2005; Plummer and Phillips on Bishop creek glaciers, California). This allows modeling of glaciers on real-world topographies represented by DEMs, on which one may explore the proper characterization of the climate required to generate glaciers that extend to LGM positions documented by end-moraine, the effects of radiation input to the glacier surface, and so on. [figure xx]

Paleo-climate estimates from glacial valleys. Now that we know something about how glaciers work, let us use this knowledge to address questions of past glaciers. One of the goals of glacial geology is to estimate the past footprints of glaciers, and from them determine the past climate needed to produce glaciers of that size. It is often assumed that the mean annual 0°C isotherm roughly coincides with the ELA. Above it the temperatures are too cold to melt all the snow that arrives, and vice versa below it. If one assumes that the temperature structure of the atmosphere obeys a lapse rate of say 6.5°C/km or 0.065°C/m, then the depression of the ELA in meters can be translated into a cooling of the climate in °C. But how do we find the paleo-ELA? We use two methods (Figure 19). First, we note that the upvalley ends of lateral moraines correspond to the ELA. If these can be located in a particular valley, then, one can estimate the paleo-ELA from the upvalley elevation of their ends. We will discuss further these moraines in the end of the chapter. The second method utilizes an empirical relationship of the mapview of modern glaciers: the accumulation area is roughly 65% of the total area of the glacier. The accumulation area ratio (AAR=accumulation area/total area) is therefore 0.65. If this holds true for glaciers in the past, and one can map the footprint of the past glacier using its terminal moraine, then one can determine at what elevation a contour would enclose an accumulation area of 65% of this. This method is more commonly used than is that based upon lateral moraines because terminal moraines are more likely to remain visible than are the upper ends of lateral moraines. We have already seen in Figure 2 how this has been used to estimate the ELA lowering during the LGM. In many ranges such estimates suggest a lowering of order many hundred meters, from which climatic cooling is estimated to have been 6-10°C. While this is valuable information, we note several weaknesses in the method: AARs vary from 0.6 – 0.8 on modern glaciers, past lapse rates are not necessarily equivalent to those of today, and glacial health is dictated not solely by temperatures, but by rates and patterns of snowfall that can vary with climate as well.

Icesheet profiles

Ice sheets are always steepest at their outer margins, and decline in surface slope toward their centers. Why is this? The argument goes as follows. An interesting manifestation of the nonlinearity of ice rheology captured in Glenn’s flow law is that one may treat ice to first order

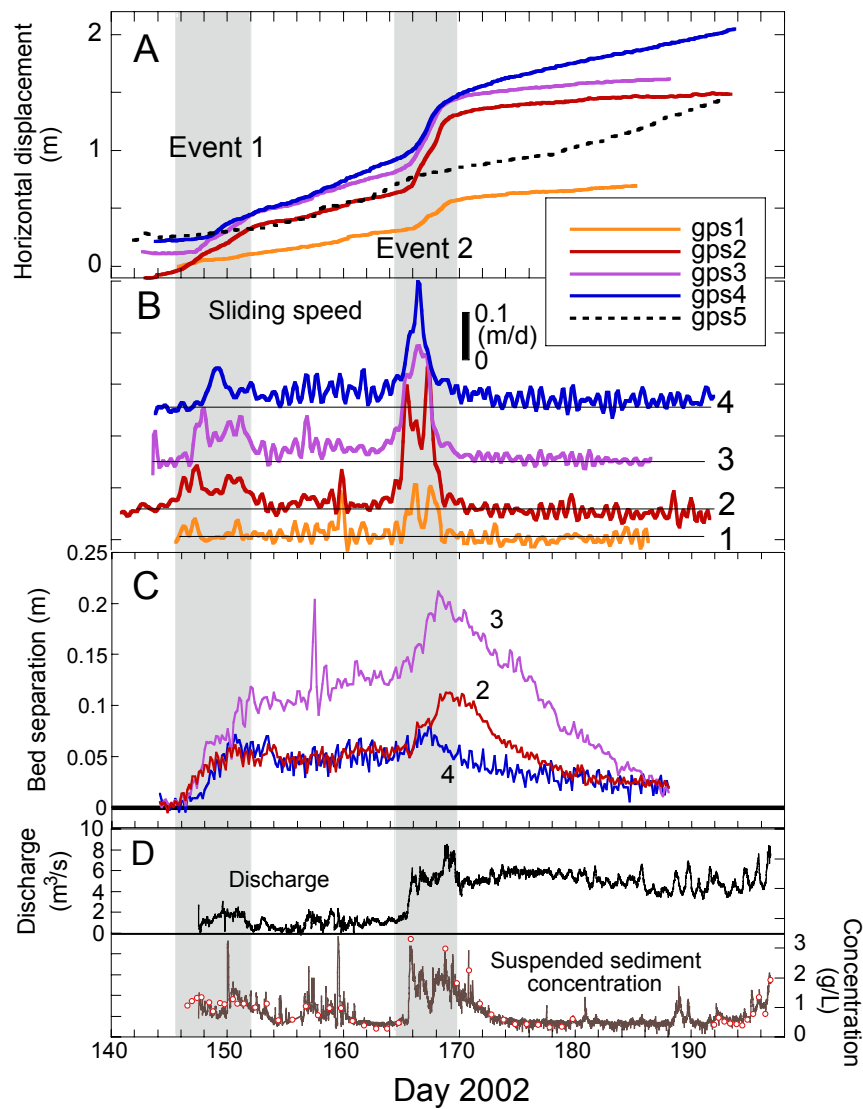


Figure 18. The record of surface motion of 5 GPS monuments on the surface of 100-180 m thick Bench Glacier, Alaska (A), their speeds (B), the uplift of the surface not attributable to surface-parallel motion (C), and both the discharge and the suspended sediment concentration of the exit stream (D). Acceleration associated with increases in sliding occurred in two events separated by 2 weeks of roughly steady sliding. The termination of the 2nd event coincides with a major increase in stream discharge, interpreted to reflect completion of the subglacial conduit that bleeds high pressures from the glacier bed. Uplift of the surface reflects block sliding up stoss slopes of bumps in the bed, and collapse of the resulting cavities after termination of sliding. (after Anderson et al., 2004, Figure 7).

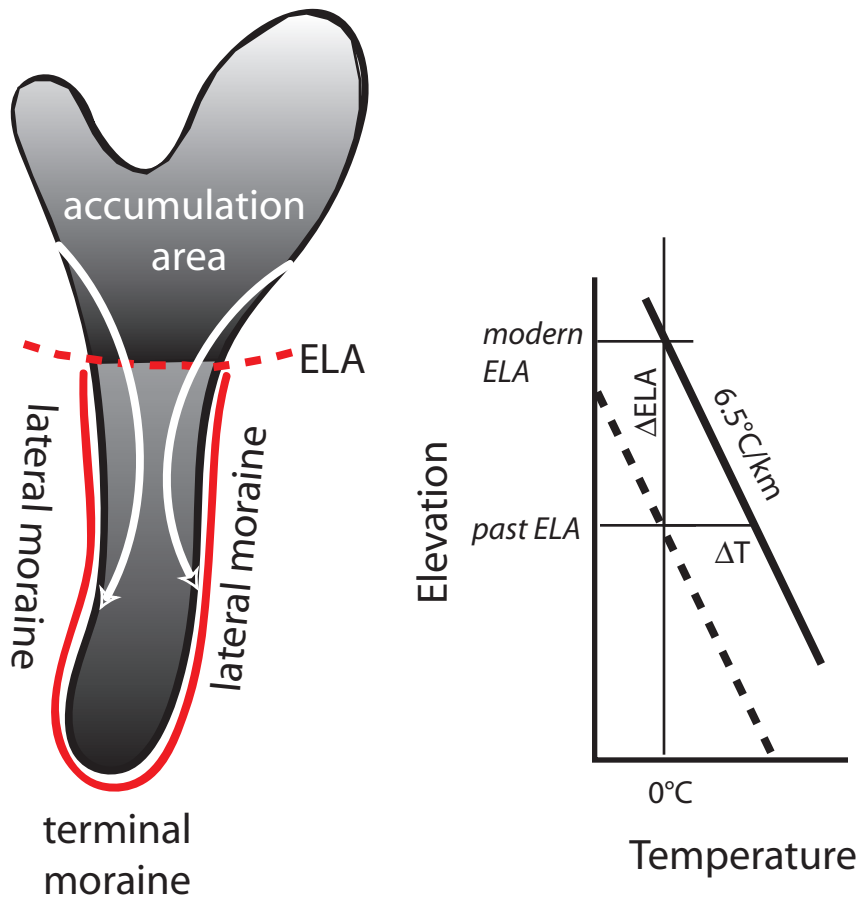


Figure 7.19. Methods for estimating paleo-ELAs are based upon the features of glaciers illustrated. Up-valley ends of lateral moraines coincide with the ELA on a glacier because the trajectories of blocks falling onto the ice are as shown in white arrows: they move toward the glacier center in the accumulation area, and outward to the edge in the ablation zone, responding to the local slopes of the glacier. Typical AARs, ratios of accumulation area to total area of a glacier, are 0.65. If the paleo-area of a past glacier can be measured using terminal moraines, the AAR can be estimated using this AAR. Translation of the change in ELA into an estimate of change in mean annual temperature is based upon application of an assumed lapse rate shown in the figure at the right.

as a plastic substance. A plastic material is one in which there is no deformation up to some 'yield' stress, beyond which there is an infinite ability to flow. It has no strength beyond this limit. On a rheological plot, this looks like the broken line in [Figure 10](#). As you can see from this plot, a nonlinear substance with a power $\gg 1$ approaches the behavior of the plastic substance. If a glacier were plastic, there must be no place within it that falls above this failure envelope.

Now consider the ice sheet profile sketched in [Figure 20](#). At some point on the bed, the shear stress is $\rho_i g H \sin(\theta)$. If the substance is plastic, and this shear stress is above the yield strength, then infinite strain rates would occur and the ice at the bed would rapidly move, thinning the ice there. This thinning would continue until the shear stress diminished below the yield strength. The argument is therefore that the ice sheet maintains a shape at which the shear stress at the base of the sheet is exactly the yield strength for ice. All we need to know is what this value is, and the handy number to carry in your head is: 1 bar, or, in the mks system, 10^5 pascal. Conceptually, then, given that the shear stress involves the product of surface slope and ice thickness, near the edge of the ice sheet the slope must be high in order to reach the yield stress, and as the ice thickens toward the center the surface slope must decline. We can cast this a little more mathematically. Let's consider an ice sheet on a flat continental surface. All we need is shear stress = constant:

$$\rho_i g H \sin \theta = C \quad (7.24)$$

Given that the surface slope can be expressed as dH/dx , where H is the thickness of the ice, we can separate the variable H , yielding the ordinary differential equation:

$$H dH = \frac{C}{\rho_i g} dx \quad (7.25)$$

This can be solved by integrating both sides

$$H^2 = \frac{2C}{\rho_i g} x$$

or

$$(7.26)$$

$$H = \sqrt{\frac{2C}{\rho_i g} x}$$

The shape of the profile should be a very specific one, obeying a square root law. There are several things we can do with this relationship. If we have an ice sheet to measure, given that we know the density of ice, the acceleration due to gravity, and can measure both H and x , we can deduce the best-fitting value of C , the yield strength of ice. We show in [Figure 20](#) the shape of the present day ice sheet in Antarctica. The simple model we have just described is shown as one of the lines on the plot. While the fit is not great, only slight modification of the theory is required to accommodate the data very well.

Another use of this simple analysis is reconstruction of past ice sheet thickness profiles. For this reconstruction problem, all we know is the outline of the ice sheet, derived from say the map view pattern of terminal moraines. Using the yield strength derived from present day ice sheets in the above exercise, we can reconstruct how thick the ice must have been as a function of distance from the margin.

Note that we have made many simplifying assumptions in the above analysis, including the characterization of the rheology as a simple plastic. More detailed reconstructions of ice sheets take into account better representations of the nonlinear (Glenn's flow law) rheology, and must

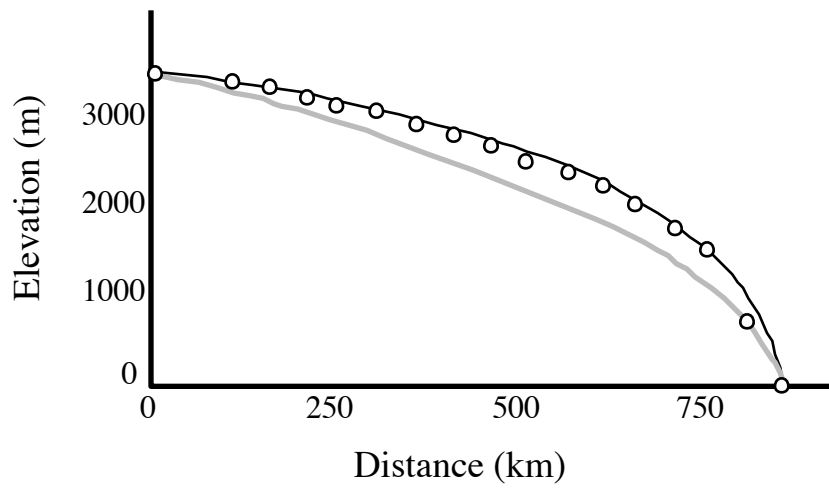


Figure 7.20 Profile of the Antarctic ice Sheet from Mirny (circles), along with theoretical profiles: parabola (gray line) and curve that incorporates a uniform accumulation rate (black line). (after Paterson, after Vialov, 1958)

also handle the thermal problem that dictates where an ice sheet is frozen to its bed (behaving as a polar glacier), and where it is temperate, and therefore can slide.

Surging glaciers and the stability of ice sheets

We have focused so far on glaciers that will likely look the same this year as the next. Exceptions to this rule are the surging glaciers, whose surface speeds can increase by orders of magnitude during a surge phase. Surges of valley glaciers may last one or two years, and be separated by decades to centuries. Surging glaciers generate beautifully looped medial moraines, making the glacier tongue look more like a marbled cake than a glacier (see [photo in Figure 21](#)). A surge also leaves the glacier with a chaos of crevasses that should be avoided at all costs as a climbing route. And on a larger scale, ice streams in Antarctica bear some resemblance to surging glaciers surrounded by non-surging ice. Understanding surge behavior, therefore, has been a highly sought after prize within the glacial community.

What is our current understanding of surges? Our understanding comes largely from the intense and long-lasting study of the 25-km long Variegated Glacier near Yakutat, in coastal southeast Alaska ([Figure 21](#)). This glacier was apparently in surge when photographed in 1905, again in the 20s, then the 40s, was well documented by a pair of air photos in 1964 and 1965. The apparently ~20 year interval between surges suggested that the next surge might happen in the mid-80s, and a study was initiated in the late 1970's with the intent to characterize a glacier as it approached its surge, and then to document well the behavior during the surge. Several teams from at least 4 institutions poked and prodded and photographed and surveyed the glacier as it approached its surge, which culminated in a two-phase period of rapid motion in 1982 and 1983.

The surge itself can be characterized as a wave of rapid motion that translates through the glacier. At the front of the wave the glacier might be moving at 0.1-0.3 m/day, while in the middle of the high velocity region it might be moving at 60 m/day ([Figure 22](#)). This wave of high velocity translates at yet higher velocities (several times 60 m/day). The crevasse patterns result from the pattern of velocities. At the leading edge of the wave, the ice is in extreme compression, to which it responds by thickening, by thrust faulting, and by folding, in a dramatic analog to the structural geologic evolution one might expect in convergent tectonics. It thickens so much more in the center of the ice than at the edges that it actually fails in tension, generating longitudinal crevasses. On the trailing limb of the high velocity wave, velocities again drop to lower values, and the ice is put into tension in the longitudinal direction, which in turn generates transverse crevasses. The two sets of crevasses chop up the glacier surface into an amazing chaos of ice pillars that are the signature of the passage of a surge.

[Water in the surge...](#) Interestingly, the surge halted rapidly on July 4th 1983 with a coincident huge flood of very turbid water ([Figures 23-26](#)).

The data taken together lead to this simplified cartoon of a surge. In the aftermath of the last surge, the glacier is left with a lower than average surface slope throughout, and has been significantly thinned. It therefore moves slowly, as both slope and thickness play into lower internal deformation and importantly sliding velocities. The net balance in the following years then rebuilds the glacier accumulation area, and thins the accumulation area, as there is lower than average transfer of ice from accumulation to ablation areas. So the glacier thickens and

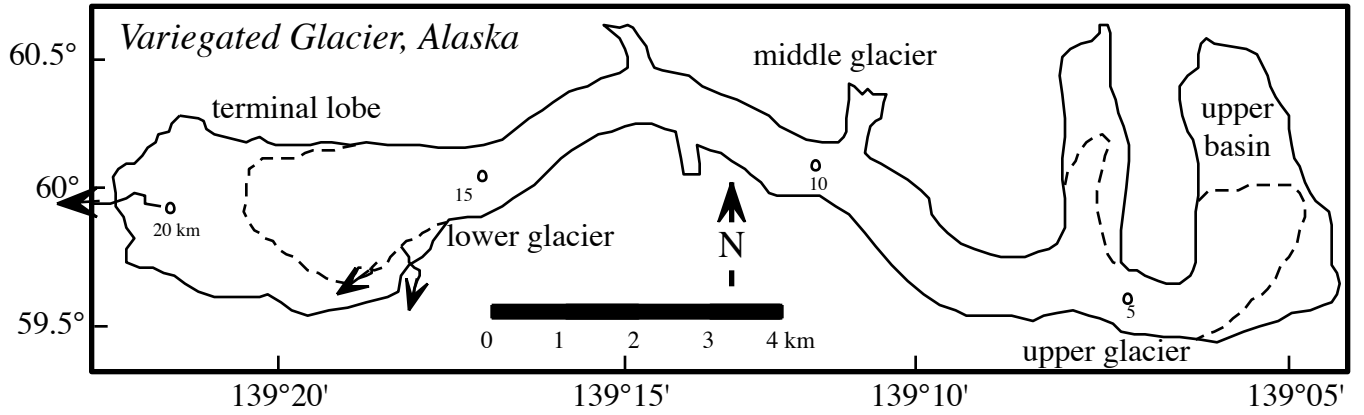


Figure 7.21 Map of the Variegated Glacier, Alaska, showing area of glacier involved in the 1982-83 surge (dashed lines), a few of the km stake locations, and the locations of the major outlet streams near the terminus. (after Kamb et al., 198x)

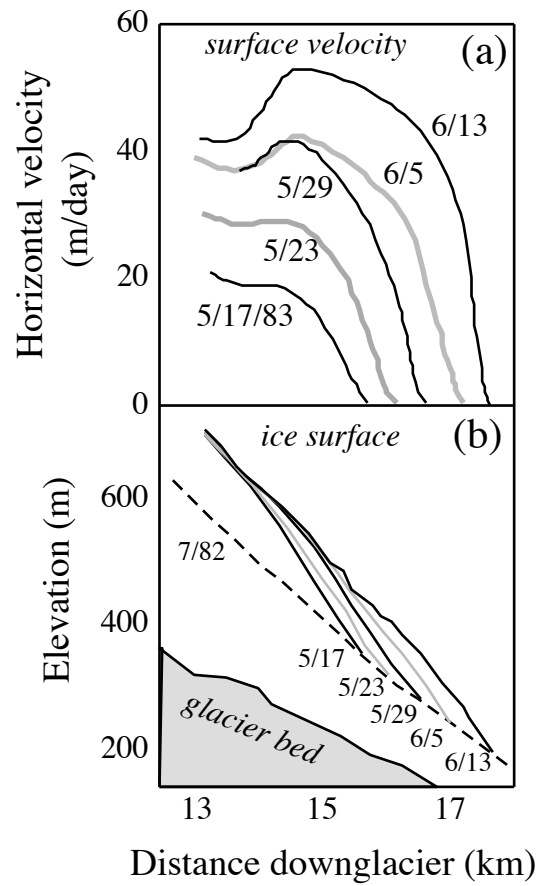


Figure 7.22 a) Ice surface velocity profile, $u(x)$, and b) ice surface topography, $z(x)$, in a 3 km reach of the lower glacier, during the 1983 surge of the Variegated Glacier, Alaska. (after Kamb et al., 19xx Science, Figure 4)

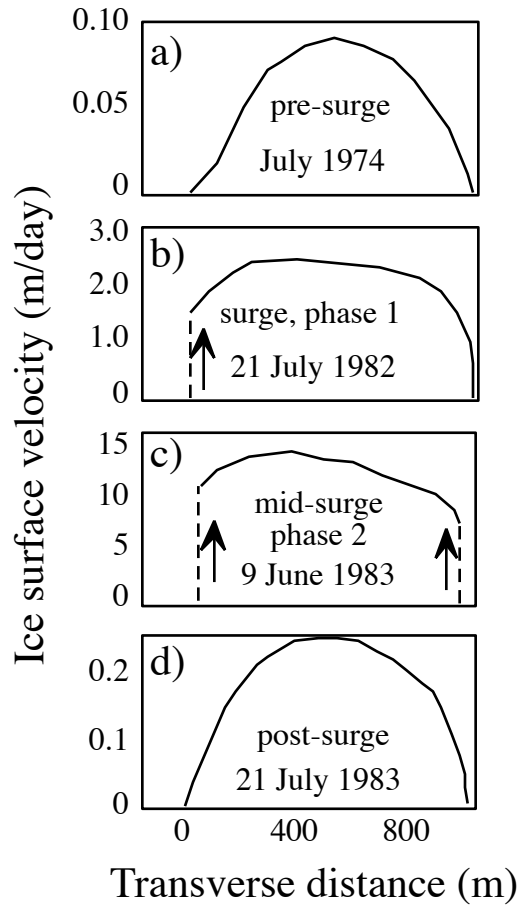


Figure 7.23 Cross-glacier ice velocities in the Variegated Glacier in (a) pre-surge, b) phase 1 of the surge, summer 1982, c) mid-phase 2 of the surge, and d) post-surge. Note the different velocity scales, showing more than 100-fold increase in speeds during maximum of the surge. That the surge velocity profile is so plug-like implicate strongly the role of sliding at the bed. (after Kamb et al., 198x, Science)

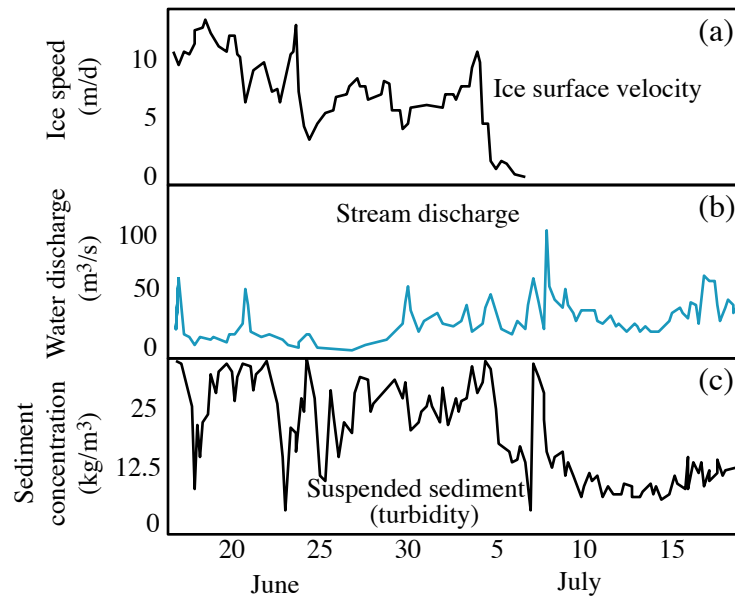


Figure 7.24 a) Ice surface velocity at km 9.5 (after Kamb et al., 1985), b) water discharge and c) sediment concentration deduced from turbidity measurements in the weeks surrounding the abrupt termination of the 1983 surge of the Variegated Glacier, Alaska. (after Humphrey and Raymond, 19xx)

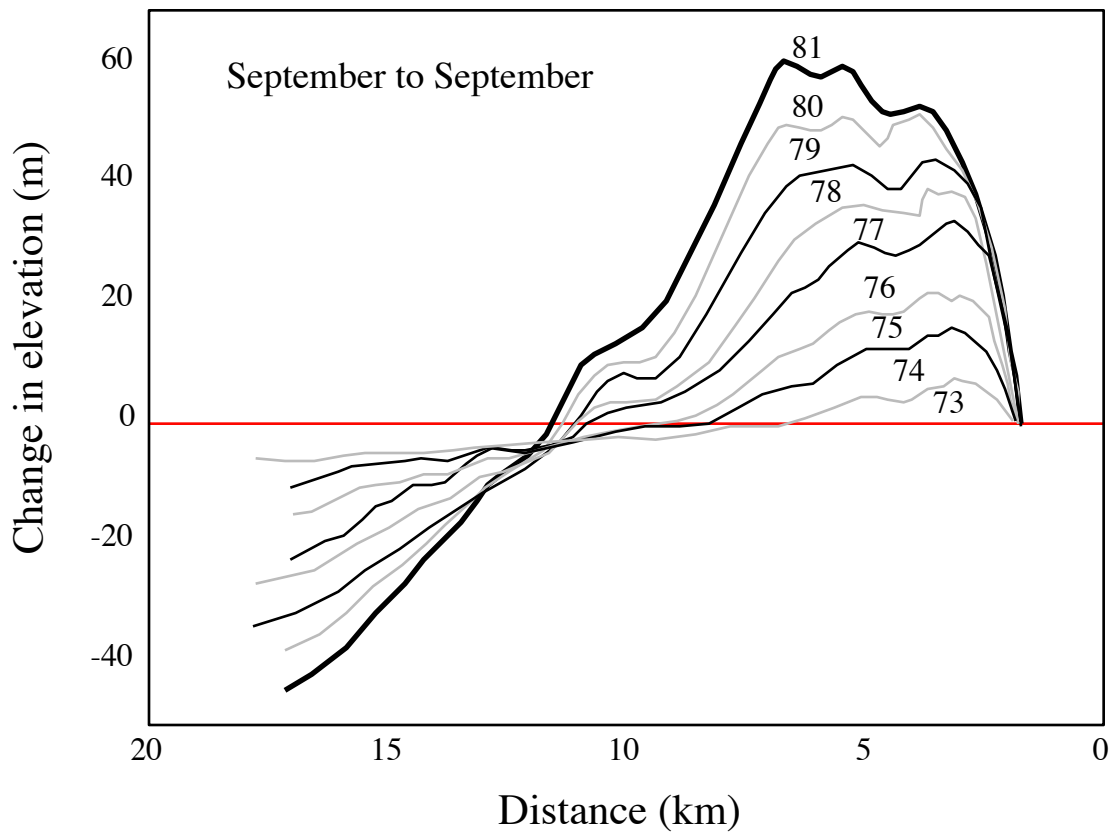


Figure 7.25 Evolution of the elevation anomaly in the decade leading up to the 1982-83 surge of the Variegated Glacier, Alaska. The glacier thickens by more than 60 m in the accumulation area, while thinning by more than 50 m in the ablation area. (after Raymond and Harrison, 19xx)

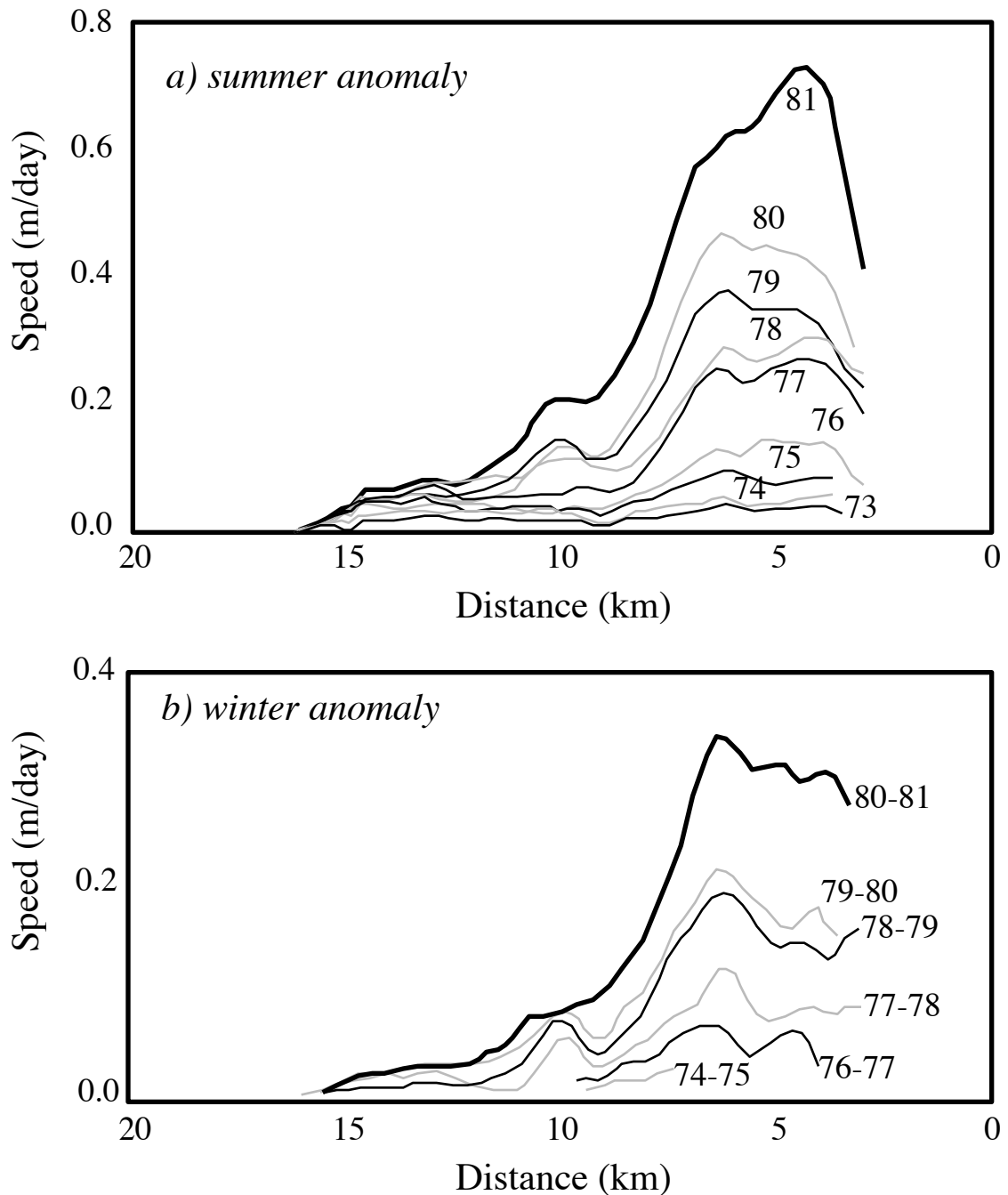


Figure 7.26 Summer (a) and winter (b) velocity anomalies on the Variegated Glacier centerline in the decade preceding the 1982-83 surge. Note different scale for the summer vs. winter anomalies, attesting to the enhancement of sliding in the summer melt season. The anomaly grows by at least an order of magnitude over the decade. (after Raymond and Harrison, 19xx)

steepens. Each year, its maximum sliding speed rises. Finally, the sliding speed increases sufficiently to disrupt the subglacial fluvial network, and the water that would normally find its way out the glacial conduit system is trapped beneath the glacier. High water pressures result, with attendant positive feedback on the sliding speed. The runaway process is the surge. The surge terminates when, for whatever reason, the water finds a way out, usually resulting in a catastrophic flood.

Tidewater glaciers

When a glacier extends its terminus down to the ocean, we call it a tidewater glacier. Some of the largest and fastest glaciers are tidewater glaciers. While the snout of a tidewater glacier may be in the water, the glacier is still grounded, still in contact with a solid substrate. The ice tongue is not floating. (In contrast, the analog in Antarctica is ice shelves, which are indeed floating beyond a point called the grounding line.) Tidewater glaciers differ from typical alpine glaciers in several ways, all due to their interaction with the ocean. Most importantly, they can lose mass through a mechanism other than melting – they can lose mass by calving of icebergs (see photo in [Figure 27](#)). This can be very efficient. On Alaska’s Pacific coastline the termini of these tidewater glaciers are the targets of tourist ships, as the white icy terminal cliff is the scene of dramatic iceberg calving events. But this is not all. Because the ice extends into water body, the lowest the water table within the glacier can get is sealevel. We have already seen the importance of state of the hydrologic system within the glacier on its sliding rate. In particular, our simplest working model for sliding speed involves the effective pressure at the base of the glacier in the denominator of the expression:

$$U_{slide} = c \frac{\tau_b}{P_i - P_w} \quad ()$$

where the denominator represents the effective pressure on the bed, and c is a constant with units of speed. When the water pressure rises to the overburden pressure, the effective pressure goes to zero and this expression suggests the sliding speed should go infinite. While this does not actually happen, the essence is captured: as this flotation condition is approached, sliding speeds ought to increase dramatically. Now consider the tidewater glacier sketched in [Figure 28](#). If it has the profile shown, the effective pressure at the bed must dramatically plummet as the ice tongue extends into deeper water. If the sliding speeds obey our simple rule, then the sliding speed ought to increase dramatically as well. This pattern of sliding is one of the factors that leads to the extensive fracturing of tidewater glacier snouts. In effect, the glacier ice therefore arrives at the terminus already prepared for calving. It is already riddled with fractures.

Calving. Given its importance in the operation of these massive glaciers, we know surprisingly little about the mechanics of calving. This is a complicated process involving the propagation of fractures within the ice, either from the bed upward or the surface downward. Interaction with the body of water includes potentially efficient melting of the terminal cliff by seawater, buoyancy of the seawater (really no different from the effective pressure we have already talked about), and the presence of tidal swings in sealevel. Where calving rates have been measured, they have been shown to be related closely to water depth; the greater the water depth the greater the rate of calving. In [Figure 29](#) we show data collected by Brown and others (1982), showing a nearly linear relationship of calving rate to water depth, D :

$$U_{calve} = aD^p \quad (7.28)$$



Figure 7.27. Aerial photograph of tidewater glaciers calving into fjord near NyAlesund, Svalbard archipelago. Note prominent plume of sediment-laden water exiting from beneath the uppermost portion of the foreground glacier. The medial moraines separate ice emanating from various tributary valleys in the headwaters. Ice cliff at the sea is roughly 100m tall. Photo by Suzanne Anderson.

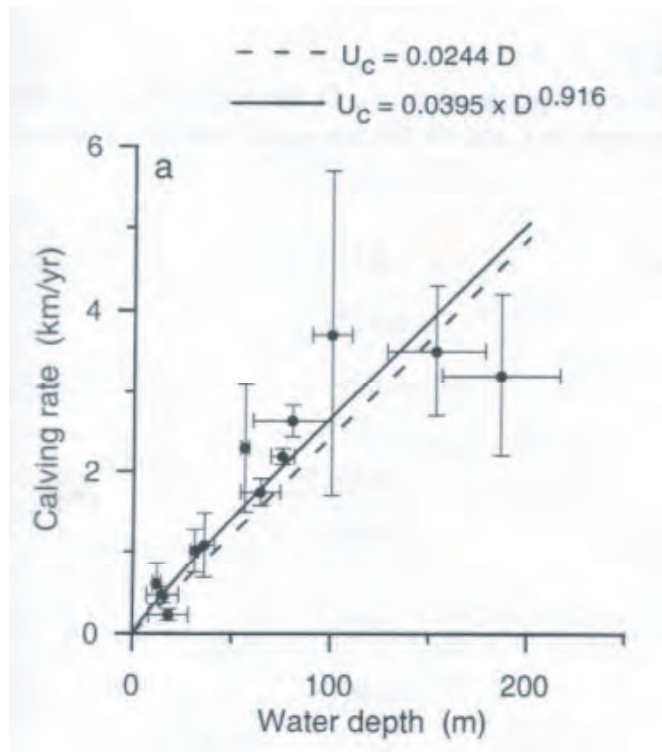


Figure 7.29. Dependence of calving rate on water depth. After Brown and others (1982).

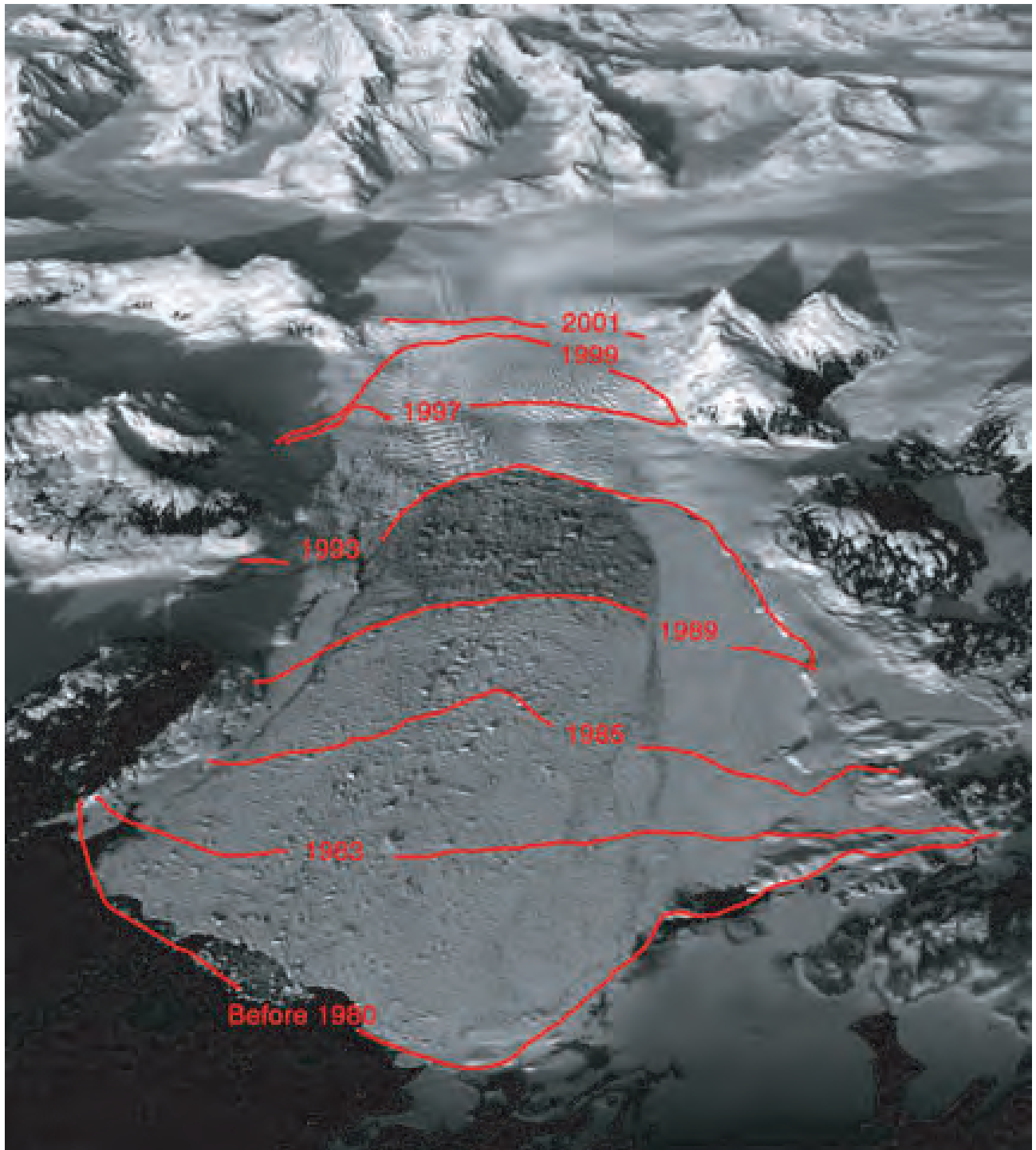


Figure 7.31. Columbia Glacier in retreat, view looking roughly east toward headwaters in the Chugach Range, Alaska. The retreat between 1988 and 2001 is 13 km, averaging roughly 680 m/yr. Image courtesy Mark Meier and Tad Pfeffer.

From the plot one may deduce that $p=0.92$, which is sufficiently close to 1 to allow simplification to $U_c = 0.02D$.

Tidewater glacier cycle. The implications of this dependence of calving on water depth were recognized in the 1960s by Meier and Post, who proposed what has been called the tidewater glacier cycle. If a tidewater glacier is to extend across deepening water, it must effectively bring along some protection against this calving loss. The proposed mechanism involves a morainal shield. These are big glaciers, and they deliver large amounts of sediment to the sea, presumably both as till at the base of the ice and as sediment delivered to the terminus in the subglacial drainage system. One can see well the muddy plume of water marking the position of this exit stream in the photo in [Figure 27](#). As well, one can imagine sediments at the bed of the fjord being distorted or pushed by the advancing front of ice. All of these sediments get smeared along the glacier terminus by marine processes (ref. Powell). The resulting shoal acts to guard the glacier terminus against the more efficient calving that would otherwise attack the ice front. This allows it to propagate into deeper water. The rate of advance is slow, and is presumably set by both the rate of delivery of ice to the front (the glacier mass balance) and the rate at which the shoal can be built into deeper water. Notice the vulnerability as the ice extends, however. If for some reason the snout retreats off its shoal, the terminus will experience increased water depth, and the calving rate should increase. Once started, this should result in a retreat that will last until the glacier is once again in shallowing water. Meier and Post suggested that tidewater glaciers undergo periodic cycles of slow advance and catastrophic retreat in this sort of bathymetric setting ([Figure 30](#)). Note that the cycles have little to do with the mass balance of a glacier. This is an instance in which the retreat of a major tidewater glacier could be completely decoupled from climate. One tidewater glacier may be advancing slowly while another in an adjacent fjord may be in catastrophic retreat. The behavior is self-organized.

In coastal Alaska, these tidewater glaciers have recently retreated up their fjords, exposing brand new landscapes within the last century. When John Muir visited what is now Glacier Bay National Park in the 1890s?, the bay was fully occupied by a large glacier. Now one must paddle a kayak tens of kilometers up the fjord to find the remnants of this glacier, each tributary of which has all pulled its toes out of the water.

The most recent example of this retreat is presently occurring on Columbia Glacier, just north of Valdez ([Figure 31](#)). This glacier was of special interest due to its proximity to the terminus of the Alaska pipeline. As icebergs calved from the Columbia could potentially enter the shipping lanes traversed by oil tankers, the behavior of the calving front of the Columbia has been closely watched. Indeed, the retreat predicted in the 1980s is now in full swing. Luckily, the terminal moraine serves as a very effective barrier to the transport of icebergs. They must grind and smash each other into smaller bits before they can escape the moraine sill, and are therefore small enough not to pose a significant risk before they are cast off into the open ocean.

[Expected duration of retreat into next decade, opening a new fjord, Columbia Bay. New figures, photo.](#)

Contribution to sealevel change. That tidewater glaciers extend to the sea implies that they have large accumulation areas in high elevations, that the accumulation rates are high due to proximity to the storms coming off the ocean, or both. The low elevations of the ablation zones

lead to very high melt rates as well, rates of many meters per year. In a recent study of glacier change in Alaska, comparison of the glacier centerline profiles collected using a laser altimeter mounted on a small plane with those derived from the 1950s USGS maps showed that the glaciers in Alaska alone could account for roughly half of the sealevel rise attributable to glaciers (the other half of the 1-2mm/yr rate of rise being attributable to thermal expansion of the water column). Most of this change came from the great changes in profiles of the large tidewater glaciers. [summary of Meier et al., 2007 Science piece, incl figure]

ice streams

stability of ice sheets -- thermal, causes of Heinrich events, surging, binge-purge etc.
Summary of the large ice sheets. Antarctica and Greenland. Utility of inSAR

Dyke work to document outline of LIS. Utility of 14C dating of shorelines and bedrock, shells...

Thermal problems. Advection in ice sheets. Polythermal alpine glaciers. Clark and Marshall on LIS thermal evolution and the 40k-100k problem.

Response times to climate change. Scaling. Big or little respond fastest?

Glacial Geology

Now that we have some solid understanding of how glaciers work, let us focus on how glaciers modify their physical environment. Glaciers both erode landscapes, generating characteristic glacial signatures, and they deposit these erosional products in distinctive landforms. We will describe the origins of these features, starting with erosional forms, and starting at the small scale. Again, the goal is not to be encyclopedic, but to address the physics and chemistry of the processes that gave rise to each of the forms.

Erosional forms and processes

Any visit to a recently deglaciated landscape will reveal clues that it was once beneath a glacier. The bedrock is often smooth, sometimes so smooth that it glints in the sun as if it has been polished. The bedrock is often also scratched. The small bumps have been removed, leaving a landscape dominated by larger bumps and knobs that have characteristic asymmetry. And at the large scale we see U-shaped valley cross sections, hanging valleys, fjords and strings of lakes dotting the landscape. At an even larger scale, fjords bite through the margins of most continents that have been subjected to repeated occupation by icesheets. Each of these features cries out for an explanation, beyond “this valley was once occupied by a big moving chunk of ice”.

abrasion

The scratches, called striations, are the products of individual rocks that were embedded in the sole of the glacial ice as it slid across the bedrock. The sum of all these scratches is the process called subglacial abrasion. It is abrasion that smooths the bed. It is the short wavelength bumps in the bed that are gone, making it look smoother. This should trigger recollection of the regelation process by which glaciers move past small bumps. Consider again that bump, and think about a rock embedded in the ice approaching the bump. The bottom line is that while the ice can get around the bump with its magic act, the rock cannot. Instead, it is forcefully pushed against the bump (Figure 15), the force being great enough to cause the rock to indent, scratch or striate the stoss side of the bump. As it is still being dragged along by the ice, this indentation streaks out to gouge a micro-channel that is the striation.

The theory of glacial abrasion requires that we handle the effects of each such striator, and that we have some knowledge of the number of them in the basal ice. The theory was worked out by Bernard Hallet, and is summarized here (Figure 32). The abrasion rate, e , goes as the number of indentors per unit area of bed, C , the cross sectional area of the indentation that they induce in the bedrock, A , and the rate at which the striators are dragged across the rock, U_c .

$$e = CAU_c$$

We must determine what sets the cross-sectional area of the indentation. Experimental work shows that the depth of the indentation increases as the force imparted by the indenter increases. Hallet argued that one should consider the clast doing the work as being embedded in a fluid (ice) that is moving toward the bedrock at a rate comparable to the sliding rate, U_{sl} . If the ice is disappearing at the stoss side of the bump, and the rock is not, then ice has to move past, around the rock. In this view, the force involved is that associated with the viscous drag of the ice as it moves around the rock to disappear at the stoss side of the bump. From the theory of fluid flow past obstacles, such as that employed in thinking about settling of clasts in a fluid, and

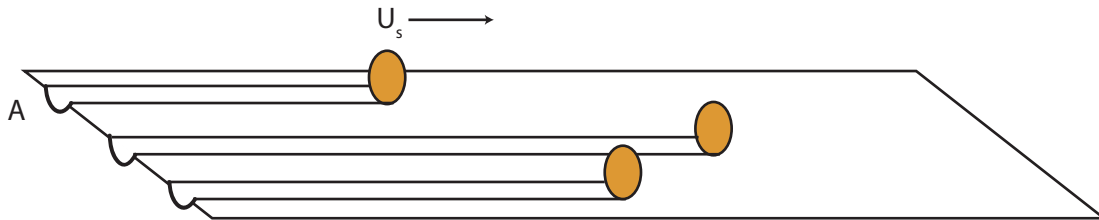


Figure 7.32. Sketch of glacial erosion by abrasion. Multiple striations of the bedrock by rocks embedded in the sole of the glacier, moving at the sliding speed U_s , lead to lowering or erosion of the bed. The rate depends upon the number of striators per unit area of bed, the cross-sectional area of the eroded striation, A , and the rate of growth of the striation, U_s . That the cross sectional area is proportional to the drag force of the ice as it regelates past the rock clast, implies that the lowering rate of the bed ought to go as the square of the sliding rate.

recognizing that the flow is likely to be very low Reynolds number (viscous as opposed to turbulent) flow, the drag force can be written

$$F_d = \frac{1}{2} A \rho_f C_d U_{rel}^2$$

where C_d is the drag coefficient, A the cross-sectional area of the clast, and U_{rel} is the relative velocity of the fluid and the rock. For low Reynolds numbers, Re , the drag coefficient is $24/Re$, or $24\nu/DU_{rel}$. This leaves the expression for the drag force as:

$$F_d = \frac{1}{3} \pi D \mu U_{rel}$$

But the relative velocity of the ice relative to the clast is some fraction of the sliding speed, U_{sl} . Combining these expressions reveals that the abrasion rate should go as the square of the sliding speed:

$$e = c U_{sl}^2$$

We note for completeness the other view of the origin of the drag force. Why is the relevant force not the weight of the overlying column of ice? This overlying column of ice has to be pretty heavy, given that ice is about 1/3 as dense as rock. The problem with this view is that the ice is not a solid, but must be considered a fluid. The rocks at the base of the glacier are engulfed in the fluid, so that not only do they not support the weight of a column of ice overhead; instead, they are themselves buoyed up by the surrounding fluid. It is the buoyant weight of the rock that counts. In this view, then, the depth of the scratches that could be imparted to the bed are greater when you drag a rock across the bed *in air* than they would be under ice. Try it. The scratches are very minor compared to the striations that must have occurred subglacially.

We note that recent work (Iverson and coworkers, 2005) has suggested that the rock-rock friction associated with these striators provides a significant brake on the sliding of the glacier. This would serve as a negative feedback in the glacial erosion system, as the more clasts there are the more the glacier will be slowed, and the less rapid the erosion will be.

Given a pre-glacial irregular bed consisting of bumps of all wavelengths, this abrasion process will most effectively remove bumps of small wavelength, leaving the bed smoother at these scales. At some scale, however, larger bumps persist. No glacial valley is perfectly smooth. When we look closely at these larger bumps, they often have an asymmetry, with a smooth up-valley stoss slope that shows signs of abrasion, and an abrupt, steep downvalley or lee side that looks like it has been quarried. These forms are called *roche moutonnee*, apparently named for the similarity of their shapes with that of the back side of a sheep. Their origin requires introduction of the other major subglacial erosional process: quarrying.

quarrying

The larger bumps in the bed can generate subglacial cavities on their lee sides (Figure 33), as the ice speeding over the top of the bump separates from the bed on the lee. All but those subglacial cavities at the very edges of the glacier will be filled with water. The quarrying process involves the generation of cracks in the bedrock at the edge of the cavity, and results from imbalance of forces on the top and sides of the rock bump. The theory of subglacial quarrying has been addressed recently by Neal Iverson and by Bernard Hallet, quite independently. Cracks grow at a rate dictated by the stresses at their tips. It is therefore the magnitude and the orientation of the stresses within the bedrock bump that are crucial to the problem.

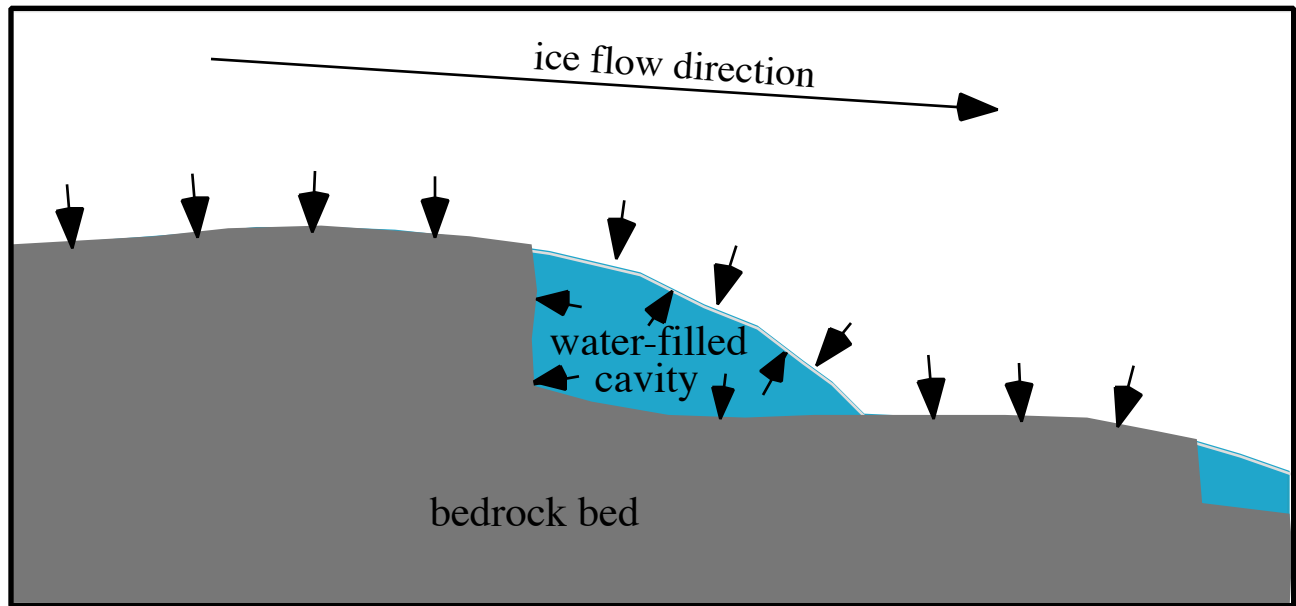


Figure 7.33 Schematic diagram of a water-filled cavity beneath a temperate glacier. Arrows represent normal stresses.

Consider the down-glacier edge of the bump, which is often quite abrupt due to quarrying and can be idealized as a square corner. The ice presses downward against the bedrock that comprises the top of the bump. The water pressure in the cavity, which acts equally in all directions, presses against the lee side of the bump. If there is a large difference between the water pressure and that exerted by the overlying ice overburden, then there will be a large stress difference, and crack growth will be promoted. Iverson generated a model of the orientation of the stresses (Figure 34), and the expected orientation of cracks under various pressure difference scenarios. One can see that the orientation of cracking to be expected is that parallel to the lee face of the cavity. The growth rate would be proportional to the pressure difference. One end-member calculation would be to remove the water in the cavity, reducing its pressure to atmospheric. For some period of time, that required for the cavity to fill with ice as it relaxes into the low pressure void, the entire weight of the ice overburden would be borne by the top of the bump, very large pressure gradients would exist, and cracks would grow that are nearly vertical.

But why would pressures in the cavity system vary at all? The origin of the water in the cavity system is melt of the glacier surface. Variations in the rate of production of melt, which occur on both daily and seasonal time scales, are the most likely culprits. Boreholes drilled to the base of glacial systems have recorded huge swings in the subglacial water pressure on quite short time scales (Figure 35).

Iverson experiment in artificial cavity beneath Engabreen 2005 (Figure 30)

How do we know these cavities exist at all? There are a couple ways. The most direct evidence is from air-filled cavities (caves) at the edges of some glaciers. Here subglacial spelunking allows us to walk around in the cavity system and to observe first-hand the operation of the plucking mechanism. By their nature, such air-filled cavities are overlain by only minor thicknesses of ice. Nonetheless, direct observation of the edges of the ledges from one year to the next have shown significant modification of the ledge takes place in a single year's sliding. A time lapse movie taken of the ice roof as it slides by such a ledge edge beneath about 15 m at the Grinnell Glacier, Montana, reveals that there are numerous small chips and blocks torn off the ledge. They become embedded in the basal ice (the roof of the cavity), and, importantly, are therefore available to act as abraders when the ice roof reattaches to the bed at the downstream boundary of the cavity.

In limestone bedrock, the nature of the subglacial water system can be well mapped out upon deglaciation of the valley. Numerous studies, notably Hallet et al. (1980) and Hooke (19xx) have produced maps of these surfaces, making use of the solutional forms of the bedrock when it is in intimate contact with liquid water, and the evidence of clear abrasional erosion elsewhere. These maps commonly show sets of cavities, occupying significant fractions of the bed, linked to one another through relatively narrow passages. This 'linked cavity' system is now a dominant feature of many conceptual models of the subglacial hydrologic network.

Large scale erosional forms

This brings us to the large scale erosional forms imposed by glaciers on the landscape. We all learn in introductory geology classes that one can identify a valley that has been shaped by glaciers when it has a U-shaped cross section, and when it is dotted with alpine lakes. Hanging valleys whose floors are perched well above the floor of a main valley are also attributed to

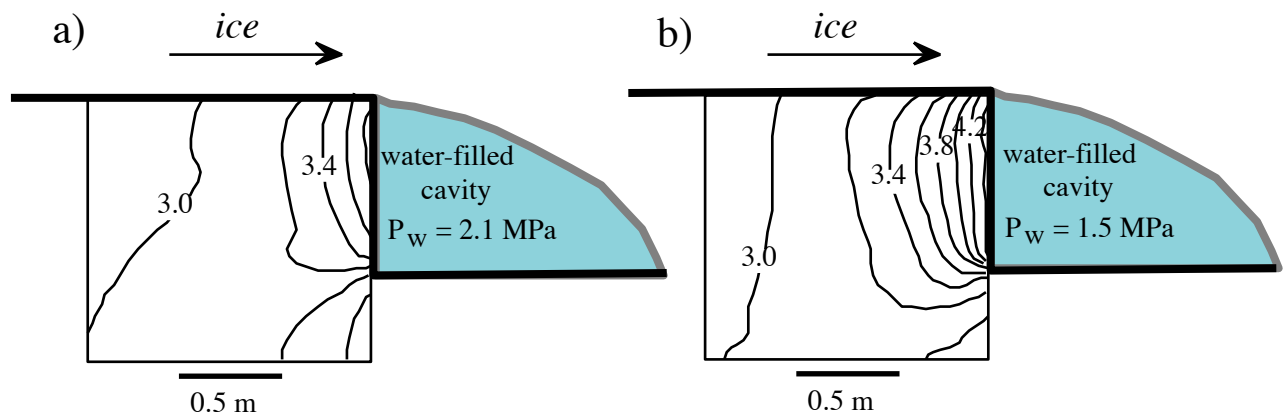


Figure 7.34. Contours of stresses (in MPa) within bedrock corner at ledge edge. Ice sliding from left to right. No vertical exaggeration. a) with water pressure steady at 2.1 MPa, and b) with water pressure reduced to 1.5 MPa. Note strong stress concentrations at ledge face. (after N. Iverson, 19xx)

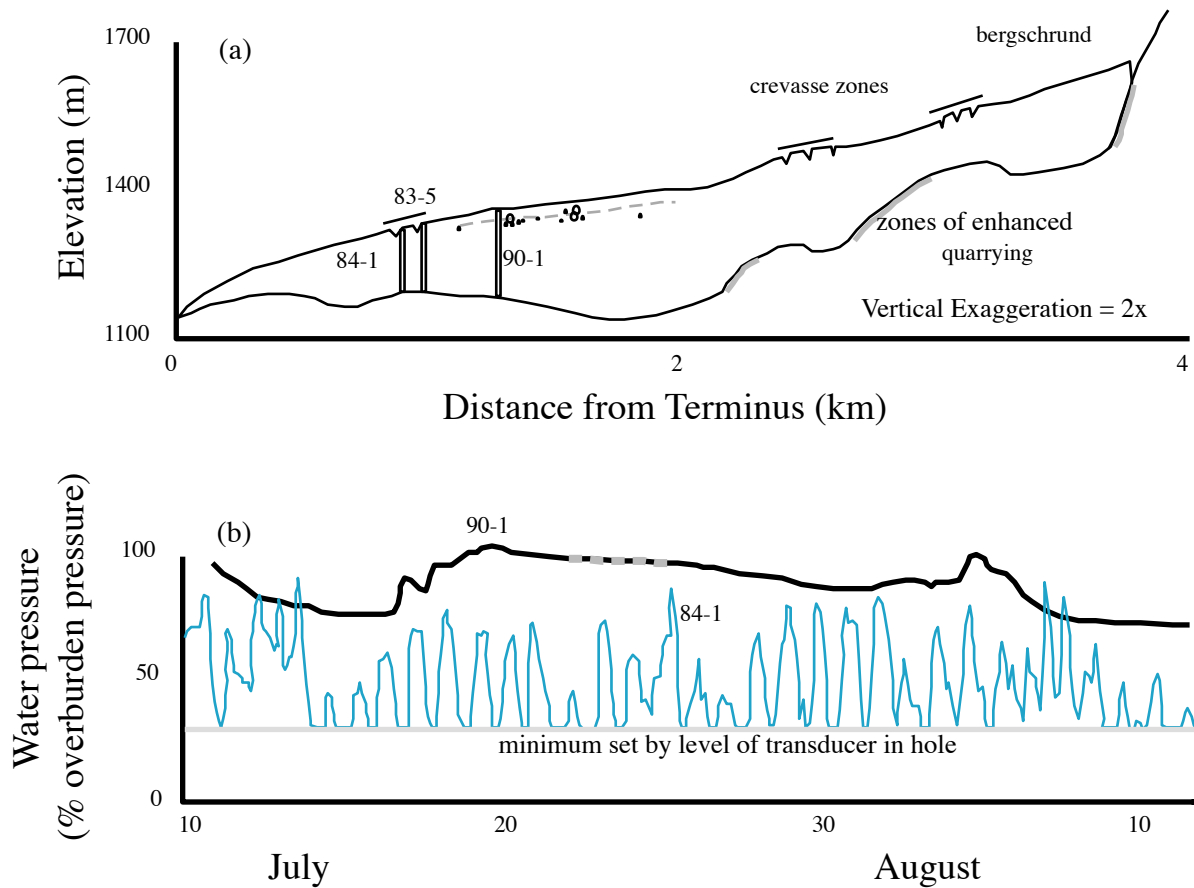


Figure 7.35. Topographic profiles of ice surface and bed (a), and water pressure records (b) from Storglacieren, Sweden. Profile shows several overdeepenings of the bed and major crevasse zones in regions of extension. Borehole locations in major overdeepening and at crest of bedrock bump are shown, along with spot measurements of the water pressure in the middle of the overdeepening. These measurements are all close to the level expected for flotation of the ice: 90% of the ice thickness, shown in gray line. Pressure records are very different for two sites, that in the middle of the overdeepening showing little variation around 90-100% of flotation, that at the crests of the bump showing major diurnal fluctuations between 70-90% flotation and that pressure associated with the depth of the transducer (gray line). Similar pressure fluctuations are inferred to promote enhanced quarrying of the bed at sites shown in (a). (after Hooke et al., 19xx, figures 2&3).

glaciers. But just how do these features become imprinted on the landscape? This is in fact a topic of considerable recent and ongoing research.

The U-shaped valley

First let us deal with the cross section (**Figure 36 – photo**). How does a classic V-shaped cross section indicative of fluvial occupation of a valley get replaced by a U-shape? And how long does it take? Jon Harbor has addressed this problem using a 2-dimensional glacier model. As in most models of landscape evolution, an initial landscape form is assumed (the “initial condition”), the glacier flow through that landscape is assessed, the pattern of erosion is calculated, the landscape shape is updated, and the flow is then recalculated (**Figure 37**). In the first suite of model runs, the glacier is allowed to achieve a steady discharge through the cross section, after which the ice discharge remains the same. In other words, climate change is ignored. The pattern of sliding, and hence of erosion in the valley bottom is non-uniform, leading to evolution of the shape. In particular, the sliding is reduced in the bottom of the triangle, and the sliding rate reaches a maximum in the middle of the valley walls. This results from the dependence of sliding rate on the water pressure field assumed in the glacier. This leads to widening of the valley walls with time. The form of the valley evolves toward one in which the form no longer changes (a steady form), one that subsequently propagates vertically as a U-shape form (**Figure 38**). In more elaborate model runs, Harbor explored the role of glacial cycles on the evolution of the valley cross section. He found that sufficient shape change occurred over roughly 100 ka that the imprint of glacial occupation of alpine valleys could be imparted in as little as one major glacial cycle.

Cirques, steps and overdeepenings: the long valley profile

The shape of a glacial valley in the other dimension is just as characteristic. In contrast to fluvial bedrock valleys, which display smooth concave up profiles, glacial valley profiles display steps and flats. Many of these steps occur at tributary junctions. In addition, the upper portions of alpine glacial valleys display knobby less well-organized topography rather than the expected smooth U-shape. Finally, many tributary valleys are said to hang above the trunk valleys upon deglaciation. The valley system disobeys what has come to be called “Playfair’s Law”, which states that the trunk and tributary streams join “at grade” (see discussion of this in the Bedrock River chapter).

Oerlemans (1984) was the first to attempt to model these features numerically. By embedding an erosional rule in a 1-dimensional glacial model, he modeled the evolution of valley long profiles (**Figure 39**). The model glaciers were driven by a simple climate in which the ELA was allowed to vary sinusoidally through time, which in turn moved a mass balance profile up and down. Interestingly, the glacial valley deepened so dramatically over several glacial cycles that the glaciers declined in size through time. While Oerlemans countered this by asserting a net cooling of the climate, the effect may be real. Glaciers likely do deepen their valleys through time. In so doing they both hide more effectively from direct insolation, reducing the melt rate, and decline in elevation, which should both reduce accumulation and increase melt rate.

More recently, MacGregor and others (2002) targeted the stepped nature of the long valley profile. Again a 1-dimensional glacial long valley model was employed in which a net mass balance pattern was imposed. A simple balance profile pivoted about the ELA, and climate change was modeled by an imposed history of ELA scaled to the $\delta^{18}\text{O}$ deep sea record. Glacier dynamics included both internal deformation, and a rule for sliding. Like in Harbor’s models,

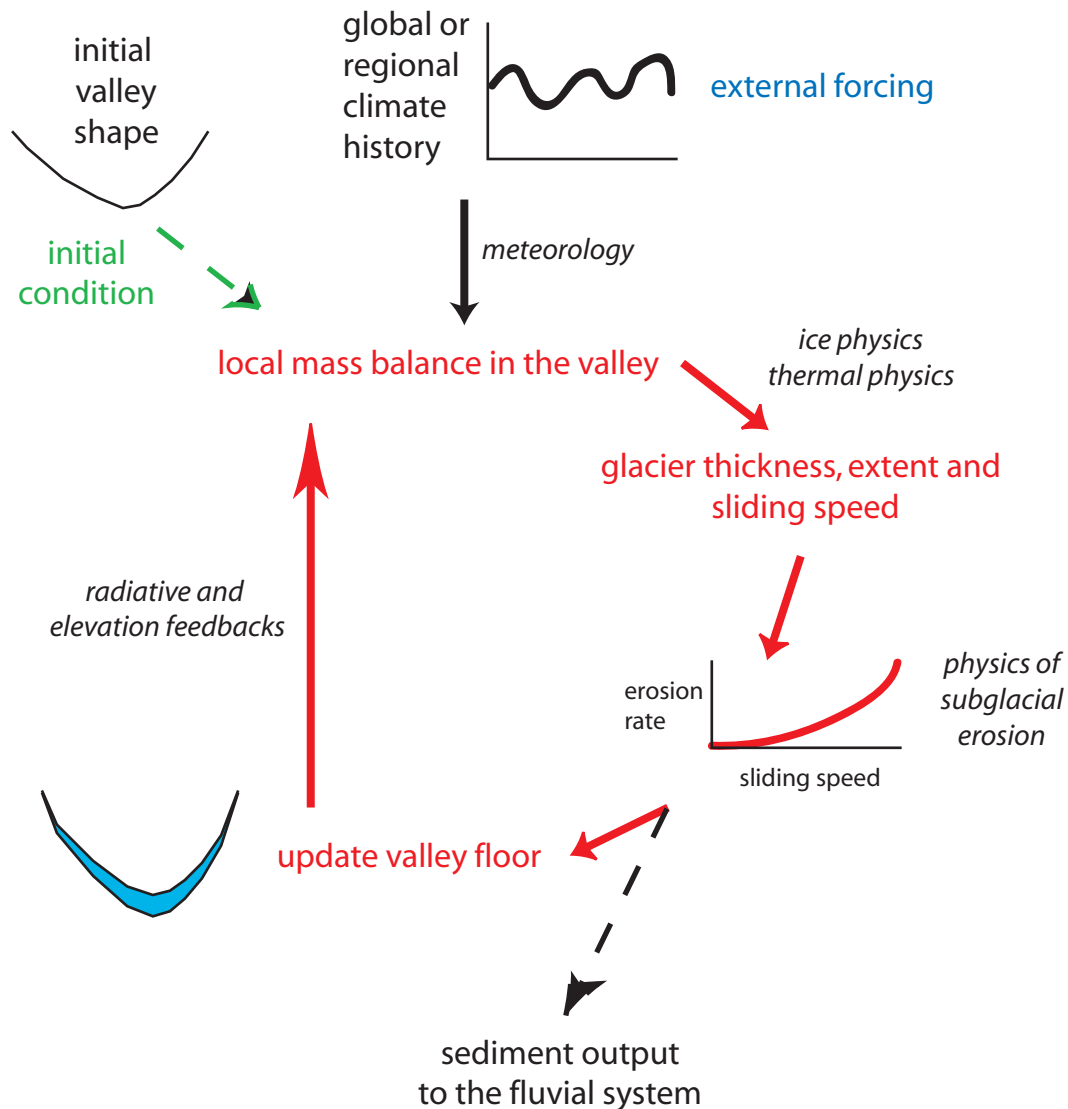


Figure 7.37. Structure of a glacial landscape evolution model. Relevant processes are in italics. Model is initiated by a specified valley geometry (the initial condition), and is driven by a specific climate history (external forcing, which here serves as a boundary condition on the glacier surface). Local valley geometry modifies the global or regional climate to generate the local mass balance profile on the glacier. Ice physics determines motion of the ice, which is thermally dependent in that both the viscosity of the ice and the ability to slide are dictated by the temperature of the ice. The sliding pattern dictates the pattern of subglacial erosion, which then both modifies the bed and generates sediment that is passed to the river downstream. The modified valley profile can then modify the local mass balance by both radiative feedbacks (hiding in a deeper valley) and elevational feedbacks that dictate both local temperatures and rates of snow accumulation. The red arrows form a loop that is repeated, interacting with the external world through climate forcing and delivery of sediment from the system.

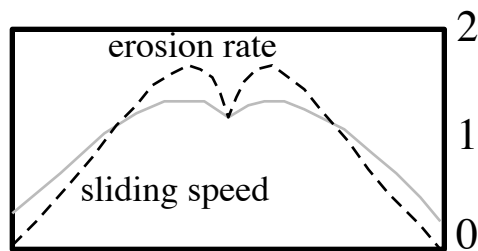
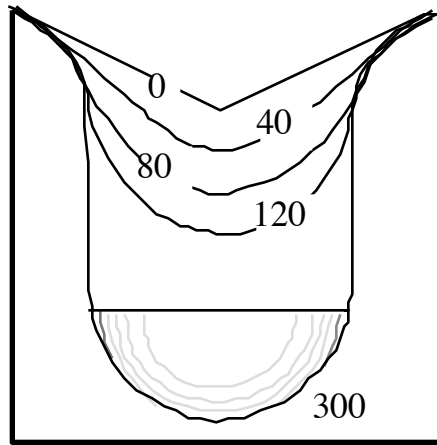


Figure 7.38 Numerical simulation of cross-valley profile evolution during steady occupation of the valley by a glacier. Initial fluvial v-shaped profile evolves to u-shaped profile characteristic of glacial valleys in roughly 100 ka, given the sliding and erosion rules used. Bottom graph shows initial distribution of sliding speed and corresponding erosion rate. Low erosion rates in valley center allow faster rates along the walls to catch up. Final erosion rate is roughly uniform, causing simple downwearing of the form once u-shaped. (after Harbor et al. Nature, 19xx)

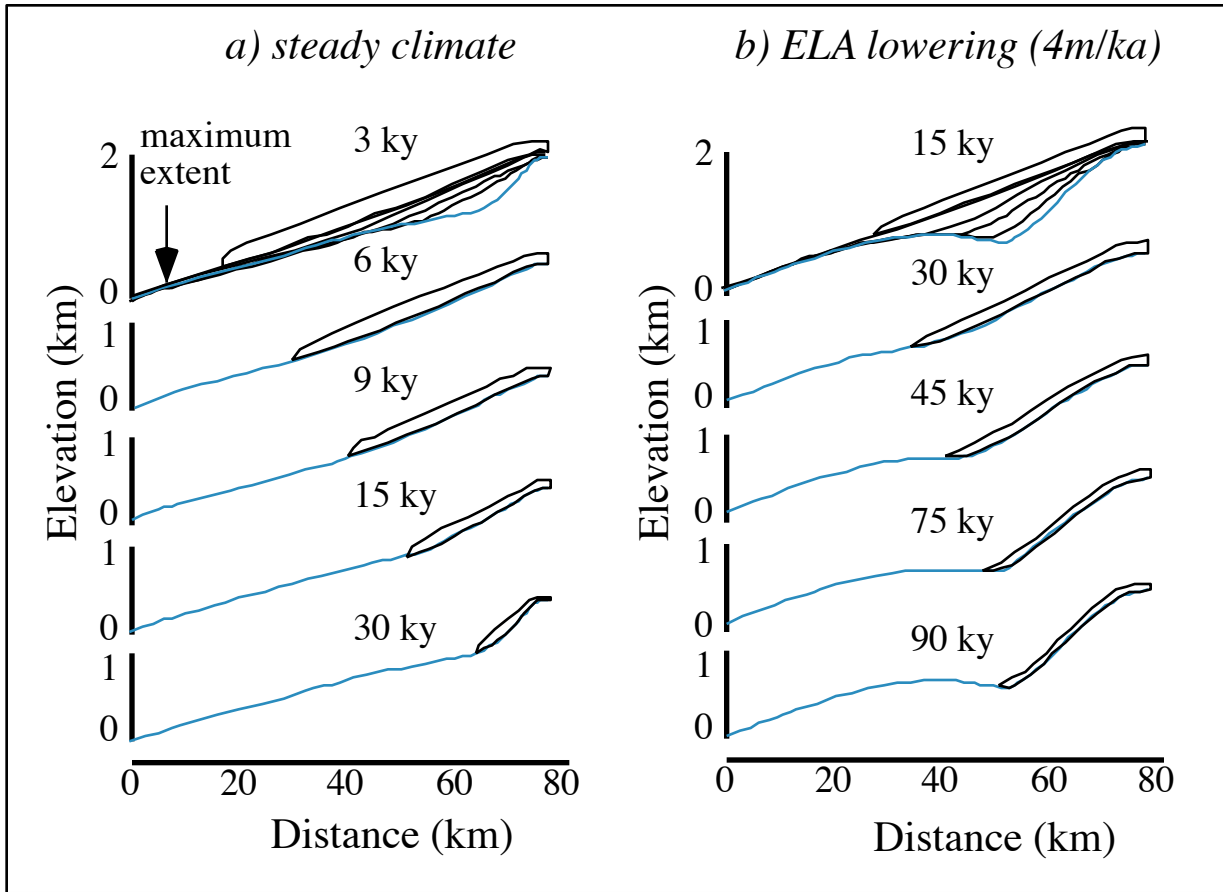


Figure 7.39 Numerical models of long valley profile evolution of a glaciated valley in the face of a) steady climate, over 30 ky, and b) climate in which the ELA lowers at 4 m per thousand years, for 90 ky. Initial profile is a linear (uniform slope) valley. Top diagram shows all time slices in the respective simulation as light lines. (after Oerlemans, 1984)

the algorithm for sliding included an imposed water table, and assessed sliding rate based upon the effective stress. The rule for the erosion rate was varied between model runs, but in all cases involved the sliding rate. The basic patterns produced were found to be insensitive to the rule chosen. Models of the single trunk glacier valley inevitably resulted in flattening of the valley floor downvalley of the long-term mean ELA and steepening of the valley profile upvalley of this (Figure 40). Only when more complicated valleys were modeled did a discrete step in the valley floor appear (Figure 41). In model runs including a single tributary valley, the erosion of the tributary valley floor was outpaced by that of the adjacent trunk stream, leading to disconnection of the two profiles, and a step appeared in the main valley. This led to the generation of model hanging valleys, and associated steps in trunk valleys. A chief result of the calculations was that the long-term pattern of erosion mimicked the pattern of long-term discharge of ice. Tributary valleys see less ice discharge than trunk streams that drain larger areas. Trunk streams immediately downvalley of a tributary must accommodate the long-term discharge of ice from the tributary, and therefore see more ice.

That the time steps in these complex models were very small in order to remain stable numerically meant that it was difficult to explore a wide range of valley shapes. Anderson and others (2006) build upon the observation that ice discharge was a faithful proxy of erosion rate in MacGregor's models. They employ analytic models of ice discharge patterns based upon the assumption that the glacier is at all times close to steady state. This implies that the discharge must at all times reflect the integral of the mass balance upvalley of a point (equation 3). These simplifying assumptions allow efficient exploration of the roles of climate variability and valley hypsometry (distribution of valley width with elevation). They show that in the simplest case of a linear mass balance profile and a uniform width glacier, a parabolic divot should be taken out of the valley floor, with the maximum of erosion located where the ELA intersects the valley profile (Figure 42). As in MacGregor's models, the valley flattens downvalley of the ELA and steepens upvalley of it. Incorporation of climate variability can be accomplished in a couple ways. One could simply assert a history of the ELA, and numerically chop out parabolas of differing magnitudes and lengths. More efficient still, one can assert a probability distribution function (pdf, see Math Appendix) that captures the spread of ELAs. The pdf of the $\delta^{18}\text{O}$ curve looks approximately Gaussian over the last 3 Ma since global scale glaciations began in the last glacial cycle (Figure 43). Using this pdf, they show that the erosion pattern should feather into the fluvial profile downvalley, and that again the maximum of erosion occurs where the long term ELA crosses the valley profile. This simple expectation can break down when more realistic planview shapes of valleys are acknowledged. Most glacial valley systems are much wider in the headwaters than they are in their lower elevations, reflecting the inheritance of the dendritic fluvial network. The ice discharge pattern predicted from equation 3 must therefore include both the pattern of mass balance and of valley geometry (width). But recall that the principal driver of erosion is the sliding rate. Ice discharge per unit width of the valley should be a better proxy for the sliding rate. This means that where the valley narrows, the more ice is being shoved through per unit width than in a wider portion of the valley. When this element of reality is incorporated in the analytic models, the pattern of erosion begins to include a bench in the upper valley below which the erosion rate increases dramatically (Figure 44). This reflects the funneling of the ice into a narrower throat as the tributary valleys in the headwaters coalesce.

Fjords

Figure 45-46, from Kessler et al. in review 2007

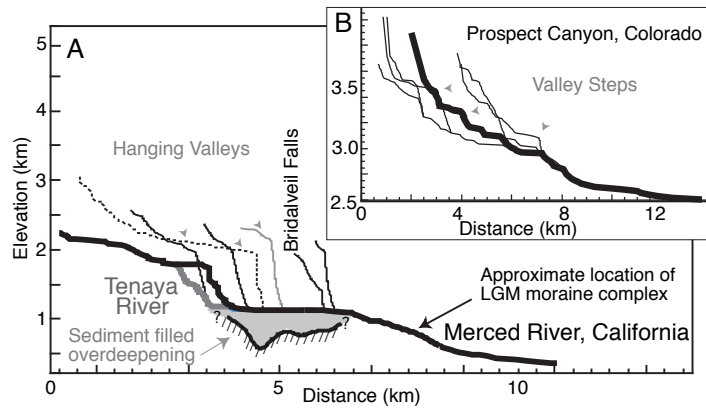


Figure 7.40. Longitudinal profiles of two glaciated valleys, showing steps and overdeepenings. (after MacGregor et al., 2000, Fig. 1)

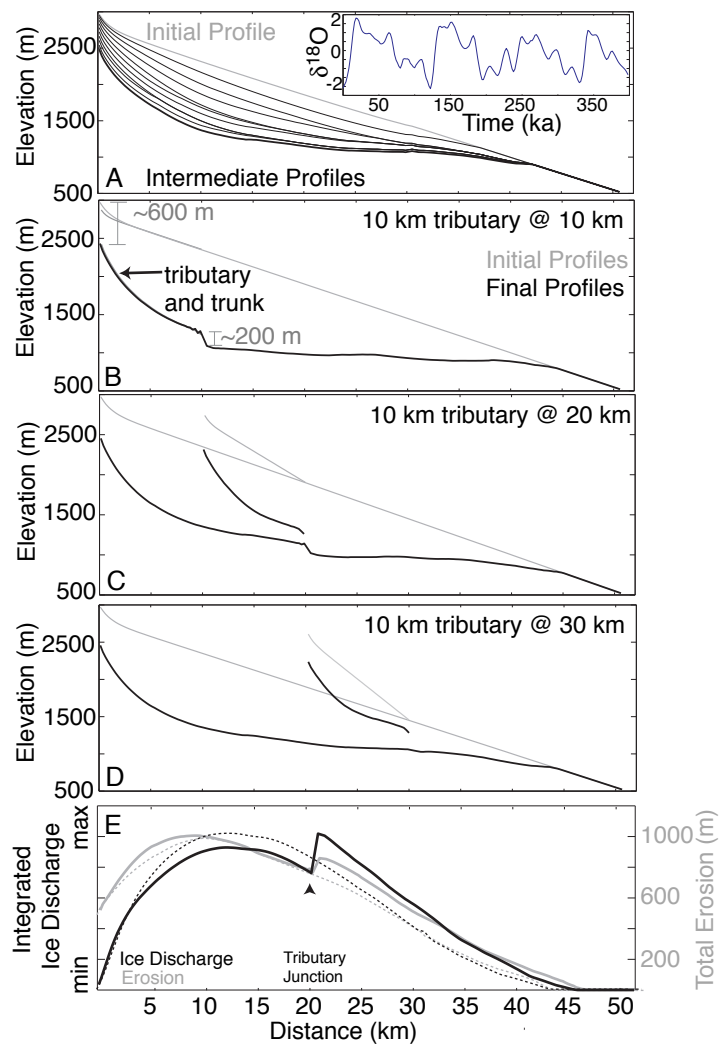


Figure 7.41. Modeled evolution of the long profile of a valley with one tributary subjected to repeated glaciation. Steps develop in the valley profile, and the tributary valley is hung. The height of the step and the height of the hang depend upon the position of the tributary, and the long-term ice discharge. (after MacGregor et al., 2000, figure 3)

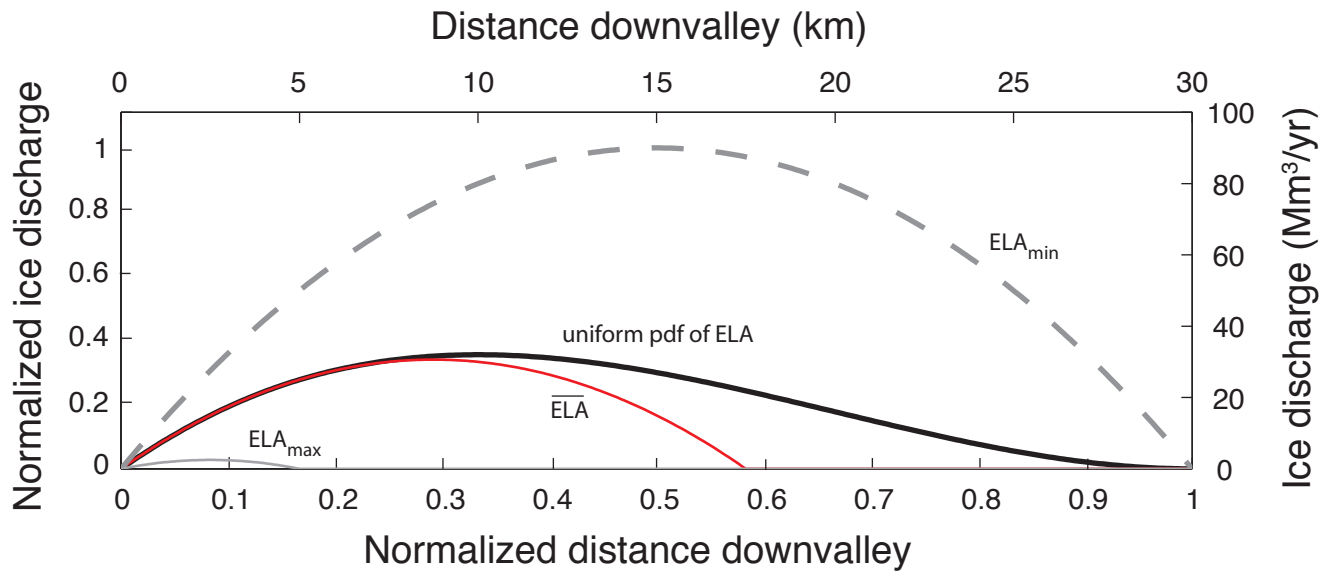


Figure 7.42. Analytic solution for ice discharge patterns resulting from steady state glaciers driven by a simple mass balance function, in a linear valley profile, and a uniform distribution of ELAs. Maximum and minimum glaciers corresponding to minimum and maximum ELAs, respectively, are shown along with the glacier discharge expected from the average ELA, and a long term average resulting from a uniform distribution of ELAs between maximum and minimum. The symmetry is broken when a distribution of ELAs is permitted. Maximum discharge occurs down-valley from that corresponding to the mean climate, at roughly 1/3 of the glacial limit (the maximum terminus position), and smoothly tapers to zero discharge there. Distance and ice discharge are normalized using glacier length and ice discharge associated with the lowest ELA. (from Anderson et al., 2006).



Figure 43. Marine isotopic record for last 1.5 Ma (after Zachos et al. [2001]), and a histogram of it. The distribution is roughly symmetric, and appears to be normally distributed (after Anderson et al., 2006)



Figure 7.47 Glacial erratic in glacial valley floor east of Mt Whitney in the Sierras. Isolated block of granite lies on granitic bedrock, but was transported into place in the last glacial maximum glacier. (photograph by R.S.Anderson)

Rock balance in a glacial valley

Set up the balance (Figure 45), here it goes from the walls and from the bed. Moraine volumes, glacial lake volumes, use of crns to place limits, etc. (Fig 46)

Depositional forms

Glacial deposits come in all shapes and forms, including as isolated glacial erratics (Figure 47), and are the subject of numerous books. The reader is pointed to Meinzes, and to Bennett and Glasser for recent more comprehensive summaries of this portion of the glacial system. We treat here only the basics. Many glacial deposits consist of poorly sorted sediments that run the gamut in terms of grain size. What were once called boulder clays and are now called simply tills. The first order classification comes from distinguishing those materials that have from those that have not seen the bed of the glacier.

Moraines

Most moraines, be they lateral, terminal, or medial (Figure 48), are derived from supraglacial debris, debris that has never seen the bed of the glacier. While this might be obvious in the case of the lateral moraines, which are accumulations of debris found along the sidewall margins of a glacier, and are often delivered to those sites by hillslope processes, it is less clear for the other two classes of moraines. Lateral moraines consist largely of angular blocks riven from the valley walls by periglacial processes, and delivered by individual rockfall events, landslides, or avalanches that incorporate rocky debris as they slide against the wall. Rarely are there blocks that show striated facets indicating time spent at the glacier bed. A point of caution: It is worth noting that some lateral moraines near present day margins of glaciers are ice-cored. These are not the simple triangular piles of rock that they look to be, but are instead a rather thin carapace of angular rock covering glacial ice.

Terminal moraines are accumulations of debris at the snout or terminus of a glacier. The larger terminal moraines are generated when a glacier remains in the same position for some time, continuing to deliver debris to the margin on an annual basis. Upon retreat, this pile of debris is left behind, smaller piles being generated each year (annual moraines) as a signature of the retreat history.

Medial moraines are the dark stripes we see gracing the interiors of many longer glaciers. Some of the more famous are in Alaska (Figure 49 - photo of Barnard glacier). There is no less striking evidence that the flow of ice is laminar, and that most glaciers are very steady in their motion, than that these debris stripes are so straight. In fact, it is the rare exceptions to the straightness of these medial moraines that indicates that something has 'gone wrong' up one or another tributary; the looped moraine signature of a surging glacier is telltale.

While there are exceptions, by far the majority of the medial moraines result from the welding together of lateral moraines at interior tributary junctions such as those on Barnard Glacier (Figure 49). The debris is swept into the seam between the two ice streams. It is angular debris, and has never seen the bed. The ice on either side of the seam has very little debris content, while that in the seam has at least some. In the ablation zone, below the ELA, this debris emerges toward the surface of the ice as the ice melts. Because the ice can melt (and therefore vanish), while the debris cannot, the debris accumulates on the surface of the glacier. At this point another element comes into play, however. The presence of any significant debris

on the surface of the ice leads to reduction of the melt rate of the ice. As shown in [Figure 51](#), only 10 cm of debris cuts down the melt rate by a factor of e (2.72). So the adjacent debris-free glacier surface melts faster, leaving the debris covered ice higher. This produces a slope away from the debris cover, which in turn promotes the down-slope motion of the debris ([Figure 52](#)). The result is a stripe of debris that widens downglacier as more debris ‘erupts’ to the surface, and is continually being spread laterally. Walking on practically any portion of a medial moraine will reveal that the hillslope processes are indeed very efficient. The debris is everywhere very thin, usually only one clast thick. Medial moraines typically display a rounded crest and relatively straight limbs. Indeed, this problem has been treated as a hillslope evolution problem (Anderson 2000), resulting in parabolic profiles. We will see in Chapter [x](#) (Hillslopes) that this is the expected steady state profile of a hilltop.

An interesting feedback occurs in complicated glacier networks. As each tributary junction spawns a new medial moraine, and as every moraine widens down-glacier, it is common for these medial moraines to merge, eventually covering the entire glacial cross section with debris. This will inevitably lead to the reduction in the mean ablation rate, and will promote the longer extent of a glacier. This appears to be the case, for example, in the Karakoram range, where highly debris covered snouts of glaciers extend well down the valleys. Similarly, in the easily eroded volcanics of the Wrangell Range in Alaska, debris-covered glacial snouts abound, as seen in [Figure xx \(photo\)](#).

eskers

There is one distinctive depositional feature attributable to the subglacial fluvial system: eskers. These are sinuous ridges with triangular cross-sections that consist largely of gravels. They can be up to several tens of meters in relief. An esker represents the operation of a subglacial tunnel through which significant volumes of surface meltwater passed, entraining and transporting the gravel as it did so. As such, their present shape and location in the landscape provides a probe of the hydrologic and glaciological conditions during which they formed. The most extensive systems of eskers were formed beneath the continental scale ice sheets.

One of the most striking features of eskers is that they do not obey the contours of the landscape on which they currently rest. This could be explained in two ways. The first is that these conduits in which the gravels were initially deposited were englacial rather than subglacial conduits, and were simply laid down over the landscape as the glacier retreated. The second is that they are indeed subglacial, and that something inherent in the subglacial hydrologic system allows water to flow uphill. Sounds outrageous, but this is the most likely. Arguments against the englacial explanation include the fact that the gravel deposits have intact stratigraphy that is not deformed by such a superposition on uneven ground. Most importantly, however, the apparent uphill flow, the details of where this uphill flow occurs, and the style of deposition in the various divides, can all be explained. We are very used to thinking about water responding only to topographic gradients, as it does when running in open-topped channels on the surface of the earth. But eskers represent flow in closed conduits – pipes – beneath the glacier. Just as water in a hose can be made to flow upward by water pressure gradients, so too is the flow in the conduits dictated by the water pressure field, running down-gradient. The pressure field is established not by the bed topography, but by the ice thickness profile, which involves both the ice surface and the bed profiles ([Figure 30](#)). The equation dictating the pressure field is that for the total head, which is the sum of the elevation head, and the pressure:

$$\phi = \rho_w g z + \rho_i g (H - (z - z_b))$$

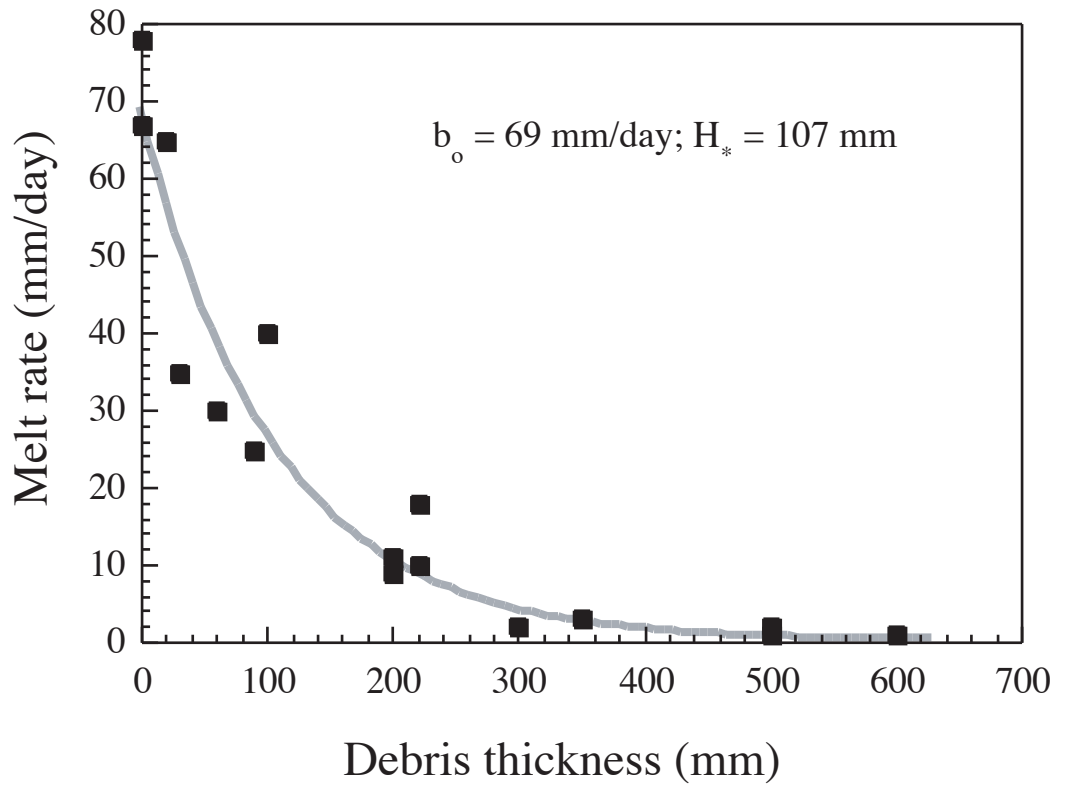


Figure 7.51. Dependence of ice ablation rate on debris thickness. Note scale length for exponential decay of ablation rate is roughly 11 cm. (after Anderson, 2002; data from S. Lundstrom, 19xx).

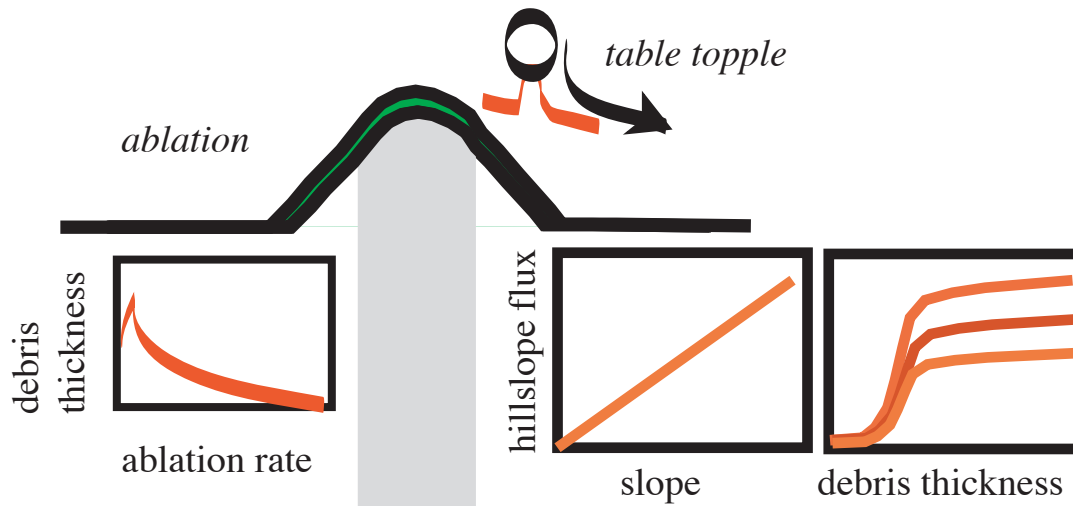


Figure 7.52. Schematic of medial moraine problem. Debris from a debris-rich septum of ice (gray) erupts to the surface at a rate dictated by the ablation rate. Debris ravel down the slope by the table topple mechanism at a rate that depends upon slope. The total debris discharge depends on both local slope and debris concentration. The moraine widens beyond the margins of the debris-rich septum through time. The moraine crest is convex, while the side-slopes beyond the debris-rich ice septum are straight.

where z is the elevation, z_b the elevation of the bed, and H the thickness of the ice. Water within a glacier or an ice sheet flows perpendicular to lines of equipotential within the glacier. These lines, or planes of equipotential, can be calculated by setting the gradient, $d\phi/dx$ to zero:

$$\frac{d\phi}{dx} = \rho_w g \frac{dz}{dx} + \rho_i g \frac{d(H - (z - z_b))}{dx} = 0$$

Solving this for the dip of the equipotential lines, dz/dx , we find that

$$\frac{dz}{dx} = \frac{\rho_i}{\rho_w - \rho_i} \frac{d(z_b + H)}{dx} = \frac{\rho_i}{\rho_w - \rho_i} \frac{dz_s}{dx}$$

As we can see from equation x, and from [Figure 53](#), the lines of equipotential essentially mirror the topographic contours of the ice surface, but dip 11 (917/(1000-917)) times more steeply than does the surface. Therefore the flowfield of water within the glacier is canted at a high angle to the surface, pointing down-glacier. When the englacial channels intersect the bed, of course, the flow is trapped at the ice-rock interface. It must still obey the pressure gradient. The equation for the head gradient (the derivative of [equation x](#)) has two terms, one related to the ice surface slope, the other to the bed slope. We now seek the expression for the potential gradient along the ice-rock interface, i.e., when $z=z_b$:

$$\left. \frac{d\phi}{dx} \right|_{bed} = (\rho_w - \rho_i)g \frac{dz_b}{dx} + \rho_i g \frac{dz_s}{dx}$$

The term associated with the bed slope, dz_b/dx , is 1/11th as important as that associated with the slope of the surface of the ice, dz_s/dx . The flow will go in the down-glacier direction, i.e. in a positive x direction, as long as this gradient is negative (flow is driven down potential gradients). This can be cast as requiring that

$$\frac{dz_b}{dx} < -11 \frac{dz_s}{dx}$$

For example, if the surface of the ice slopes at -0.01, or 10m/km downglacier, then water will continue to flow downglacier as long as the bed slope is less than 0.1. This is a steep *upward* slope. When the ice sheet is removed to reveal the esker deposit, it looks as if the water in the subglacial tunnel had flowed uphill, while in fact it had flowed down the total head gradient. The bottom line is that the surface topography of the glacier is 11-fold more important in dictating the direction of flow than is the topography of the landscape over which it flowed.

One of the classic examples of esker systems is the Katahdin esker system, in Maine. This system drains 150 km from central Maine, wraps around Mt Katahdin, a nunatak poking through the ice sheet during the last glacial maximum, to the calving margin at roughly the present coast. In a classic pair of papers, Shreve (1985a,b) uses the physics of water flow in a subglacial conduit to explain a wide variety of the features of these eskers. As one follows any particular esker down-ice, the esker disobeys present day contours in a particular way, and it changes shape in a characteristic pattern. Shreve first explained these patterns, and then made use of them to reconstruct the shape of the ice sheet then (about 12.7 ka) covering this portion of Maine. As shown in [Figure 53](#), the shape change is such that on the flat the esker tends to be sharp-crested, and triangular in cross section. As it climbs toward a divide, it first becomes multiple-crested, and then broad-crested, losing its triangular cross section altogether. Over the top of the divide, there may be a gap in the esker before it resumes its course, again sharp-crested. Shreve focused on what is happening to the water in the ice-walled tunnel. Heat is generated as the water flows, due to frictional interaction with the walls. This energy can be used either to warm up the water or to melt the walls or both. Note also that as the water flows into regions of thinner ice, it is moving into warmer ice (recalling the thermal profile within a temperate glacier). The faster the ice is thinning, the more of this energy being released must be consumed in warming the water to keep pace with the warming of the walls. If this pace of warming is not sufficient, the water will

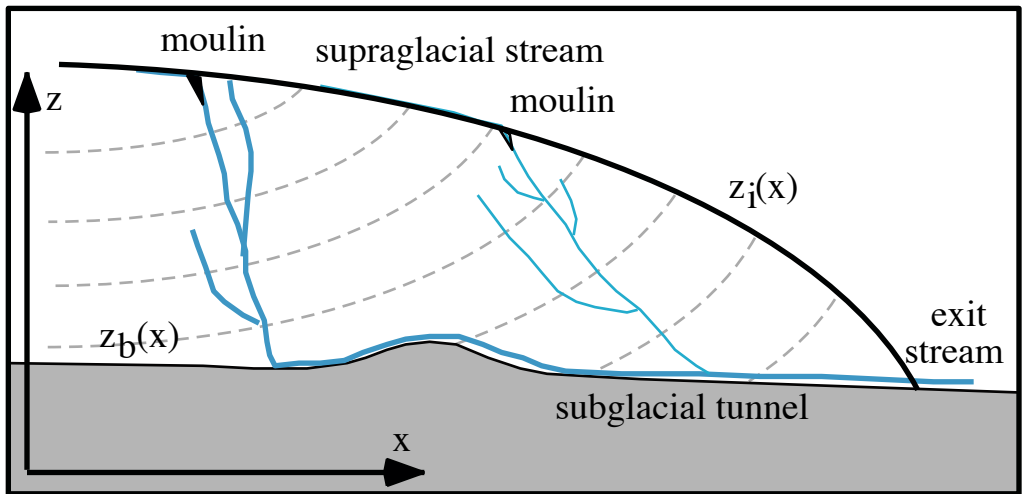


Figure 7.53 Schematic of the water flow paths within a glacier profile. Melt water enters the glacier through moulins and crevasses. Englacial water flows normal to equipotential lines (dashed) until it encounters the bed. Flow at the bed occurs in tunnels in the ice and/or the bed, and remains dictated by pressure gradients. These are more strongly determined by the ice surface gradient than by the bed gradient. (after Shreve, 1985 GSA Bulletin)

be below the pressure melting point of ice, and will freeze onto the wall. Shreve deduced that the condition for freezing is when the bed gradient is positive, and is more than 1.7 times the magnitude of the ice surface gradient (Figure 54). It is at this point that the ice is thinning too rapidly for the water to warm up fast enough. Rapidly melting walls allow ice with all its basal debris to move toward the ice conduit; in addition, the shape of the conduit is tall, the melting rates being highest where the water is thickest. Freezing walls pose the opposite case. With no new ice moving toward the conduit, the roof is low-slung, the freezing rates being highest there. New sediments are not supplied, and sediment already in the pipe is simply reworked, generating better sorted deposits.

Shreve also reconstructed the ice surface morphology. Wherever he found well-defined transitions from sharp-to-broad crested, he could pin down the ice surface slope. In addition, he made use of the divergence between modern topographic gradient and the path of the esker over it to deduce the ice surface slope. At seven places along the 140-km Katahdin esker system, surface gradients constrained the shape of the ice sheet (Figure 55a). The thickness profile was then integrated, constrained to have the proper surface gradient at each location. In other words, knowing dz/dx at several locations, $z(x)$ was obtained by integration. Note that no assumptions were made about the rheology of the ice, its thermal profile, whether or not it was sliding, or the nature of the underlying material. This independently documented ice sheet profile could then be used to assess the pattern of the basal shear stress of the ice sheet (Figure 55b). Recall that we used the assumption that the basal shear stress was uniform, and on the order of 1 bar (10^5 Pa) in our simple reconstructions earlier. Shreve found that the shear stress varied from $0.2 - 0.3 \times 10^5$ Pa (relatively low compared to estimates from modern ice sheets of about 1×10^5 Pa), and viewed this as supporting claims of others that the history of the demise of the local portion of the Laurentide icesheet from its last glacial maximum had been first to deflate (lower in slope), and then to retreat from its margins. The eskers were formed when the ice sheet was in its deflated state.

Erosion rates

Just how efficient are glaciers at eroding the landscape? What means do we have of constraining erosion rates beneath hundreds of meters of ice? [quick summary of all available methods (Figure 56)] Our principal probe is the sediment output from glacial streams. By its nature, this yields only a spatially (and perhaps temporally) averaged measurement of the erosion rate. It is impossible to tell unambiguously where the sediment has come from beneath the glacier. Even so, this number is useful in that it allows comparison with fluvially dominated systems, and it allows comparison amongst glacial systems from which one might ferret out what variables are the dominant ones. If we can measure well the sediment discharge, Q_{sed} , then the spatially averaged rate of erosion of the glacier whose basal area is $A_{glacier}$ is:

$$\bar{e} = \frac{Q_{sed}}{A_{glacier}}$$

It is not at all trivial to measure sediment load in a river, however. As discussed in the fluvial chapter, one must measure both suspended sediment and bedload transport rates. Using this method, one can obtain a near real-time record of the sediment output from the glacier. There is no doubt that this records the sediment output from the glacier. We are not assured, however, that this is equivalent to the rate at which sediment is being produced by erosion at the glacier bed. The problem is that sediment can be stored temporarily at the glacier bed, to be exported from the subglacial system later.

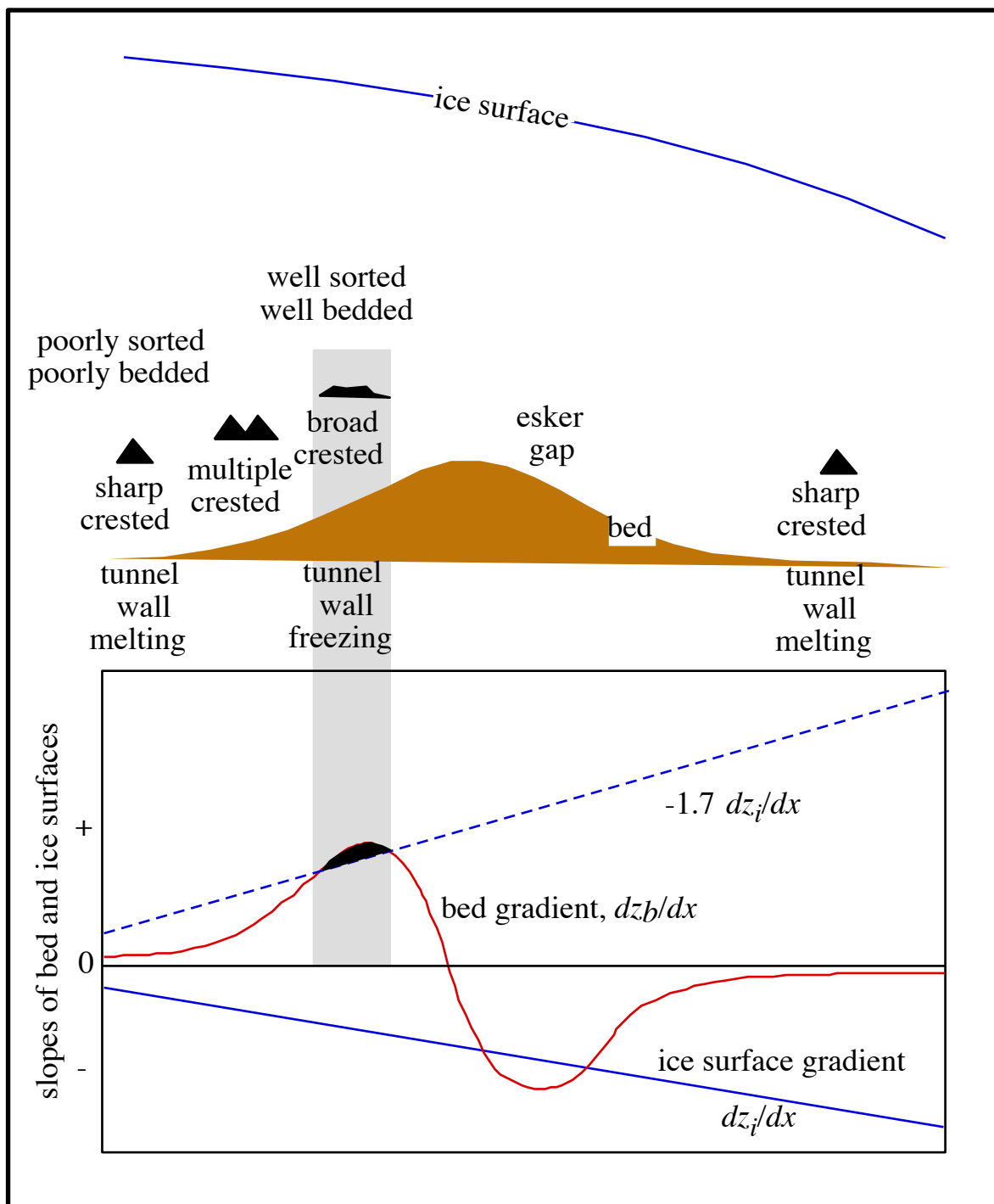


Figure 7.54 Esker styles. Types of eskers and their locations in the topography beneath an ice sheet. Eskers evolve from sharp-crested on flat topography to multi-crested and broad-crested as the water in the subglacial tunnel is forced over a pass in the basal topography. (after Shreve, 1985 GSA Bulletin)

An intermediate time scale (one to several years) estimate of erosion rates can be obtained in special circumstances. In Norway, much of the hydropower used in the nation derives from water tapped subglacially, high up on the walls of the fjords where glaciers are still clinging. Engineers have drilled tunnel networks into the mountains that deliver subglacial water to conduits, which descend through the mountainside to turbines below. The problem is that the subglacial water is carrying a sediment load, which would damage the turbine blades. They have therefore built a set of monster reservoirs to trap the sediment before the water roars through the pipes. The traps are emptied periodically, the number of dump truck loads being tallied to estimate the volume of sediment involved since the last cleaning.

Another technique yields yet longer-term rates of glacial erosion. This relies upon the volume of sediment in a depositional basin that arrived at the site over a given period of time. For example, the basin may be the interior of a fjord, or the continental shelf of Alaska. Drilling the deposit, or seismically imaging it, can constrain the geometry and hence the volume of the deposit. And time lines can be drawn within it by obtaining an age from some marker horizon within the deposit.

The results of many studies utilizing these methods have been summarized by Hallet and others (Figure 57). The rates vary greatly, but can range up to several mm/yr. They also vary in a systematic way geographically. The glacial basins in Alaska are very productive of sediment, while those in Norway are 1-2 orders of magnitude less so. This presumably reflects both the erodability of the substrate, and the delivery of snow to the region. The Alaskan coast is dominated by young rocks of an accretionary prism, while the Norwegian coast is a Precambrian shield. And the Alaskan bight enjoys huge snowfalls relative to Norway. A steady state Alaskan glacier must therefore transport much more ice down valley than its Norwegian counterpart. To the degree to which this is accomplished by enhanced sliding, the erosion rate ought to be enhanced.

Role of rock type (joint density) in determining erosion rate.

Iceberg Lake story from the deltas and laminated sediments. (Loso et al., 2004)
Riihimaki et al. 2005

Use of CRNs to measure erosion rates over an entire glacial cycle. Fabel, Briner, 4th of July valley, Guido et al., 2007 Geology, on retreat pattern rather than erosion in San Juans, Colorado.

Drumlin fields...and their use as flow indicators

Case study of Yosemite Valley, California

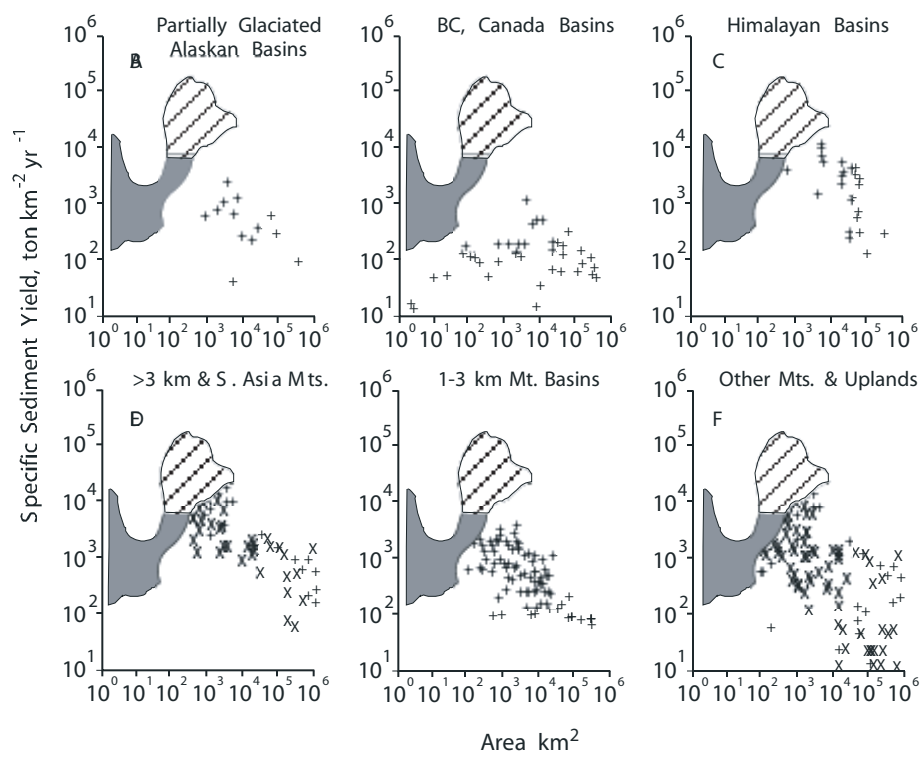


Figure 57. Sediment yield from glacial basins around the world (shaded pattern), and comparison with fluvially dominated basins (x's). (after Hallet, Hunter and Bogen, 1996)

Further reading

Bennett and Glasser

Drewry, David. Glacial Geologic Processes

Hooke, Roger leB. Glacial Mechanics

Lock, The Growth and Decay of Ice

Meinzes

Paterson, 3rd edition, The Physics of Glaciers

Pfeffer AGU monograph on Columbia

Sharp, Robert P. Living Ice

Shreve on eskers

Sugden and John

References

Figure Captions

Figure x.x Schematic diagrams of a glacier (white) in a mountainous topography (gray) showing accumulation and ablation areas on either side of the equilibrium line altitude (ELA). Mapped into the vertical, z (left diagram), the net mass balance profile, $b(z)$, is negative at elevations below the ELA and positive above it. We also show the net balance mapped onto the valley-parallel axis, x (follow dashed line downward), generating the net balance profile $b(x)$. At steady state the ice discharge of the glacier must reflect the integral of this net balance profile (bottom diagram). The maximum discharge should occur at roughly the down-valley position of the ELA. Where the discharge goes again to zero determines the terminus position.

Figure x.x Mass balance profiles for the year 1998 on the Nigardsbreen, a coastal Norwegian glacier. a) Specific balance in meters of water equivalent. Winter balance from snow probe surveys, summer balance from stake network (circles). Net balance is shown in gray; net balance is zero at 1350 m, the ELA. b) The volume balance derived by the product of the specific balance with the altitudinal distribution or hypsometry of the glacier. That the glacier has so much more area at high elevations is reflected in the high contribution of accumulation to the net volume balance of the glacier (gray fill). In 1998, the net balance is highly positive; there is more gray area to the right of the 0 balance line than to the left), so that the integral of the gray fill is > 0 . In this year the positive total balance represents a net increase of roughly 1 m water equivalent over the entire glacier. (after NVE, 1999)

Figure x.x Specific mass balance profiles from several glaciers around the world, showing the variability of the shape of the profiles. Mass balance gradients (slopes on this plot) are quite similar, especially in ablation zones (where the balance < 0) except for those in the Canadian Arctic (Devon and White ice caps). (adapted from Oerlemans, Nature October 7, 1992)

Figure x.x Profiles of topography (solid line), equilibrium line elevation (ELA) and glacial extent (solid, present day; dashed, last glacial maximum (LGM)) along the spine of Western North America from California to the Arctic Ocean. Note many hundred meter lowering of the ELA in the LGM, and corresponding greater extent of the glacial coverage of the topography. (after Skinner and Porter, 19xx)

Figure x.x Temperature profiles in polar (top) and temperate (bottom) glacier cases. Kink in profile in the polar case reflects the different thermal conductivities of rock and ice. Roughly isothermal profile in the temperate case is allowed by the downward advection of heat by meltwaters. Temperature is kept very near the pressure-melting point throughout, meaning it declines slightly (see phase diagram of water).

Figure x.x Density profiles in two very different glaciers, the upper Seward Glacier in coastal Alaska being very wet, the Greenland site being very dry. The metamorphism of snow is much more rapid in the wetter case; firn achieves full ice densities by 20 m on the upper Seward and takes 100 m in Greenland. Ice with no pore space has a density of 917 kg/m^3 . (after Paterson, 19xx)

Figure x.x Profile of the Antarctic ice Sheet from Mirny (circles), along with theoretical profiles: parabola (gray line) and curve that incorporates a uniform accumulation rate (black line). (after Paterson, after Vialov (1958))

Figure x.x Diagrams to aid in the derivation of the velocity profiles in linear fluids (top row) and in nonlinear fluids (second row). In each row the shear stress profile is the same, linearly increasing from 0 at the top of the fluid to the basal shear stress τ_b at the base. The middle box shows the shear deformation rate profile, $dU/dz(z)$, and the third box shows its integral, the velocity profile, $U(z)$. Bottom box shows graphically the shear strain associated with three different levels in the fluid. Recall that shear strain can be measured by the change in angles in a box with originally orthogonal sides.

Figure x.x Four measured deformation profiles of an initially straight vertical borehole in the Worthington Glacier, Alaska. Measurements made with borehole inclinometer; only down-glacier component of deformation shown. Ice depth at this location is roughly 190 m. (after J.T. Harper, pers. comm. 1996; see Harper et al., Science 19xx)

Figure x.x Velocity profile of the Athabasca Glacier, Canada, derived from inclinometry of a borehole and measurement of surface displacement of the borehole top. Projection to the base yields estimate of the contribution from sliding (gray box). (after Paterson, 19xx; data from Savage and Paterson (1963))

Figure x.x Distribution of down valley ice speeds in cross section of the Athabasca Glacier, Canada. a) As interpolated from measurements in 7 boreholes (labeled gray lines), from Raymond (1971), and b) as predicted by a theory by Nye (1965). (after Paterson, 19xx). Center diagram shows cross-valley distribution of sliding speed as deduced by the intersection of the velocity contours with the bed in (a). Note strong broad peak in the sliding speed in the center of the glacier.

Figure 7.11 Flow profiles for $n=1$ (green) and $n=3$ (red) fluids, normalized against maximum height above bed and maximum flow speed. The mean speed is shown as the vertical lines, and the position above the bed at which this mean speed would be measured is signified by the dashed horizontal lines. As the nonlinearity of the rheology increases, the mean speed approaches the surface speed, and the depth at which it would be measured is found nearer the bed.

Figure x.x Phase diagram $P(T^\circ)$ for the molecule H_2O . Note the negative slope of the melting curve separating water and ice. This allows melting, favoring the higher density phase, when pressure is increased, and is at the root of the regelation process. (after Locke, 19xx)

Figure x.x Schematic diagram of the regelation process by which temperate glaciers move around small bumps on the glacier bed. ice melts on the high pressure (stoss) side of the bump, moves around it as a thin water film, and refreezes in the low pressure shadow on the lee side. The heat released by the refreezing is conducted back through the bump to be used in the melting process. It is therefore an excellent case of coupling between thermal and fluid mechanics problems.

Figure x.x Map of the Variegated Glacier, Alaska, showing area of glacier involved in the 1982-83 surge (dashed lines), a few of the km stake locations, and the locations of the major outlet streams near the terminus. (after Kamb et al., 198x)

Figure x.x Evolution of the elevation anomaly in the decade leading up to the 1982-83 surge of the Variegated Glacier, Alaska. Glacier thickens by more than 60 m in the accumulation area, while thinning by more than 50 m in the ablation area. (after Raymond and Harrison, 19xx)

Figure x.x Summer (a) and winter (b) velocity anomalies on the Variegated Glacier centerline in the decade preceding the 1982-83 surge. Note different scale for the summer vs. winter anomalies, attesting to the enhancement of sliding in the summer melt season. The anomaly grows by at least an order of magnitude over the decade. (after Raymond and Harrison, 19xx)

Figure x.x Cross-glacier ice velocities in the Variegated Glacier in (a) pre-surge, b) phase 1 of the surge, summer 1982, c) mid-phase 2 of the surge, and d) post-surge. Note the different velocity scales, showing more than 100-fold increase in speeds during maximum of the surge. That the surge velocity profile is so plug-like implicate strongly the role of sliding at the bed. (after Kamb et al., 198x, Science)

Figure x.x a) Ice surface velocity profile ($u(x)$), and b) ice surface topography, $z(x)$, in a 3 km reach of the lower glacier, during the 1983 surge of the Variegated Glacier, Alaska. (after Kamb et al., 19xx Science, Figure 4)

Figure x.x Ice surface velocity at km 9.5 (after Kamb et al., 1985), b) water discharge and c) sediment concentration deduced from turbidity measurements in the weeks surrounding the abrupt termination of the 1983 surge of the variegated Glacier, Alaska. (after Humphrey and Raymond, 19xx)

Figure x.x Trajectories of clasts embedded in basal ice as it encounters big (top) and little (bottom) bumps in the bed. Ice can deform sufficiently to accommodate the larger bumps, allowing clasts in the ice to ride over the bumps. In the small-bump case, the ice trajectories intersect the bed, reflecting the regelation mechanism. Clasts in the ice will be brought forcefully into contact with the bed, and cause abrasion of the front sides (stoss) of these bumps, leading to their elimination.

Figure x.x Schematic diagram of a water-filled cavity beneath a temperate glacier. Arrows represent normal stresses.

Figure x.x. Contours of stresses (σ_1 , in MPa) within bedrock of corner at ledge edge. Ice sliding from left to right. No vertical exaggeration. a) with water pressure steady at 2.1 MPa, and b) with water pressure reduced to 1.5 MPa. Note strong stress concentrations at ledge face. (after N. Iverson, 19xx)

Figure x.x. Topographic profiles of ice surface and bed (a), and water pressure records (b) from Storglacieren, Sweden. Profile shows several overdeepenings of the bed and major crevasse

zones in regions of extension. Borehole locations in major overdeepening and at crest of bedrock bump are shown, along with spot measurements of the water pressure in the middle of the overdeepening. These measurements are all close to the level expected for flotation of the ice: 90% of the ice thickness, shown in gray line. Pressure records are very different for two sites, that in the middle of the overdeepening showing little variation around 90-100% of flotation, that at the crests of the bump showing major diurnal fluctuations between 70-90% flotation and that pressure associated with the depth of the transducer (gray line). Similar pressure fluctuations are inferred to promote enhanced quarrying of the bed at sites shown in (a). (after Hooke et al., 19xx, figures 2&3).

Figure x.x Numerical simulation of cross-valley profile evolution during steady occupation of the valley by a glacier. Initial fluvial v-shaped profile evolves to u-shaped profile characteristic of glacial valleys in roughly 100 ka, given the sliding and erosion rules used. Bottom graph shows initial distribution of sliding speed and corresponding erosion rate. Low erosion rates in valley center allow faster rates along the walls to catch up. Final erosion rate is roughly uniform, causing simple downwearing of the form once u-shaped. (after Harbor et al. Nature, 19xx)

Figure x.x Numerical models of long valley profile evolution of a glaciated valley in the face of a) steady climate, over 30 ky, and b) climate in which the ELA lowers at 4m per thousand years, for 90 ky. Initial profile is a linear (uniform slope) valley. Top diagram shows all time slices in the respective simulation as light lines. (after Oerlemans, 1984)

Figure x.x Schematic of the water flow paths within a glacier profile. Melt water enters the glacier through moulins and crevasses. Englacial water flows normal to equipotential lines (dashed) until it encounters the bed. Flow at the bed occurs in tunnels in the ice and/or the bed, and remains dictated by pressure gradients. These are more strongly determined by the ice surface gradient than by the bed gradient. (after Shreve, 1985 GSA Bulletin)

Figure x.x Types of eskers and their locations in the topography beneath an ice sheet. Eskers evolve from sharp-crested on flat topography to multi-crested and broad-crested as the water in the subglacial tunnel is forced over a pass in the basal topography. (after Shreve, 19xx)

Figure x.x a) Profile of the ice sheet along flow line over Maine, through Mt Katahdin, at roughly 11 ka, as deduced from esker topography (bottom continuous line) as it crosses various passes (isolated bumps). Two profiles shown bracket maximum and minimum estimates. b) Basal shear stress profile for same section of the ice sheet. Stress is everywhere below 1 bar (100 ka) and over much of the profile is only 20-30 kPa. (after Shreve, 198x)

Figure x.x . Two types of glacial outburst flood geometries. Tributary stream dammed by trunk valley glacier generates floods through tunnel outflow. Tributary glacier damming trunk stream valley typically fails through subaerial breach at the valley margin. (adapted from Fountain and Walder, 1998)

Outline

why should we be interested in glaciers
sea level
measures of global change
nifty objects we encounter en route to summits
analog to simple rocks at or near their melting points
whole satellites and planets made with a carapace of ice

Glaciology

glaciers definition
what glaciers are not -- sea ice
mass balance of a glacier, hypsometry, total mass balance as a measure of the health of a glacier, defn of the ela, snowline
example profiles from around the world. Oerlemans work.

glacial types
temperate
polar
tidal
surging
ice caps and ice sheets

expected ice discharge profile max at the ela
general flow pattern above and below the ela and influence on locations of moraines

ice transfer technologies
internal deformation. nonlinear flow law Glens flow law
sliding
internal deformation enhanced around bumps
regelation

ice sheets profiles go as square root of distance from margin -- the plastic endmember

thermal regime dictates polar glaciers are slow and dont erode their beds
crevasses

surging
Variegated
ice streams

stability of ice sheets -- thermal, causes of Heinrich events, surging, binge-purge etc.

Glacial Geology

Erosional forms

Small scale

- Striae
- Smooth beds, removal of bumps
- Roche moutonee: plucking and abrasion
- Channel forms
- Linked cavities...Blackfoot and Castleguard

Large scale

- Ushaped valleys
- Long valley profiles
 - Paternoster lakes
 - Hanging valleys
 - Fjords
- Aretes and horns

Depositional forms

- The materials: tills, boulder clays
- Moraines. Note the angular nature of the debris, indicating its derivation supraglacially
 - Terminal
 - Lateral
 - Medial
 - Stripes indicative of laminar flow of ice
 - Looped moraines indicators of surging behavior
 - Debris cover promoted by widening of medial moraines
 - Ground moraine, till
- Eskers
 - Tunnels can be driven over divides
 - Subglacial fluvial channels. note rounded nature of the gravels
 - Shreve story of nature of eskers in Maine

Products and where they go once they leave the glacial system

- braided river systems
- loading of the shelves, e.g., Alaskan sediment sinks
- erosion rates derived from these volumes